2007

Technical analysis of adjustable melt rotation and numerical analysis of polymer flow using CFD software

Michael John Wolbert
Lehigh University

Wolbert, Michael John Jr.

Technical Analysis of Adjustable Melt Rotation and Numerical Analysis of Polymer Flow...

May 2007

Technical Analysis of Adjustable Melt Rotation and Numerical Analysis of Polymer Flow using CFD Software

by

Michael John Wolbert Jr.

A Thesis

Presented to the Graduate and Research Committee

of Lehigh University

In Candidacy for the Degree of

Master of Science

in

Mechanical Engineering and Mechanics

Lehigh University

May, 2007

LEHIGH UNIVERSITY

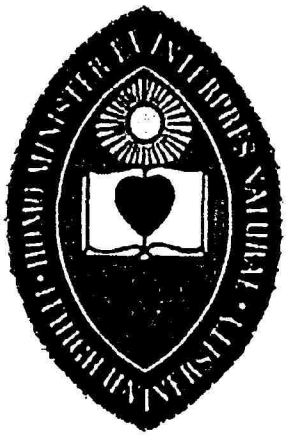

Bethlehem, Pennsylvania

This thesis is accepted and approved in partial fulfillment of the requirements for the

Master of Science.

John P. Coulter, Ph.D.,
Thesis Advisor

Herman F. Nied, Ph.D., Chair,
Mechanical Engineering and Mechanics

April 26, 2007
Date

Acknowledgments

I would like to thank Dr. John Coulter for his guidance and support throughout this project. He is solely responsible for helping me make my decision to attend Lehigh University to further my education. He is also responsible for keeping me going through the many obstacles that occurred during my research project.

I would also like to thank Dr. John Beaumont of Penn State Behrend and Kevin Boell of the Plastics CAE Center. Their advice and guidance was greatly appreciated throughout my research project.

Finally I would like to thank the department of Mechanical Engineering and Mechanics for providing me with the financial support that I needed in order for me to attend Lehigh University while I pursued my Masters of Science degree. I would also like to thank Greg Layser and Mike Casarrela who contributed in helping me throughout my research project.

Table of Contents

List of Tables

List of Figures

Abstract

The use of multi-cavity molds has become increasingly popular in injection molding. They allow for a high production output which ultimately increases profits. The geometrically balanced runner system has been adopted as the best way to deliver melt from the sprue to the cavities. Studies have shown that fill imbalances still occur between cavities in molds with geometrically balanced runners. A contributor to this imbalance is the creation of shear thinning in a polymer during the injection molding process. These imbalances often serve as the cause for costly design considerations and mold fabrication and re-fabrication. Melt rotation is used to help eliminate the flow imbalances, but melt rotation also requires design and fabrication. The objective of this research study is explore the possibility of an adjustable melt flipper which would reduce a majority of design considerations, and to do a feasibility study on a CFD software to see how accurately it can predict shear and the imbalances associated with it.

The following is a study on the use of adjustable melt rotation technology, where the degree of melt rotation can be varied, and a study on the use of Polyflow as simulation software capable of predicting shear and flow imbalances. The results of these studies will help with the understanding of melt rotation technology and the use of software programs to aid in design.

1 Introduction

Present day injection molding often requires high part production in short production times. This leads to the use of multi-cavity molds which need to be designed quickly so as to get the product to market as soon as possible. The geometrically balanced runner system is the most widely used runner system in multi-cavity molds for its ability to create an equal distance between each part and the sprue. However, geometrically balanced runner systems have been shown to still create fill imbalances. These fill imbalances can greatly affect part quality and uniformity. As a result, solutions are needed in the design of runner systems to eliminate flow imbalances and create more uniform parts at the highest production rates possible.

1.1 Purpose of the Study

The geometrically balanced runner system is industrially accepted because the total distanced traveled by the melt in the runner system from sprue to each cavity is equal. While this leads many to believe there will be no fill imbalance problems, this assumption has now been proven incorrect. Research has led experts to believe that the fill imbalances are caused by the non-Newtonian characteristics of polymers. The shear rates created during injection have a great effect on the filling imbalances found in multi-cavity molds. These fill imbalances are partially predictable and through design can be overcome. Melt rotation technology, invented by John Beaumont, is the design answer to fill imbalances. These fill imbalances can be generally predicted, but

not yet in a quantitative way. Thus to date the correction for fill imbalances has been done only through trial runs and the re-design of runner systems using melt rotation technology. The goals of this study were to: 1) use a CFD software package to try and quantitatively predict the fill imbalances found in geometrically balanced runner systems; and 2) to experimentally test adjustable melt rotation technology that could be utilized to correct for fill imbalances in a tunable way.

1.2 Target Problem Description

Melt rotation technology was first proposed by John Beaumont in 1997 as a solution for runner imbalances [6]. Since that time, the technology has been implemented in a number of cases to help eliminate imbalances in multi-cavity molds. The specific melt rotation geometry must be designed for each individual mold that the melt rotation technology is being used in. The process of specifically designing the melt rotation for each mold is time consuming as well as costly. A universal solution to the specific design of melt rotation for each mold would eliminate design time and engineering costs.

Numerical simulations are presently used to help aid in the design of molds and to help understand what is occurring during the injection molding process. Currently CFD software programs on the market have difficulty simulating and predicting the imbalances currently seen in injection molding when multi-cavity molds are used.

1.3 Objectives of the Present Investigation

The development of an adjustable melt rotation insert will eliminate the need for specific melt rotation geometries to be used for each individual case. The molder will be able to adjust the melt rotation in order to meet their needs with no engineering help needed or re-design. The melt rotation insert could be used with varying core pin lengths. The various core pin lengths would be used to adjust the elevation change which causes a change in the amount of melt rotation. The molder could then use the core pin that produces the best results for their needs.

The use of Polyflow, a currently available CFD software program, to simulate imbalances in injection molding can be helpful in the design of molds. If Polyflow is capable of quantitatively predicting fill imbalances it would greatly aid in the design of runner systems and melt rotation technology. It would help to reduce design time, and ultimately the need for trials and re-design.

One objective of this investigation is to experimentally determine the feasibility of the use of adjustable melt rotation technology in correcting fill imbalance when it comes to different materials and injection rates. The other objective is to determine if Polyflow is quantitatively capable of predicting the fill imbalances, associated with shear, that are created during the injection of polymer melt.

1.4 Thesis Outline

The thesis begins with Chapter 2 which will review the evolution of runner design in multi-cavity molds. The problems with each runner design will be

discussed, especially with the widely accepted geometrically balanced runner system. Next, explanations of the fill imbalances observed through the use of geometrically balanced runner systems will be discussed. Following this, melt rotation technology will be discussed due to its ability to correct fill imbalances. Details of design and experimental results will be covered. Finally the use of CFD software packages will be discussed for their ability to predict fill imbalances.

Chapter 3 will begin with the reasoning behind the CFD software selection. The capabilities of the software will be covered, and then the simulations that were performed will be outlined. Finally the results of the simulations will be discussed and the ability of the software to predict fill imbalances will be determined.

The experimental set-up to study the potential of adjustable melt rotation will be discussed in Chapter 4. The machinery used in the production of the experimental parts will be listed. A description of the mold and mold inserts will follow. Next the polymers tested will be discussed focusing on their material properties and relevance to the study. The different trials will be laid out in order of which runner inserts were used. Following that will be the processing conditions used for each individual material, including the different injection rates. Finally the process through which the data was collected will be discussed.

Chapter 5 will include the results from the experiments. For each of the four polymers tested, resulting fill imbalance levels will be presented as a function of the melt rotation system and injection velocity utilized. From the data and graphs, correlations in the data can be made.

Correlations in the data will be discussed in Chapter 6. These correlations will be explained based on the conditions present in each trial and process. Conclusions from the work as well as suggestions for future research are presented at the end of the thesis.

2 Fill Imbalances During Injection Molding

Improving the efficiency of the injection molding process is always a concern of companies in the industry. Improved efficiency results in lower production costs. One way this is achieved is by increasing the number of parts produced during a single injection molding cycle. This is where the importance of the multi-cavity mold comes in. A common problem that arises when seemingly balanced multi-cavity molds are used is the unequal filling of cavities. This leads to a lack of uniformity in the parts, which ultimately causes a loss of profit. It was obvious with early runner designs where the cause of the fill imbalance arose; runner lengths for cavities in the mold were different. Even when runner design evolved to allow for equal runner lengths, however, fill imbalances were still observed. Along with the evolution of runner design, and increased production with lower production costs, the tolerances and quality of injection molding parts has also increased. In order to meet these tighter tolerances and higher quality standards, both industry and academia have focused on trying to find the cause of fill imbalances associated with multi-cavity molds. The focus has been placed on the runner systems, trying to find the cause of the fill imbalances that is seen between the cavities.

The current chapter presents the history of multi-cavity runner design. First it will cover the early runner designs and the problems associated with them. Then the present day geometrically balanced runner system will be looked at in detail along with the problems that surround it. The solution of melt rotation technology is

discussed next. To conclude the ability of CFD software to predict fill imbalances will be presented as a tool to help in the design of molds and their runner systems.

2.1 Multi-Cavity Runner Design

Today there are only a couple runner designs commonly used in multi-cavity molds. While most runner designs today are geometrically balanced, unbalanced "Fishbone" and "Tree" designs can also be found in the injection molding industry. The following section will discuss the differences between the traditional "Fishbone" and "Tree" runner designs and geometrically balanced runner systems.

2.1.1 "Fishbone" and "Tree" Runner

Single cavity molds quickly evolved into multi-cavity molds in the injection molding industry in order to increase productivity. The early multi-cavity molds typically had a runner system design classified as "fishbone" or "tree". With this runner design the cavities further away from the sprue had longer runner lengths then those cavities located closer to the sprue, as illustrated in Figure 2.1.

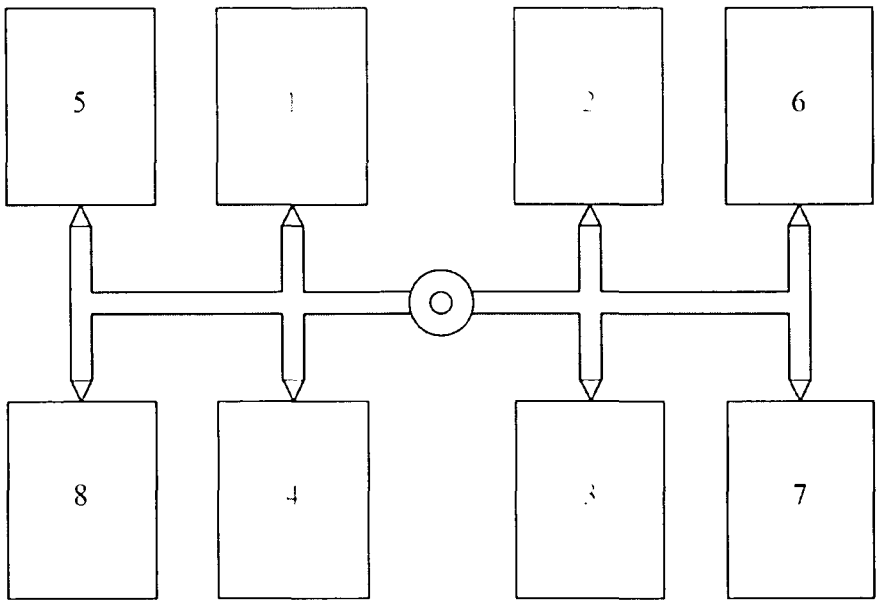

Figure 2.1: "Fishbone" or "Tree" Runner Design

This runner design typically leads to the cavities closest to the sprue to fill first. The parts created in the cavities closest to the sprue were found to be larger in dimension and weight then the parts in the cavities further from the sprue. The fill imbalance is due to uneven runner lengths and pressure drop that each cavity experiences. During the injection molding process the polymer melt will follow the path of least resistance. The cavities that experience lower pressure drops will fill faster then those cavities that experience higher pressure drops. The following equations are used to calculate the pressure drops observed in molds:

$$\Delta P_{round} = \frac{8Q\eta L}{\pi r^4} \quad (1)$$

$$\Delta P_{rectangular} = \frac{12Q\eta L}{wh^3} \quad (2)$$

In these equations, ΔP represents the pressure drop, Q the volumetric flow rate, η the viscosity, L the runner length, r the radius of the runner, w the width of the runner, and h the height of the runner. Calculations using these equations show that for a runner system with a constant runner diameter, the pressure drop at the inner cavity locations would be less then that at the outer cavity locations.

The fill imbalance problem created by the use of "fishbone" and "tree" runner systems is traditionally overcome by artificially balancing the runners. The runner systems would be re-cut so that the cavities closer to the sprue would have smaller diameter secondary runners feeding them from the primary runner. The cavities further from the sprue would have runners feeding them with diameters equal to or a little less then that of the primary runner. This difference in runner diameters would then create comparable pressure drops for inner and outer cavities allowing for more even fill. The artificial balancing though was only good for a small range of volumetric flow rates due to the equations used to calculate the pressure drop. Figure 2.2 depicts an artificially balanced runner system.

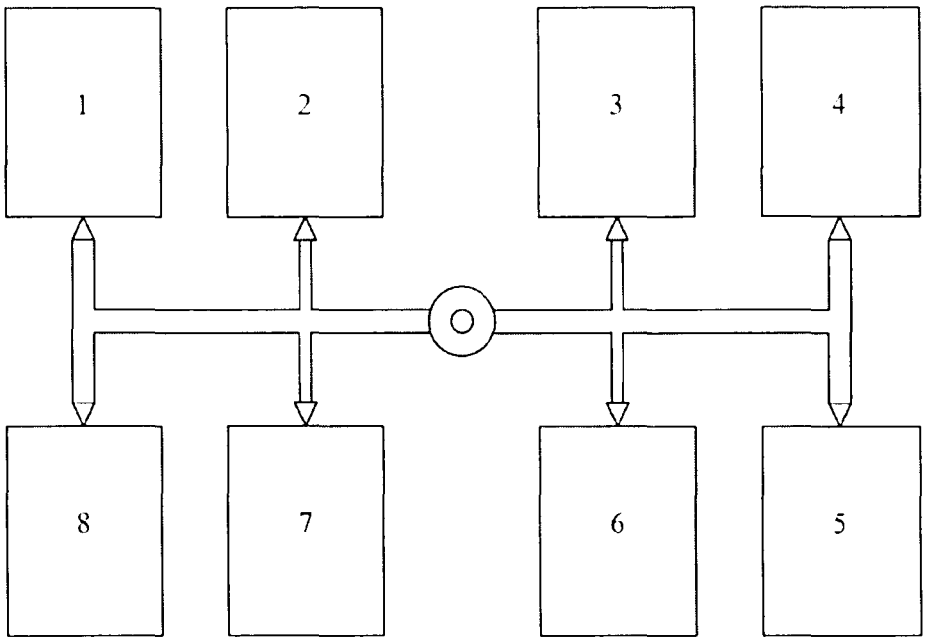

Figure 2.2: "Fishbone" or "Tree" Runner Artificially Balanced Runner Design

The incorporation of computers in design helped greatly with the artificial balancing of runner systems. Using principals like the equations above, the computer could run simulations and determine the sizing of runner systems to create a more balanced flow. These simulations help reduce design time and time needed to re-work molds in order to balance the flows. These simulations used just the basic principals though and did not apply to any complex modeling.

2.1.2 Geometrically Balanced Runner

The geometrically balanced runner was created for its ability to create equal flow lengths from the sprue to each individual cavity in a multi-cavity mold. Today it is considered superior to the prior "fishbone" and "tree" runner designs. However it is not totally the answer to fill imbalance. It has been discovered that during a short

shot, the cavities closer to the sprue still fill before the cavities located further away from the sprue, even though runner lengths are equal for all cavities. Figure 2.3 shows the layout of a typical H-shaped geometrically balanced runner for an 8-cavity mold.

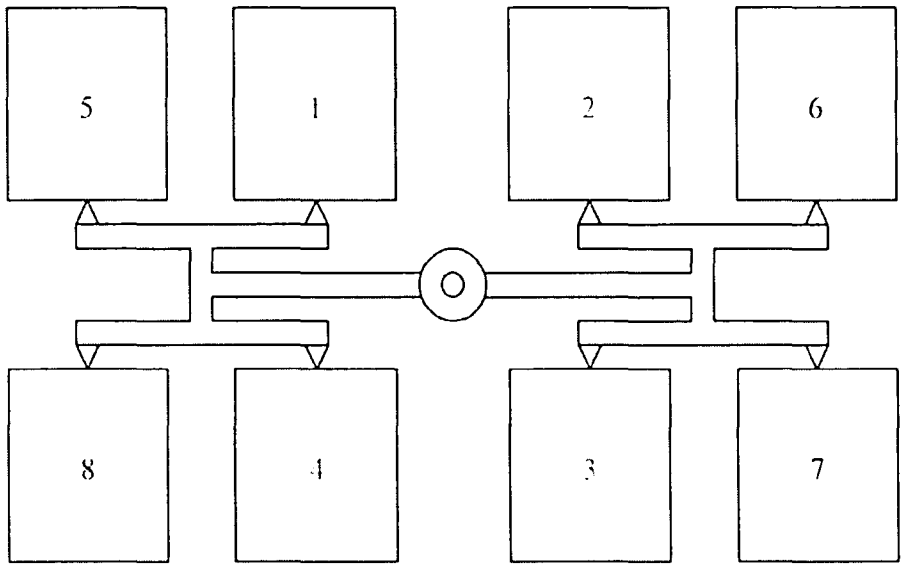

Figure 2.3: Geometrically Balanced Runner Design

Cavities 1-4 represent the "inner" cavities, those receiving flow first, and cavities 5-8 represent the "outer" cavities, those receiving flow second. During short shots it has been found that the inner cavities commonly receive melt before the outer cavities.

The fill imbalances observed in geometrically balanced runner systems greatly hinder the ability to create uniform parts. The cavities filling first tend to be heavier and larger then the other parts due to an uneven packing stage. The filling imbalance effects the packing pressures and packing duration that each cavity experiences. Flash, sinks, and partially filled parts are also observed due to the filling and packing

imbalances.[1] Tolerances are hard to achieve due to dimensional variations that result from uneven part weights and shrinkage.

2.2 Cause of Fill Imbalance

Upon the discovery of the fill imbalances in geometrically balanced runners, multiple theories and ideas of the cause arose. Some of the most popular theories involved temperature gradients in the mold, mold deflection, and the effects of sharp corners at the runner intersections. Each of these theories has been investigated and each determined not to be the cause of fill imbalances in geometrically balanced runners. Another theory arose, the theory of shear induced fill imbalances, which today is accepted as the primary cause of the fill imbalances seen in geometrically balanced multi-cavity molds.

2.2.1 Components of Shear Induced Fill Imbalance

In 1997 Beaumont developed the theory of shear induced filled imbalances. His theory is the combination of several principles of flow which begins with the no-slip boundary condition at the wall. Next is the relationship between shear rate and a polymer's viscosity and polymer temperature. The final principle that is associated with shear induced fill imbalances is the affect of temperature on viscosity. [6]

2.2.1.1 No Slip-Condition

A no-slip condition at the walls is assumed with the flow of a polymer melt since it is a viscous fluid. Where the melt is in contact with the mold surface there is

no motion between the melt and the mold surface. The boundary layer is a region just inside of this surface where large velocity gradients develop. These velocity gradients are large enough to produce significant viscous stresses and shear rates. The remaining region, which is located outside the boundary layer, is the freestream where the velocity gradients and viscous stresses are not as significant. Inside of a runner system this flow is parabolic, with the highest velocity in the center and a zero velocity at the mold surface. This flow is classified as a laminar Poiseuille flow, and illustrated in Figure 2.4.

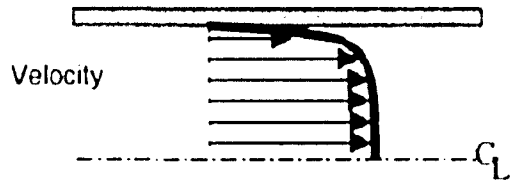

Figure 2.4: Laminar Poiseuille Flow [11]

The shear rates created inside the boundary layer are very important as they affect polymer properties and in-turn the overall process. Figure 2.5 shows the shear rate profile that is created during the flow of the polymer melt during injection.

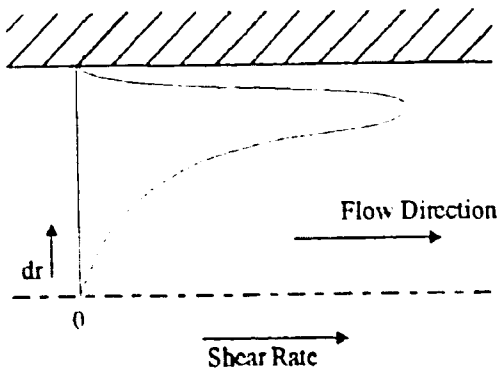

Figure 2.5: Shear Rate Profile in Runner [2]

2.2.1.2 Shear Rate Effect on Viscosity

Polymers are classified as non-Newtonian fluids. Their viscosity decreases with an increase in shear rate, this is known as shear-thinning. Shear-thinning occurs because in the high shear rate areas the polymer chains become oriented in the same direction. This orientation allows for the polymer chains to slide past each other with less effort. Since viscosity is a measurement of a resistance of a fluid to flow, less effort to make the polymer chains move past each other means the viscosity in that region is lower. Figure 2.6 shows two different shear-thinning behaviors that polymers can possess.

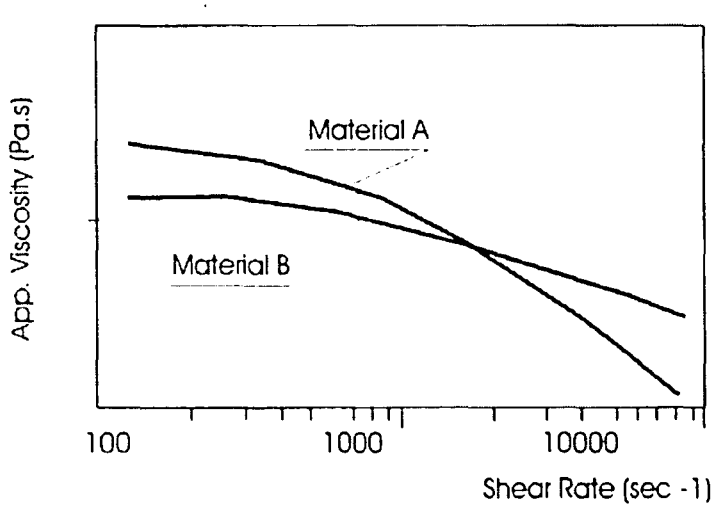

Figure 2.6: Shear-Thinning Behaviors [3]

Material A is more sensitive to shear rates and shows more shear-thinning with higher shear rates. Material B is less sensitive; its viscosity is less affected by higher shear rates.

2.2.1.3 Shear Rate Effect on Temperature

Shear rate has a large effect on the viscous energy dissipation (VED) in a fluid. The result of this is mechanical heat. The heat generated due to the friction present is proportional to the polymer viscosity and the square of the shear rate, as shown:

$$VED \propto \eta\dot{\gamma}^2 \quad (3)$$

As previously discussed the shear rate is highest at the wall and zero at the center of flow. This viscous heating created near the wall is responsible for increasing the temperature of the polymer material flowing near the walls of the runner. This higher temperature material in the outer flow layer is portrayed in Figure 2.7.

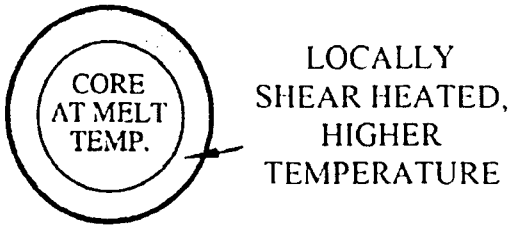

Figure 2.7: Cross Section of Runner Showing Local Shear Heating [4]

2.2.1.4 Temperature Effect on Viscosity

A polymer at a low temperature consists of highly entangled molecules that can not move past each other in their present state. The addition of heat to a polymer will allow for a polymer to turn from a solid to a viscous liquid. The glass transition temperature (T_g) is indicative of a stage between solid and liquid where the material begins to act like a rubbery elastomer. The addition of more heat above the glass

transition temperature allows for the polymer backbone to flex and create room for the molecules to slide past each other. In order for a polymer to flow there must be enough thermal energy for the molecules to be mobile to move past each other and enough space around the molecule in order for it to have somewhere to move. Therefore viscosity is dependent on the availability of free volume which is zero at 0 K and increases with a rise in temperature [5]. This is the basis for the well known fact that viscosity decreases with an increase in temperature. Figure 2.8 displays a plot of viscosity vs. shear rate for various temperatures.

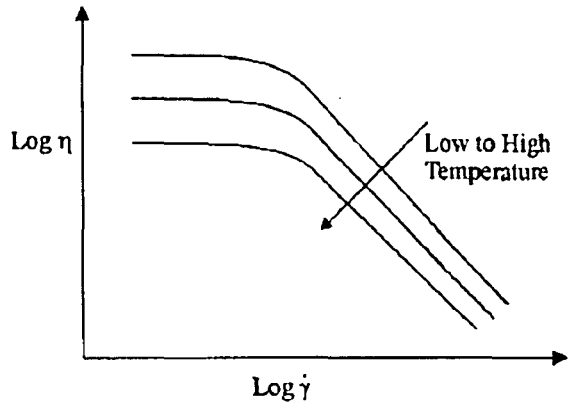

Figure 2.8: Effect of Temperature on Viscosity [6]

2.2.2 Theory of Shear Induced Fill Imbalances

With the principles of no-slip condition, shear rate, and temperature explained, how these principles combine to created shear induced fill imbalances can now be explored. The theory of shear induced fill imbalances, first published by John Beaumont [6] in 1997, is a conglomeration of all these principles.

As discussed earlier, for a fully developed laminar velocity profile there is a resulting shear rate profile. The highest shear rates are located in the boundary layer.

The viscosity in the boundary layer is a function of shear rate and therefore will be lower then the viscosity in the core of the melt. Viscosity will also be reduced more if there is an increase in temperature to the melt due to viscous heating. The combination of shear rate and temperature gradient throughout the melt causes changes in the viscosity of the polymer relative to the radial distance from the center of the runner. Viscosity located at the center of the runner will be higher then the viscosity of the melt located in the outer boundary layer. Figure 2.9 shows the combined effects of the shear rate and temperature gradient on the viscosity of the melt for slow, medium, and fast flow rates.

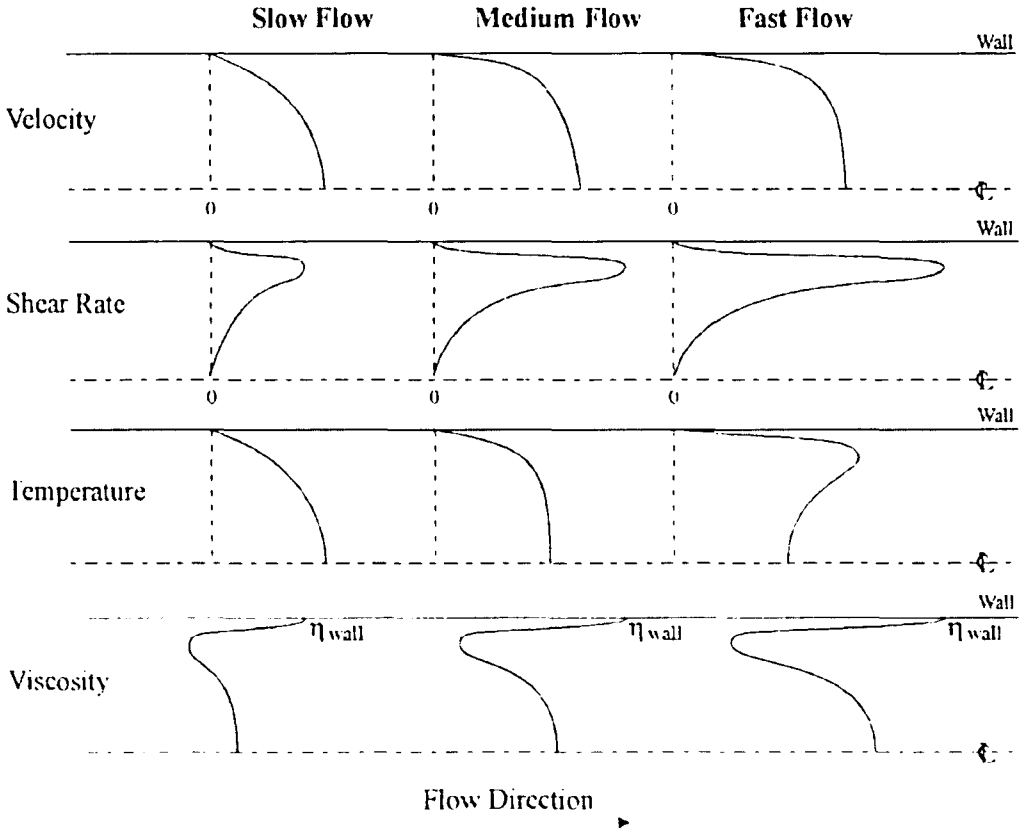

Figure 2.9: Combined Effects on Viscosity [6]

It has been observed that cavity to cavity fill imbalances are only observed in geometrically balanced molds with more then 4 cavities. Molds with 1, 2, or 4 cavities, examples of which are shown in Figure 2.10, will not have cavity to cavity fill imbalances.

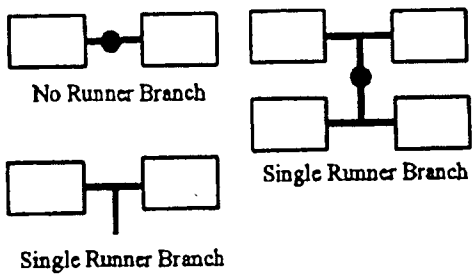

Figure 2.10: Runner Designs with No Cavity to Cavity Fill Imbalance

Fill imbalances will occur with geometrically balanced runner systems numbering 8 cavities or more. More important then the number of cavities is the number of branches in the runner system. As the melt travels through the primary runner, the melt's viscosity profile gradient will develop, but the gradient will be symmetrical. Once the melt reaches the first intersection and branches into the secondary runner the temperature and viscosity distribution will become non-symmetric as illustrated in Figure 2.11.

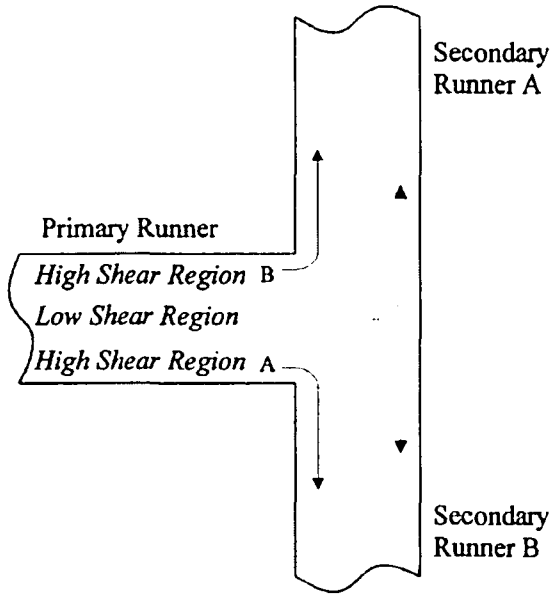

Figure 2.11: Separation of Melt Laminates into Secondary Runner [2]

The branching of the primary runner into the secondary runner causes the highly sheared, higher temperature, lower viscosity melt that was located around the perimeter to now be primarily located on the inner side of the secondary runner as shown in Figure 2.12.

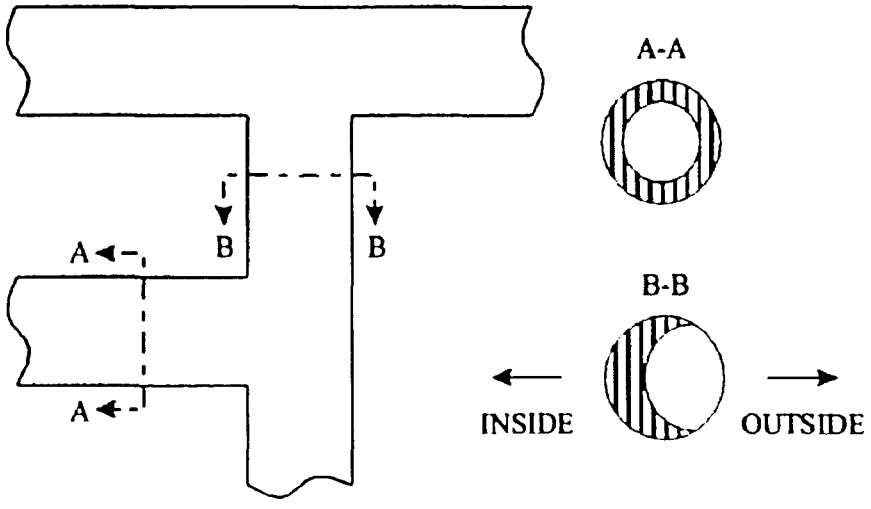

Figure 2.12: Cross Section of Viscosity and Temperature Profile [2]

At the next intersection the secondary runner branches into the tertiary runner. The highly sheared, higher temperature, lower viscosity melt that was located in the perimeter of the primary runner is now the majority of the material being directed to the inner cavities. The low sheared, lower temperature, higher viscosity melt that was located in the center of the primary runner is now the majority of the material being directed to the outer cavities. This is represented in Figure 2.13.

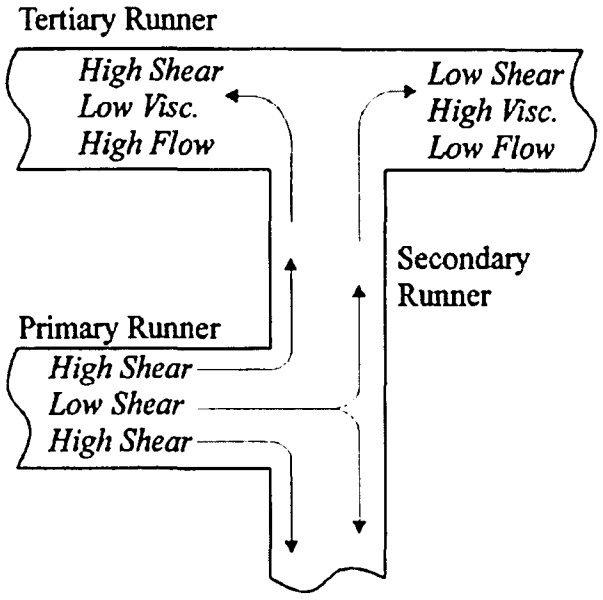

Figure 2.13: Separation of Melt Laminates into Tertiary Runner [2]

2.3 Melt Rotation Technology

Beaumont's theory states that the cooler center of the primary runner melt flow is thrust towards the outer walls when intersecting the secondary runner wall while the perimeter material of the primary runner clings to the inner walls of the secondary runner. This variation of melt properties becomes a problem when the secondary runner branches into the tertiary runner. Beaumont also believed that if the

geometry of the runner system were to be the cause on the variations in viscosity, then the runner could be altered geometrically to overcome these variations. With this Beaumont designed and developed the MeltFlipper^{TM} as the first implementation of what has now become known as melt rotation technology.

2.3.1 Design of Melt Rotation

Melt rotation technology is used to rotate the melt profile before it branches at runner intersections. Since the axial symmetry of the melt is lost in the intersections, melt rotation technology is installed at selected intersections. To create the rotation of the melt deeper and shallower runners are machined on the A and B plates at particular points as illustrated in Figure 2.14.

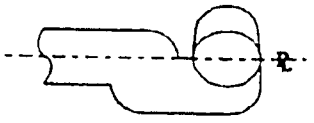

Figure 2.14: Side View of Melt Rotation Technology

These additional bends relocate the location of the cool center and hot perimeter melt regions of the primary runner to a non-symmetric pattern related to the top and bottom directions. From a side to side perspective, however, the pattern is non-homogeneous but symmetric relative to the vertical runner midplane. Thus the non-symmetry is "rotated" by 90° as illustrated in Figure 2.15.

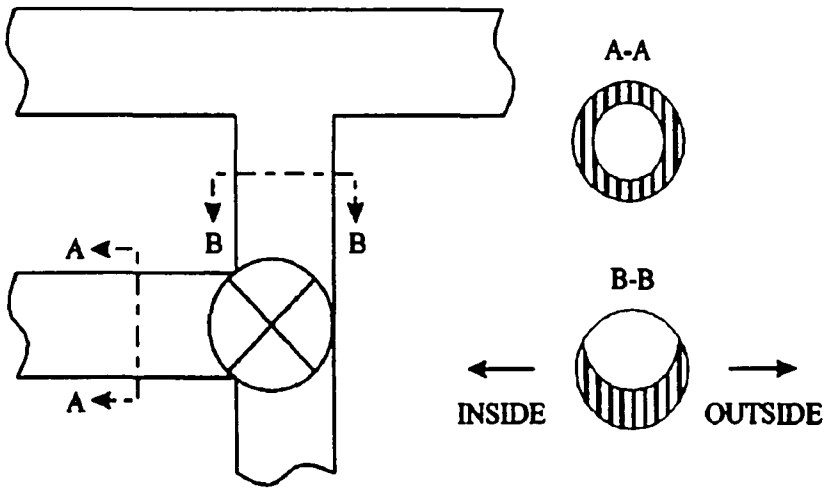

Figure 2.15: Relocation of Melt Top To Bottom [2]

When the material flows from the primary runner through the melt rotation arrangement and into the branched secondary runner, there is symmetry about the vertical axis. This leads to equal amounts of low and high shear material to the inner and outer cavities. This symmetry of melt along a vertical axis is illustrated in Figure 2.16.

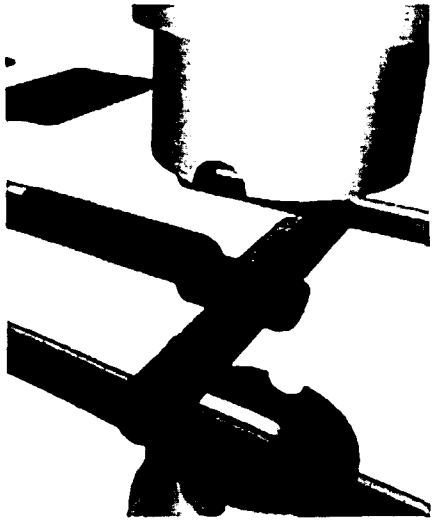

Figure 2.16: Vertical Symmetry of Melt [7]

2.3.2 Results of Melt Rotation

The implementation of melt rotation technology has led to some very promising results. In most cases a perfect fill balance can be achieved as seen in Figure 2.17

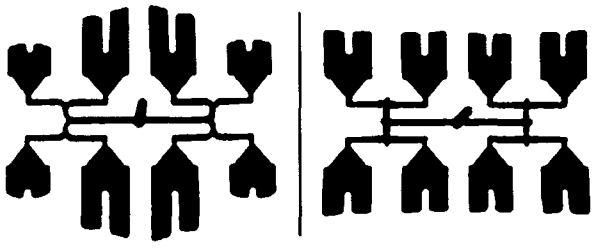

Figure 2.17: Before and After Melt Rotation Technology [7]

In some cases a 100% filling balance was not achieved, but the melt rotation technology was shown to greatly reduce the amount of imbalance as illustrated in Figure 2.18.

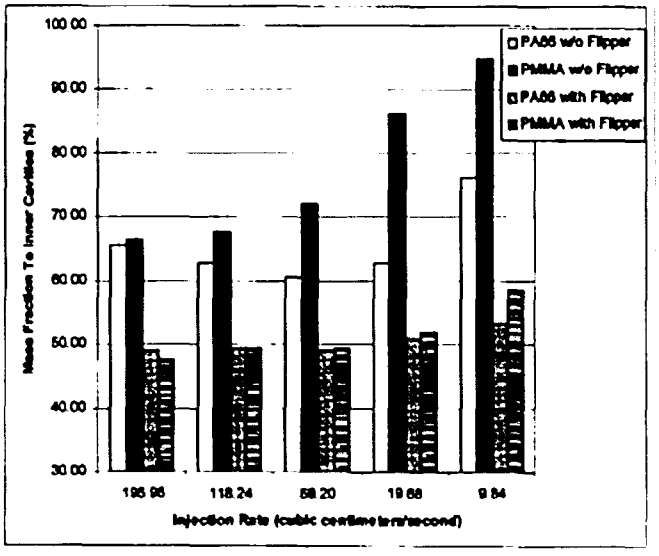

Figure 2.18: Fill Imbalances in Two Materials With and Without Melt Rotation [2]

2.4 Predicting Fill Imbalances

The first injection molding software programs used 2-Dimensional and 2.5-Dimensional meshes to calculate their simulations. Even a larger problem with these programs was the modeling of runner systems. During modeling, runner systems would be modeled as 1-Dimensional elements. The importance of simulating what was occurring in the runner systems was not understood until the shear induced fill imbalance phenomenon was discovered. With this discovery it was determined that 3-Dimensional meshes must be used for these simulations and that runner system must also be meshed with 3-Dimensional elements. There was no 3-Dimensional injection molding software on the market, so extrusion software was first looked at for its capability to simulate the effects shear has in the runner system. Eventually injection molding software was created with the ability to use 3-Dimensional meshes.

2.4.1 Extrusion Software

The flow through a runner channel is comparable to that of flow through an extrusion die. This allows for the used of 3-Dimensional extrusion software to simulate flow through a runner system. The boundary conditions are modified to allow for a cold mold. The shear induced flow imbalances can then be simulated and studied. Figure 2.19 shows results obtained by Ramsey Haylett and David Rhoades [8] using Altair Engineering's HyperExtrude extrusion software.

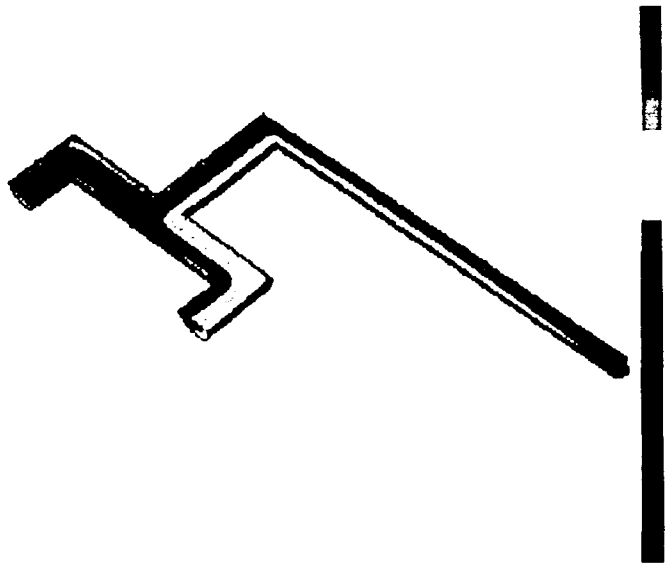

Figure 2.19: Use of HyperExtrude to Simulate Imbalance [8]

2.4.2 Injection Molding Software

Injection molding software packages realized the need for true 3-Dimensional simulations when the importance of the shear created in runner systems was discovered. This resulted in the need for the software producers to create a true 3-Dimenesional simulation program. One of those simulation packages that updated from their 2-Dimensional and 2.5-Dimensional meshes is Moldflow. Figure 2.20 show results obtained by Peter Cook, Huagang Yu, Clinton Kietzmann, and Franco Costa [9] using Moldflow's 3-Dimensional injection molding software package.

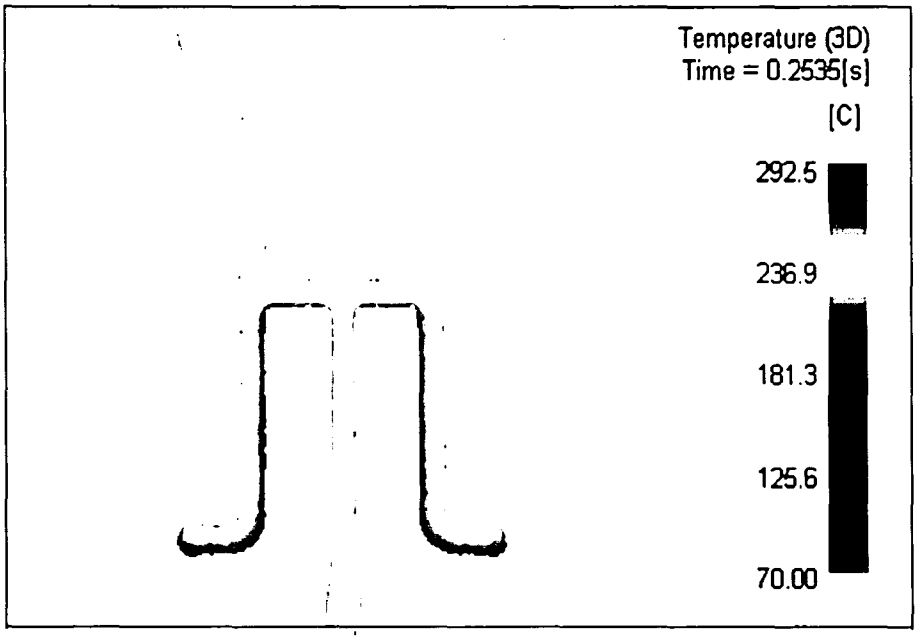

Figure 2.20: Use of Moldflow to Simulate Imbalance [9]

CoreTech System's Moldex3D started as a 3-Dimensional injection molding package. Their software has been used to simulate geometrically balanced runner systems as well as geometrically balanced runner systems designed with melt rotation technology. Figure 2.21 and Figure 2.22 respectively show the simulation results obtained by C.C. Chien, C.C. Chiang, W.H. Yang, Vito Tsai, and David Hsu [10] using Moldex3D.

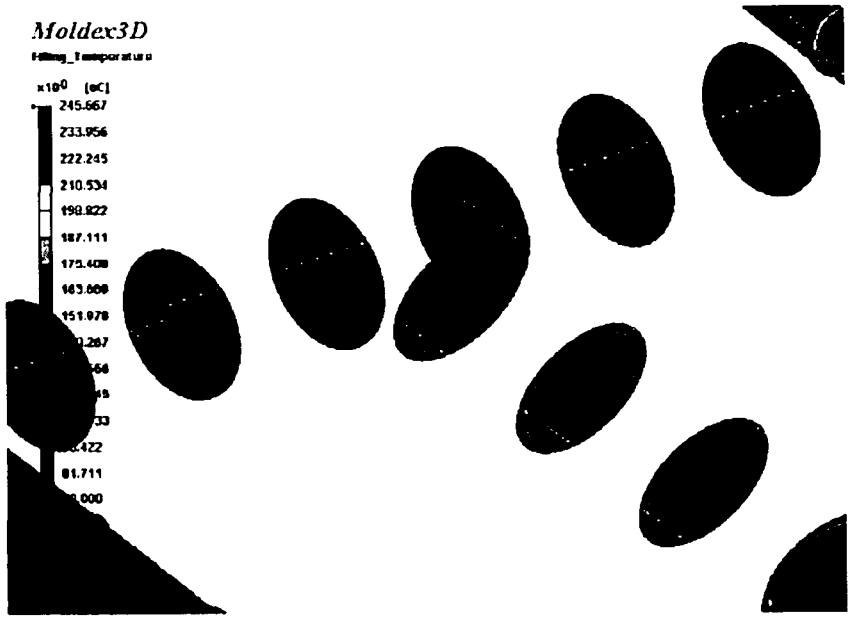

Figure 2.21: Geometrically Balanced Runner System Simulation Using Moldex3D [10]

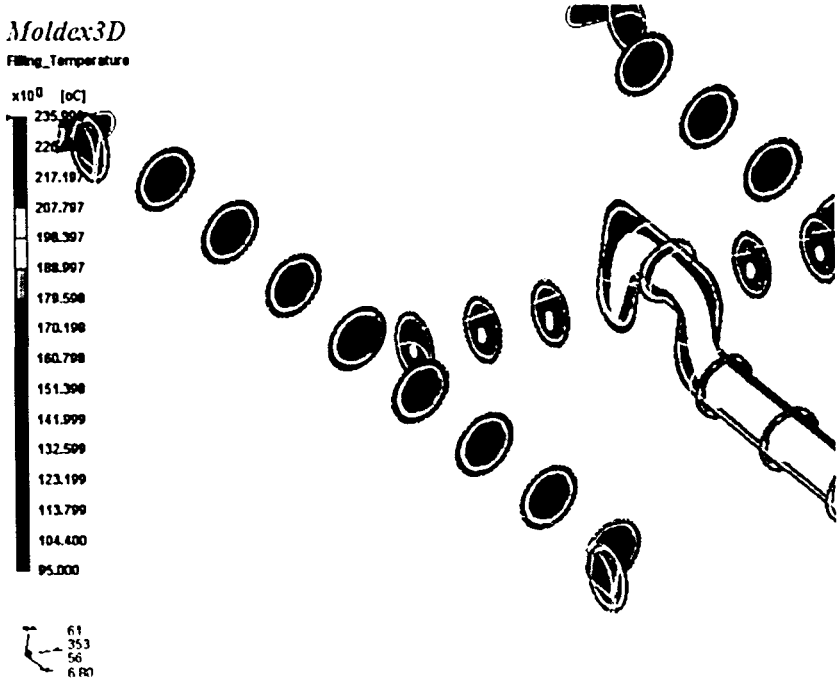

Figure 2.22: Melt Rotation Technology Simulation Using Moldex3D [10]

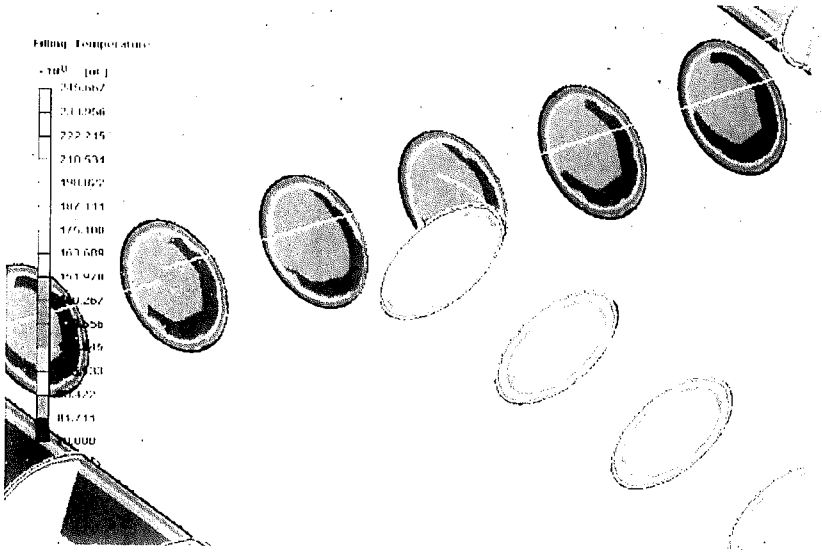

Figure 2.21: Geometrically Balanced Runner System Simulation Using Moldex3D [10]

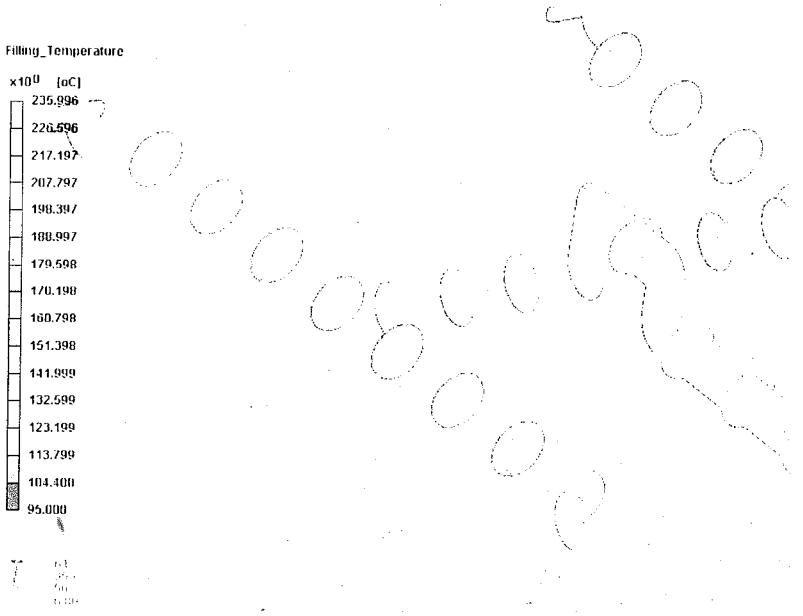

Figure 2.22: Melt Rotation Technology Simulation Using Moldex3D [10]

2.5 Need for Further Studies

Melt rotation technology has proven to be capable of correcting fill imbalances, but there is no one melt rotation technology solution. The amount of rotation differs from mold to mold, process to process, material to material. In order to achieve fill balance the melt rotation needs to be designed and in some cases re-designed. The development of adjustable melt rotation would eliminate the time needed for design and re-design.

The use of CFD software to predict fill imbalances would also help to eliminate the time needed for design and re-design of the melt rotation technology. A runner design could be simulated and the amount of melt rotation could be determined before any steel has been cut. This would eliminate any and all re-designing that a mold may need to achieve a fill balance. Current software packages can simulate the shear induced imbalances, but can not quantitatively calculate the extent of the imbalances. A CFD software that is capable of quantitatively calculating shear induced imbalances is needed in order to help in the design of multi-cavity mold runner systems.

The present research project is aimed at investigating the capabilities of melt rotation technology and CFD software as tools to eliminate fill imbalances and the design complications that occur because of them. The next chapter will cover the attempt to use Polyflow to quantitatively predict shear induced fill imbalances.

3 Numerical Study

Numerical simulations are a helpful tool in the design of molds. They help to predict what will happen in a mold before the mold is even build. This allows for problems associated with injection molding to be fixed before any steel is even cut. Shortly after the discovery of shear imbalances it was discovered that the injection molding simulation software packages on the market were unable to predict this observed phenomenon. Current software packages on the market are capable of predicting shear in the runner systems but are unable to quantitatively predict the effects of the shearing. Without being able to quantitatively predict the shear effects and resulting imbalances the simulations are not as helpful as they could be. The current chapter describes an attempt to use Polyflow, a commercially available CFD software program, to quantitatively predict shear induced fill imbalances.

3.1 Software Selection

As discussed in Chapter 2 leading injection molding software packages like Moldflow [9] and Moldex3D [10] are currently able to predict shear in the runner system to a qualitative extent only. The extrusion software package HyperExtrude [8] has also been used to qualitatively predict shear in a modeled runner system. During the present investigation, the capabilities of another popular commercial polymer processing software package, Polyflow, were explored to see what capabilities it has in predicting shear imbalances.

Polyflow, a software package originally developed in Belgium, is currently a product of the Fluent Corporation. It is an advanced general purpose finite-element-based CFD software created for the analysis of polymer processes. It is well known for its library of viscoelastic fluid models and die design capabilities. Both of these are important to any attempt to simulate runner layouts. The viscoelastic fluid models are needed for simulating polymers and dies are closely related to cold runner systems.

Along with using Polyflow for the simulations, GAMBIT was used to create the 3-Dimension meshes and Fieldview was used for post processing. GAMBIT is Fluent's geometry and mesh generation software. It was chosen for its ability to create a very refined mesh around the perimeter of the runner where the high shear gradients are located. Fieldview was used for its ability to easily take the output files from the Polyflow simulations and create easily understandable graphics of the results.

3.2 Simulations Performed

The first simulations performed using Polyflow were to explore the mesh refinement capabilities available using GAMBIT. GAMBIT would be used to create a basic mesh. Then a finer version of the basic mesh would be created. Finally a refined mesh would be created that had a higher concentration of mesh elements located around the perimeter of the geometry. Running simulations on these three meshes

would benchmark the meshing capabilities of GAMBIT and the results that were obtained by running simulations on the mesh geometries in Polyflow.

The second round of simulations was on the primary runner alone. This was to explore the capabilities of Polyflow to simulate a generalized Newtonian non-isothermal flow. The simulations would predict a multitude of outputs including viscosity, local shear rate, and viscous heating.

The third set of simulations was on an intersection of the primary runner with a branched secondary runner. This was to determine if Polyflow could predict the viscosity gradient in the primary runner and then the subsequent split of low and high viscosity regions into the secondary runner. The simulations were all performed with a focus on localized viscosity, local shear rate, and viscous heating.

3.3 Simulation Results

The results of the simulations performed were not those that were first anticipated. The mesh capabilities of GAMBIT were found to be very good, but the utilization of Polyflow on the resultant meshes was not as successful. The approach to the simulations of the runner design was time after time changed in order to try and obtain useful results from Polyflow. Still Polyflow was unable to converge on a set of results that were significant in the prediction of shear induced flow imbalances.

3.3.1 Mesh Geometry

A simple 1/8" diameter runner was created in GAMBIT. The runner geometry was then meshed with a basic mesh, a finer basic mesh, and then a refined meshed. The three different meshed are shown in Figure 3.1.

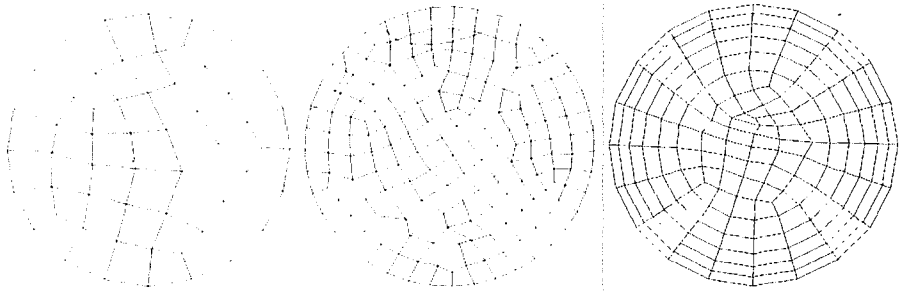

Figure 3.1: Basic Mesh, Finer Basic Mesh, Refined Mesh

The meshes were then imported into Polyflow where a generalized Newtonian non-isothermal flow simulation was run on them. The injection flow rate was 0.00127 m^3/s. The material properties were very general polymer properties because these simulations were just to show the effectiveness of the different meshes. The material properties are found later in the chapter in Table 3-1, where the properties are discussed in more detail.

Figure 3.2 shows the results of the simulations for the normal velocity. The basic mesh results are not as symmetrical as they should be. The finer basic mesh results are definitely better then the basic mesh results but still have its irregularities. The refined mesh results appear to be very symmetrical and uniform.

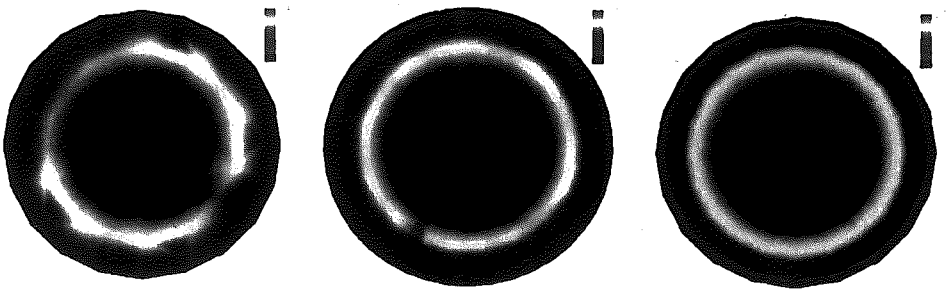

Figure 3.2: Norm Velocity; Basic Mesh, Finer Basic Mesh, Refine Mesh

This is also illustrated in Figure 3.3 which was the simulation results for the local shear rate. Again the refined mesh results are very symmetrical in appearance compared to the two other meshes.

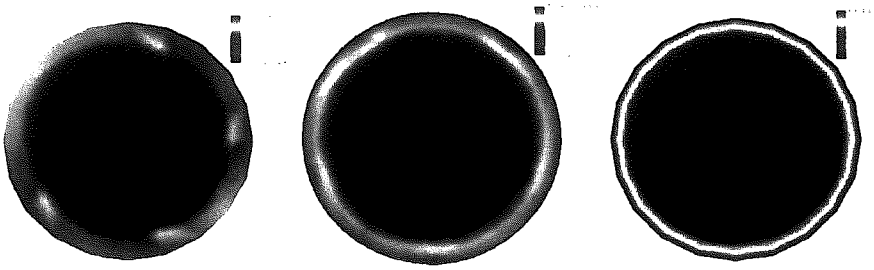

Figure 3.3: Local Shear Rate; Basic Mesh, Finer Basic Mesh, Refine Mesh

Overall these simulations proved GAMBIT was capable of producing a refined mesh that would be useful for the simulation and prediction of shear in the perimeter of the runner.

3.3.2 Primary Runner

The primary runner was created in GAMBIT with a refined cross-sectional mesh configuration throughout its length. Figure 3.4 shows the refined mesh utilized to represent the primary runner.

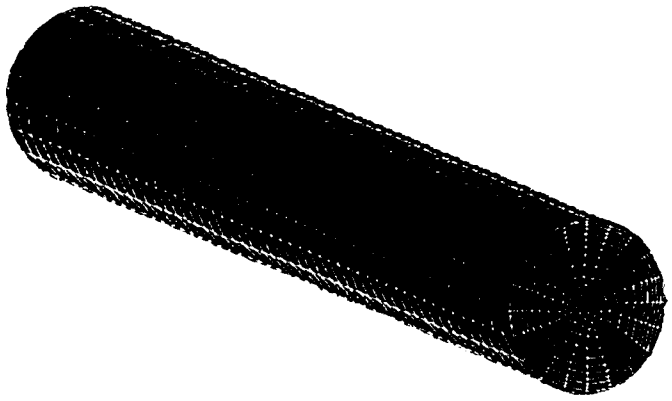

Figure 3.4: Refined Mesh Primary Runner

This mesh was then imported into Polyflow to run simulations of polymer flow through it. Polyflow has a multitude of equations used to simulate the properties of polymers. For these simulations the Cross Law was used to represent the shear-rate-dependent viscosity. The Cross Law is shown in Equation 4 where η represents viscosity, η_0 the zero-shear-rate viscosity, λ the natural time (inverse of shear rate at which the fluid changes from Newtonian to power-law behavior), γ the local shear rate, and m the Cross-law index (1-n).

$$\eta = \frac{\eta_0}{1+[\lambda\gamma]^m} \quad (4)$$

The WLF Law is used to represent the temperature-dependent viscosity. The WLF Law is shown in Equation 5 where c_1 and c_2 represent WLF constants and T_r and T_a are reference temperatures.

$$\ln(H(T)) = \frac{c_1(T_r - T_a)}{c_2 + T_r - T_a} - \frac{c_1(T - T_a)}{c_2 + T - T_a} \quad (5)$$

The material properties that were used were those of a previous experiment [11]. This is because ultimately the results of Polyflow were to be compared to other results that had been found using other programs. Table 3-1 shows the material properties that were used. These properties were corrected in order to be used in the Polyflow equations. This was achieved through derivations performed in MAPLE. The material properties in Table 3-1 are derivate for use in the following equations:

$$\eta(T, \dot{\gamma}) = \frac{\eta_0(T)}{1 + \left(\frac{\eta_0 \dot{\gamma}}{\tau^*}\right)^{1-n}} \quad (6)$$

$$\eta_0(T) = D_1 \exp\left[\frac{-A_1(T - D_2)}{A_2 + (T - D_2)}\right] \quad (7)$$

Material	ABS	PA 66	PP
Grade	GE Cycolac GPM 4700	DuPont Zytel 101 NC010	Amoco PP 1046
Thermal Properties			
Melt Density (kg/m^3)	964.5	1047.	783.9
C_p J/(kg-C)	2295	2900	3100
K W/(m-C)	0.26	0.25	0.15
Rheological Properties			
Cross-WLF			
n	0.279	0.2814	0.311
τ^* (Pa)	6.11E + 04	3.11E + 05	2.38E + 04
D_1 (Pa-s)	2.50E + 13	1.85E + 14	1.40E + 15
D_2 (K)	373.1	323.1	263.1
A_1	31.44	34.27	32.99
A_2 (K)	51.6	51.6	51.6
No Flow Temp. (K)	385	508	455

Table 3-1: Cross and WLF Properties [11]

Polyflow was set to run an evolution on the flow during the simulation. This means the simulation would begin at a fraction of the flow rate and then calculate upwards. This is in order to help make the computations easier. With this the first simulations were performed. Unfortunately the simulations would not run with a cold mold wall temperature, so an adiabatic condition was applied to the runner perimeter. This boundary condition can be reasoned because of the insulation properties of

polymers and the fact that injection through a runner system is normally extremely fast. With the use of an adiabatic condition the simulations would converge, but only if viscous heating was not taken into account. In order to get the results that were originally trying to be determined, viscous heating had to be taken into account. Simulations taking viscous heating into account were run, but they never converged. Multiple parameters were controlled with an evolution parameter, but still convergence could not be obtained. Figure 3.5 and 3.6 show the best result obtained while simulating the primary runner.

Figure 3.5: Norm Velocity Primary Runner; Flow Rate = 0.00127 m^3/s

Figure 3.6: Local Shear-Rate Primary Runner; Flow Rate = 0.00127 m^3/s

Multiple material properties such as velocity, melt temperatures, and even Cross and WLF parameters were changed in order to try and produce results that converged. This was done in order to see if there was an oversight or glitch in the program, but still no significant results were obtained.

3.3.3 Primary and Secondary Runner

An intersection of a primary runner with a branched secondary runner was created in GAMBIT with a refined mesh along the perimeter of the runner. Symmetry was used in order to minimize the number of elements which in turn would limit the number of calculations during simulation. Figure 3.7 shows the resulting mesh of the primary and secondary runner intersection.

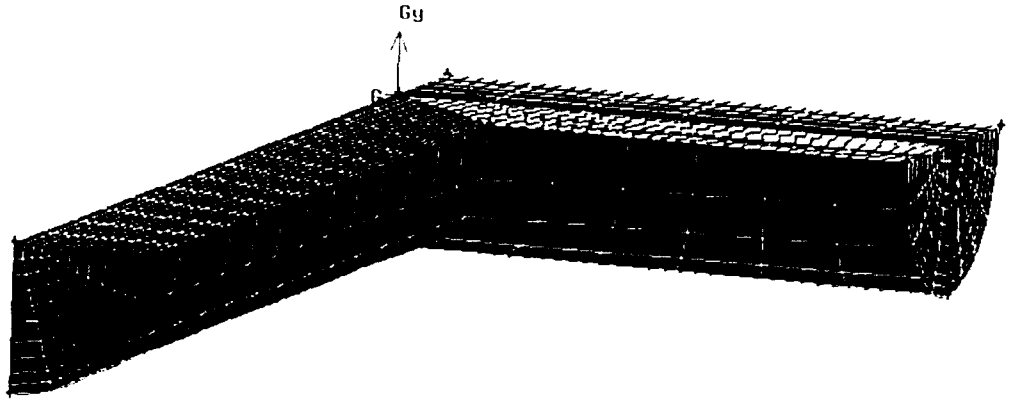

Figure 3.7: Primary and Secondary Runner Intersection

As before with the primary runner simulations a number of attempts were made to try and get flow results that converged. Parameters where changed and altered, but still convergence could not be obtained. The simulations did show some promise of the capability to predict shear imbalances, but concrete quantitative results

were never obtained. Polyflow was able to show the crescent moon that was expected after the splitting of the melt into the secondary runner, but for some unexplainable reason further down the secondary runner the amount of shear would be symmetrical again. This is illustrated in Figure 3.8 and 3.9.

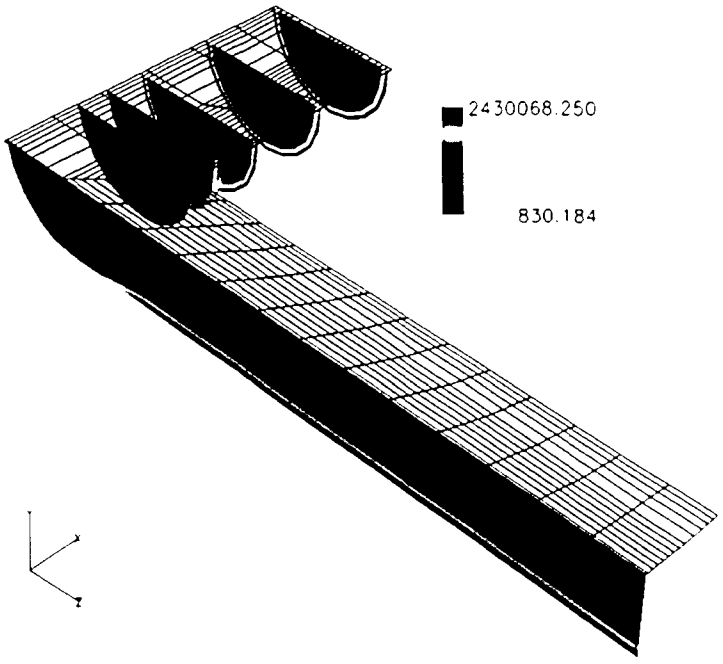

Figure 3.8: Local Shear-Rate Primary and Secondary Runner; Crescents; Flow Rate = 0.00127 m^3/s

Figure 3.9: Runner Sections from Intersection to End of Secondary Runner

Figure 3.10 and Figure 3.11 show the best results obtained for the primary and secondary runner intersection. Both show what would be expected of higher values near the intersection of the primary and secondary runners.

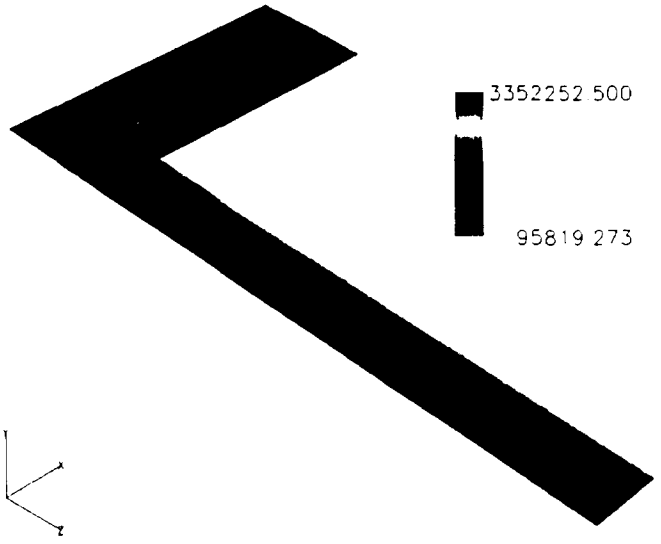

Figure 3.10: Local Shear-Rate Primary and Secondary Runner; Flow Rate = 0.00127 m^3/s

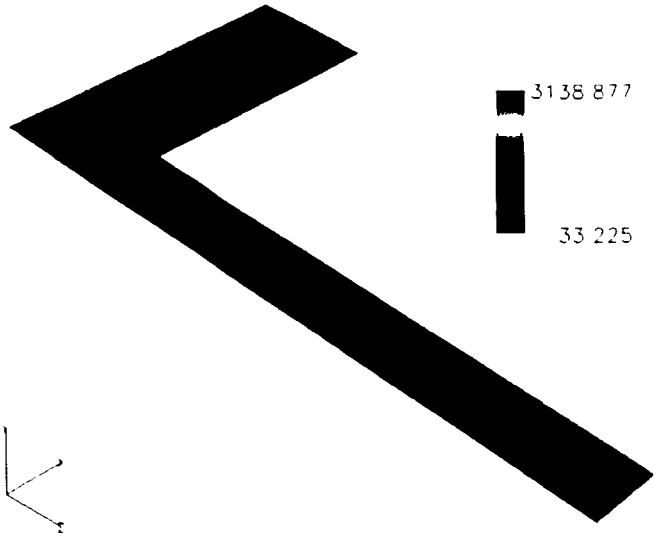

Figure 3.11: Viscous Heating Primary and Secondary Runner; Flow Rate = 0.00127 m^3/s

As seen in Figure 3.10 symmetry seemed to cause some irregularities in the simulation. A full runner geometry of the primary and secondary runner intersection was then created, but again roughly the same results were found. Figure 3.12 shows an example of results seen with the full runner.

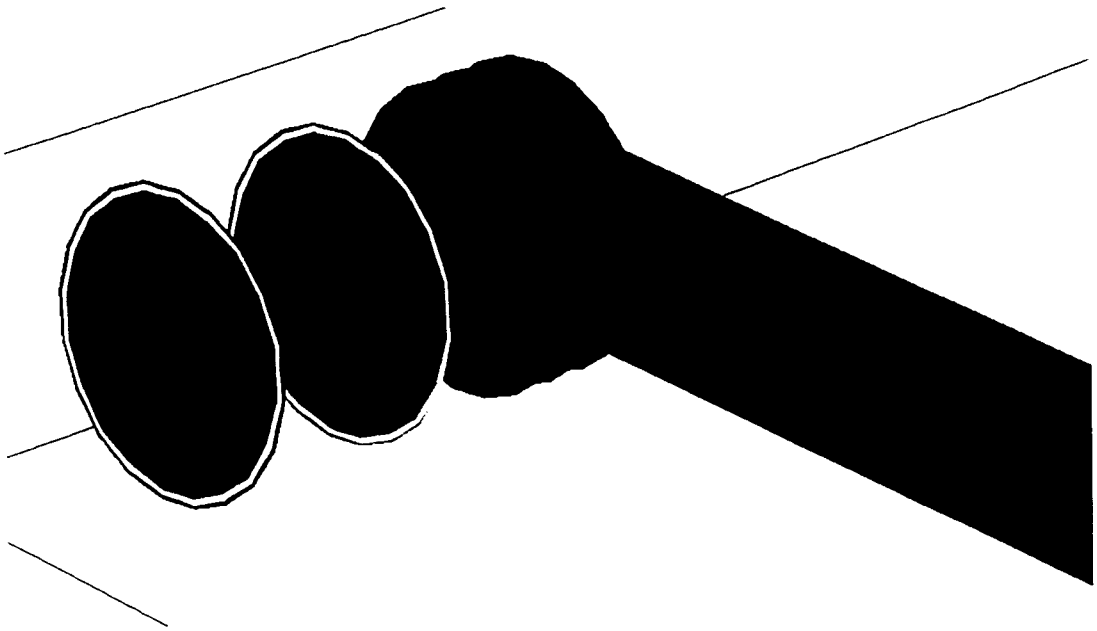

Figure 3.12: Full Runner Shear-Rate Simulation; Flow Rate = 0.00127 m^3/s

4 Experimental Study of Adjustable Melt Rotation

As stated earlier a primary goal of the investigation was to test the capabilities of adjustable melt rotation technology. A customized set of adaptable tooling was designed and fabricated to explore this concept. In the current chapter, the machinery used to perform these experiments will be described, along with the mold and its re-configurable inserts. The mold inserts formed the basis of the experiments. The inserts allowed for pins to be used to control the land height of the melt rotation. This control of land height allowed for the melt rotation to be adjustable.

During the study testing was performed with four different polymers. Different injection velocities and other processing conditions were applied with each material. Details related to the resultant experimentation protocol follow.

4.1 Machinery

All of the machinery used in this experiment is located in Lehigh University's Manufacturing Science Laboratory (MSL) in Packard Lab at the Lehigh University's ASA Packer Campus. The injection molding machine used this experiment was a Boy 15 S as pictured in Figure 4.1.

Figure 4.1: Injection Molding Machine Boy 15 S

The Dryer used to dry the materials before processing was a Dri-Air Industires DRI-AIR 2000 and the thermolator used for mold temperature control was a Thermal Care / Mayer VTC 9. These units are pictured in Figure 4.2.

Figure 4.2: DRI-AIR 2000 Dryer and VTC 9 Thermolator

In order to determine the injection velocity applied, a Linear Variable Differential Transformer (LVDT) (a DCT 2000 manufactured by the RDP Group) was obtained and connected to the injection screw apparatus. Labview 8.0 was used to collect all data. Figure 4.3 shows a picture of the LVDT and a screen shot of the associated Labview display.

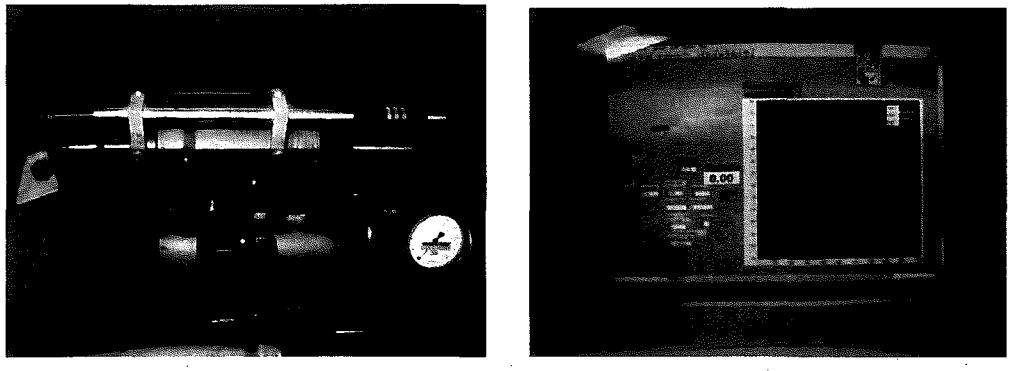

Figure 4.3: DCT 2000 LVDT and Labview 8.0

Melt flow imbalances were studied by weighing resulting products using an Acculab VIC-303. This scale has an accuracy to 0.001 grams. The scale utilized is shown in Figure 4.4.

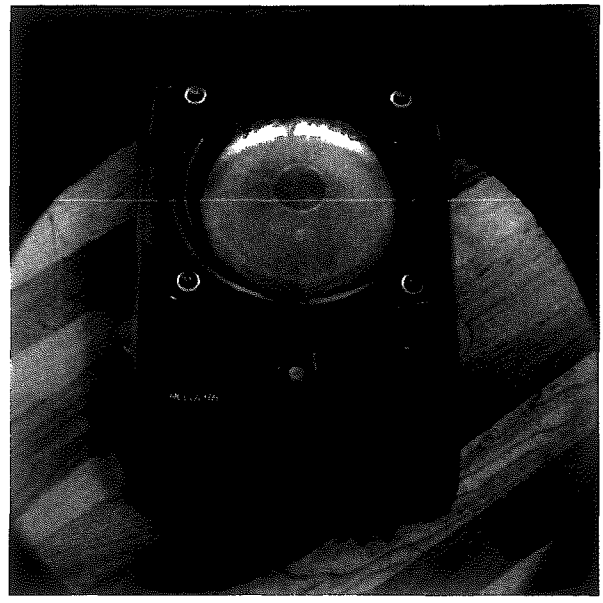

Figure 4.4: Acculab VIC-303 Scale

4.2 Reconfigurable / Adjustable Tooling Development

The mold used in this experiment was custom designed and fabricated for the present study. It utilizes a mold base that has easily inserted and interchangeable mold plates. The mold base measures 16" x 8' and is the largest sized mold that can be used on the Boy 15 S. The mold base accepts plates of 8.315" in length, 5.062" in width. The mold base can accept plate thicknesses of 0.5" to approximately 1.5". The mold base and plates can be seen in Figure 4.5 and Figure 4.6.

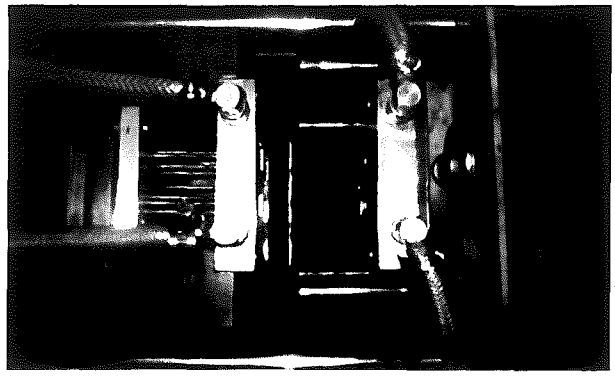

Figure 4.5: Top View of Mold and Plates

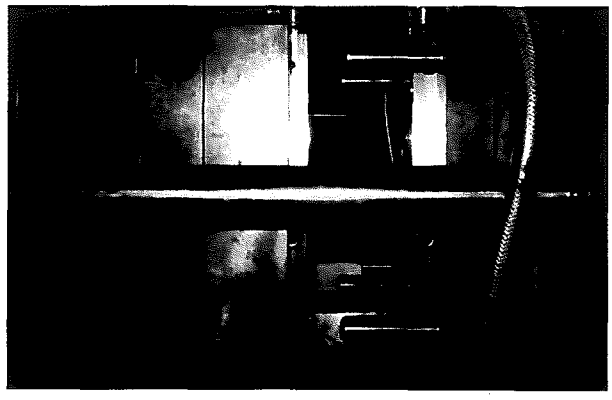

Figure 4.6: Side View of Mold and Plates

The plates located at the mold parting line in the above pictures; they also have the cooling lines connected to them. The plate located on the right hand side of the mold parting line is considered the A plate. The plate located on the left hand side of the mold parting line is considered the B plate.

Due to size constraints only half of an eight cavity mold was designed into the mold plates. The resulting four cavity mold, however, was geometrically balanced and contains a primary, secondary, and tertiary runner system identical to those found in typical eight cavity molds. Inserts were used on both the A and B plates for both the primary and secondary runner split. The inserts allowed for testing with both the adjustable melt rotation system and a traditional runner system. The mold plates and inserts were fabricated out of P-20 steel. CAD drawings of all mold plates and inserts are located in Appendix A – Mold and Insert Drawings.

4.2.1 Mold Plate A

Mold plate A was designed to have the sprue opening located in it. It also has the gates machined into it. The gates are a fan gate design and were chosen because they cause minimal fill resistance. Also machined in mold plate A is a pocket for the mold plate A insert. Finally there are cooling lines that allow for even cooling to all four cavity faces. Figure 4.7 is a picture of the Mold Plate A face.

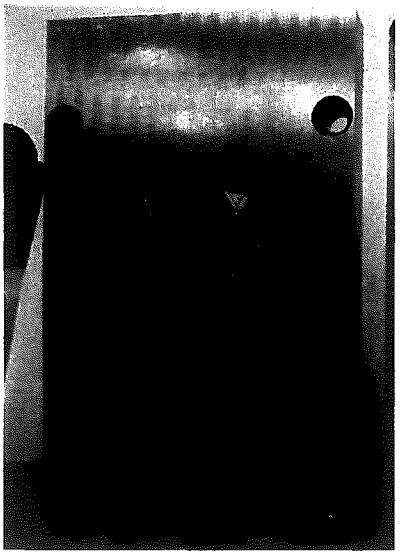

Figure 4.7: Mold Plate A

4.2.2 Mold Plate B

Mold plate B was designed to have the four cavities machined into it. These cavities were designed to show the progression of the flow fronts into each of them during a short shot. A long, narrow, and thin rectangular cavity is used in order to show the differences in filling of each cavity. Each of the four cavities in the mold is of the same dimensions; 0.75" wide, 1.5" long, and 0.1" deep. Each cavity was engraved with flow group markings in order to make data collection easier. The sections of runner from the sprue puller to the mold plate B insert and from mold plate B insert to each cavity were also machined in mold plate B. The runner design selected was a modified parabolic runner that is 0.125" deep with 10° tapered side walls. Ejector pin holes were located throughout mold plate B to allow for ejection of the parts after the molding cycle. Also machined in mold plate B was a pocket for a

mold plate B insert. Finally there were cooling lines allowed for even cooling to all four cavities during processing. Figure 4.8 is a picture of the Mold Plate B face.

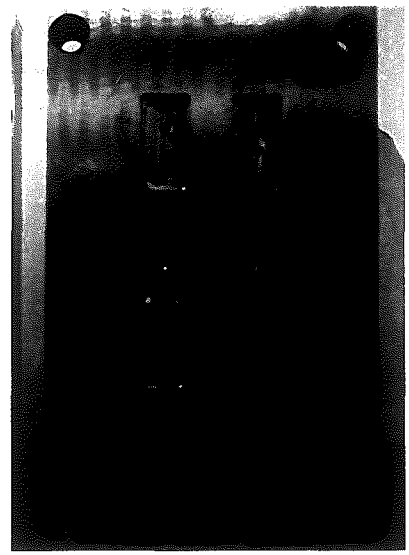

Figure 4.8: Mold Plate B

4.2.3 Insert Design

As stated, centrally located in the mold plates are pockets for the placement of runner channel inserts. Sets of inserts were designed and fabricated to yield adjustable melt rotation as well as standard runner channels.

Adjustable melt rotation is achieved by varying the height of the melt rotation geometry. By increasing the height of the melt rotation geometry from zero to the height of the runner diameter, the degree of melt rotation increases from no melt rotation to full melt rotation. Partial melt rotation is considered any degree of melt rotation between zero and full melt rotation. Figure 4.9 depicts the differences in melt rotation geometry from no melt rotation to full melt rotation.

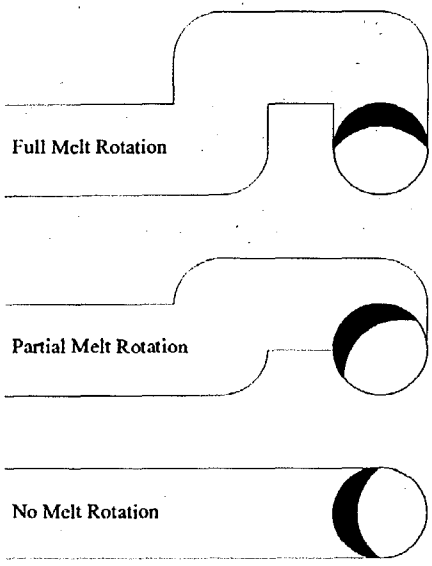

Figure 4.9: Melt Rotation Geometry Diagram [13]

4.2.3.1 Adjustable Melt Rotation A Plate Insert

The A plate insert (Figure 4.10) for the adjustable melt rotation allows for polymer transfer within the runner from the B plate past the parting line and into the A plate. There are three areas of melt rotation located in the melt rotation insert set. The first melt rotation is located at the split of the primary runner into the secondary runner. This is the position of the adjustable melt rotation. The A plate insert contains a 0.125 deep runner in the location of the first split. The full runner on the A plate insert allows for the potential of full melt rotation. The second and third melt rotations are located at the split of the secondary runner into the tertiary runner. Melt rotations at these two locations were fixed at the half rotation level. Runners in the A

plate insert for these two locations are therefore only half as deep as a full runner or 0.0625".

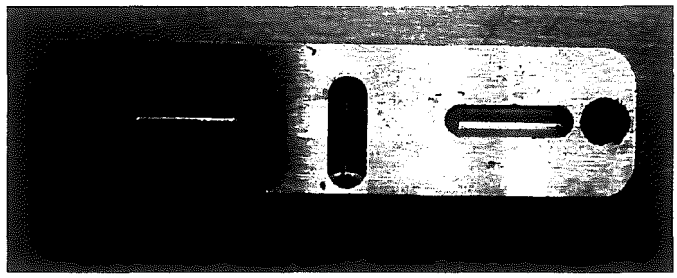

Figure 4.10: Adjustable Melt Flipper Insert A Plate

4.2.3.2 Adjustable Melt Rotation B Plate Insert

The adjustable melt rotation B plate insert (Figure 4.11) is used in conjunction with the adjustable melt rotation A plate insert. As mentioned previously, the adjustable melt rotation insert pair contains three melt rotations. Two fixed melt rotations are located at the split of the secondary runner into the tertiary runners. The rotation is created by a change in runner depth at these locations from 0.125" depth to 0.0625" depth forcing melt above the parting line. The third melt rotation is located at the split of the primary into the secondary runner. This is the location of the adjustable melt rotation.

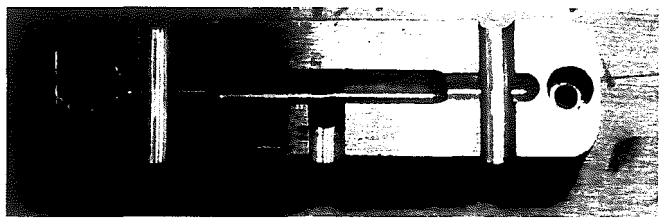

Figure 4.11: Adjustable Melt Rotation Insert B Plate

The rotation can be adjusted through the use of core pins varying in exposed height from 0.0" to 0.125" in approximately 0.020" increments. The core pins are placed in the thru hole at the intersection of the primary and secondary runners. The resulting different melt rotation settings are referred to as melt rotation 0 through melt rotation 6. Melt rotation 0 represents a pin even with the runner floor. Melt rotation 1 represents a pin height of 0.025" above the runner floor; melt rotation 2, a pin height of 0.045"; melt rotation 3, a pin height of 0.065'; melt rotation 4, a pin height of 0.085"; and melt rotation 5, a pin height of 0.105". Finally, melt rotation 6 represents a pin height of 0.125" above the runner floor. The pins used to achieve these different degrees of melt rotation are displayed in Figure 4.12.

Figure 4.12: Adjustable Melt Flipper Pins

4.2.3.3 Standard A Plate Insert

The standard A plate insert (Figure 4.13) is designed to replicate the A side plate of a typical runner system. The insert does not allow for any transfer of polymer melt past the parting line.

Figure 4.13: Standard A Plate Insert

4.2.3.4 Standard B Plate Insert

The standard B plate insert (Figure 4.14), much like the A plate insert, is designed to replicate a typical runner system without melt rotation technology. The runner system remains at 0.125" depth through the primary and secondary split. Both the standard A and B plate inserts will be used to benchmark against the adjustable melt rotation results.

Figure 4.14: Standard B Plate Insert

4.3 Materials Studied

Filling imbalances fluctuate based upon the material being molded. Each material has varying fill imbalance results. Therefore it is important to try and test a range of polymers in order to observe the varying fill imbalances. This will help

Figure 4.13: Standard A Plate Insert

4.2.3.4 Standard B Plate Insert

The standard B plate insert (Figure 4.14), much like the A plate insert, is designed to replicate a typical runner system without melt rotation technology. The runner system remains at 0.125" depth through the primary and secondary split. Both the standard A and B plate inserts will be used to benchmark against the adjustable melt rotation results.

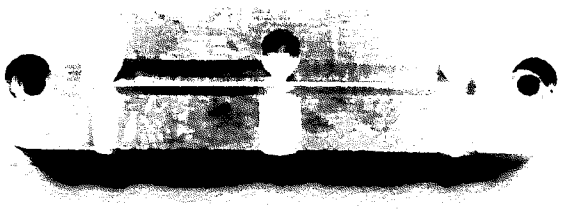

Figure 4.14: Standard B Plate Insert

4.3 Materials Studied

Filling imbalances fluctuate based upon the material being molded. Each material has varying fill imbalance results. Therefore it is important to try and test a range of polymers in order to observe the varying fill imbalances. This will help

contribute to the science base on how different materials respond to shear rates and to melt rotation technology. For this experiment four materials were chosen based on time considerations and material availability. These Materials are listed in Table 4-1.

Material	Abbreviation	Manufacturer
Polycarbonate	PC	Dow Chemicals USA
Polypropylene	PP	Basell Polyolefins
Polyamide 6	PA 6	BASF Corporation
Polybutylene Terephthalate	PBT	Ticona

Table 4-1: Materials Studied

The first material chosen was PC or polycarbonate. This material is an amorphous polymer with exceptional impact resistance, heat distortion resistance, and optical clarity. Its applications are in appliances, storage, electrical components, and lighting. PC is known to exhibit a high sensitivity to flow imbalances [12].

PP or Polypropylene was the second material. This material is semi-crystalline and considered a commodity plastic. It is known for its clarity, good stiffness, high level of cleanliness, and excellent organoleptic properties. It is used in food packaging, and reusable containers of various types. During previous experiments, PP has show a unique "reverse" fill imbalance where the outer cavities fill sooner then the inner cavities [2].

The third material used in this experiment was PA 6, Polyamide 6, better known as Nylon 6. Nylon 6 is an amorphous polymer that has good thermal and chemical properties, good strength, and stiffness retention. It is used in auto parts, machine parts, tubing, and fibers. In previous studies, Nylon 6 has shown a high sensitivity to flow imbalances [2].

The final material selected was polyester, PBT or Polybutylene Terephthalate. It is a semi-crystalline with excellent hydrolysis resistance, mechanical properties and processability. PBT is mostly used as an insulator in the electrical and electronics industries. PBT has shown a high sensitivity to flow imbalances in previous studies [2].

Once the polymers were selected it was next necessary to choose a particular manufacturer and grade of each material. There are numerous companies that produce the materials and that offer a wide variety of grades. Each grade offers different material properties and other features. Some of these features are additives such as color, glass, and other fillers. The four materials used in this experiment were:

- Dow Chemicals USA Calibre 300 EP-22 Polycarbonate (PC)
- Basell Polyolefins Purell X50109 Polypropeylene (PP)
- BASF Corporation Capron 8253 HS Polyamide 6 (PA 6)
- Ticona Celanex 3309 HR Polybutylene Terephthalate (PBT)

All of the materials are basic with no fillers except for the PBT. The PBT is the only one with an additive. The grade of PBT used in this study was filled with 30% glass.

4.4 Trials

Each of the four materials was tested at three different injection rates. These injection rates were:

1. Low Injection Rate
2. Medium Injection Rate

3. High Injection Rate

For each of these injection rates eight different runner layouts were used. These Runner Layouts were:

1. Normal Geometrically Balanced Runner
2. Melt Rotation 0, pin even with runner floor
3. Melt Rotation 1, pin height of 0.025" above runner floor
4. Melt Rotation 2, pin height of 0.045" above runner floor
5. Melt Rotation 2, pin height of 0.065" above runner floor
6. Melt Rotation 2, pin height of 0.085" above runner floor
7. Melt Rotation 2, pin height of 0.105" above runner floor
8. Melt Rotation 2, pin height of 0.125" above runner floor

In summary there were 24 runs of parts for each of the four materials.

4.5 Process Conditions

Parameters such as nozzle temperature, front zone temperature, rear zone temperature, mold temperature, injection time, cooling time, and injection pressure throttle position were determined for each material. All temperatures were determined from each materials data sheet. The times were selected to allow more then enough time for each stage of the injection molding process. Injection pressure throttle positions were determined by finding the capabilities to produce parts using the already set temperatures and times. The position of the injection pressure throttle

coincides with the injection velocity. Table 4-2 to Table 4-5 summarize all of these processing conditions for each of the materials.

Injection Speed	Low	Medium	High
Nozzle Temperature (°C)	270	270	270
Front Zone Temperature (°C)	270	270	270
Rear Zone Temperature (°C)	260	260	260
Mold Temperature (°C)	65	65	65
Injection Time (sec)	20	20	20
Cool Time (sec)	10	10	10
Injection Pressure Throttle Position	6.3	6.9	7.5

Table 4-2: PC Processing Conditions

Injection Speed	Low	Medium	High
Nozzle Temperature (°C)	230	230	230
Front Zone Temperature (°C)	230	230	230
Rear Zone Temperature (°C)	220	220	220
Mold Temperature (°C)	30	30	30
Injection Time (sec)	20	20	20
Cool Time (sec)	10	10	10
Injection Pressure Throttle Position	2.0	3.0	4.0

Table 4-3: PP Processing Conditions

Injection Speed	Low	Medium	High
Nozzle Temperature (°C)	235	235	235
Front Zone Temperature (°C)	250	250	250
Rear Zone Temperature (°C)	245	245	245
Mold Temperature (°C)	65	65	65
Injection Time (sec)	20	20	20
Cool Time (sec)	10	10	10
Injection Pressure Throttle Position	3.5	4.5	5.5

Table 4-4: PA 6 Processing Conditions

Injection Speed	Low	Medium	High
Nozzle Temperature (°C)	250	250	250
Front Zone Temperature (°C)	250	250	250
Rear Zone Temperature (°C)	240	240	240
Mold Temperature (°C)	75	75	75
Injection Time (sec)	20	20	20
Cool Time (sec)	10	10	10
Injection Pressure Throttle Position	4.5	6.0	7.5

Table 4-5: PBT 30% Glass Filled Processing Conditions

With all of the major processing conditions determined a shot size was determined that would have the lead cavity filling 70-80%. The V/P switchover was set, and the screw recovery position was adjusted until this desired shot size was achieved. All other processing conditions were kept the same for all four materials and were never changed during the length of this experiment. The PC, PA 6, and PBT all needed to be dried before processing. The PC was dried for 4 hours at 120°C, PA 6 was dried at 85°C for four hours, and PBT was dried at 120°C for 4 hours.

4.6 Collection of Data

For each trial, beginning with the traditional runner and proceeding all the way to melt rotation 6, and for each injection velocity with each material, 15 parts were collected. The first 5 parts were thrown away; these parts were run in order to stabilize the process. Then the next 10 parts were collected in order to be weighed for this experiment. Parts were labeled in order to be identified later during the weighing process. Also during the production of parts, the LVDT using LabView recorded data in order to calculate the injection rates for each trial.

The injection flow rate was determined by examining the LVDP data that was collected using LabView. A data point 1 was chosen; this data point had a position and time. Then data point 2 was chosen; also with a position and time. The difference between data point 2 and data point 1 was taken for both position and time. Then the distance traveled was divided by the time it took to travel that distance. This resulted

in an injection rate. The injection rate was then multiplied by the area of the injection barrel and an injection flow rate was determined.

After the experiment the parts were de-gated and weighed. The inner cavities were individually weighed and then their weights were added together to create a weight for Flow Group A. The outer cavities were individually weighed and then their weights were also added together to create a weight for Flow Group B. Then all four part weights were combined to determine the total weight of the parts. Both Flow Group A and Flow Group B were divided by the total weight of the parts in order to determine the percentage of total part weight for each flow group. Then the Flow Group B percentage (outer cavities) was subtracted from the Flow Group A percentage (inner cavities) to determine the fill imbalance between the cavities. Chapter 5 will present all of the data collected and discuss the different characteristics that were observed.

5 Adjustable Melt Rotation Results

This chapter will present all of the results from the trial adjustable melt rotation runs for all four materials. Graphs will illustrate the differences between degree of melt rotation and use of a standard runner for a set injection velocity. Then the results from the different injection velocities will be compared. These plots will show the different characteristics observed for each of the tested materials. Specimen weights for each trial can be found in the Appendices B through E.

5.1 Results for Polycarbonate (PC)

During testing, molding conditions were established so that the leading cavity was approximately 70-80% filled. The shot size was then held constant throughout the remainder of the testing. At each injection rate testing was conducted using a traditional runner system as well as the adjustable melt rotation system at each of its seven settings. The settings are referred to as melt rotation 0 through melt rotation 6. After the process had stabilized, ten parts were collected for each of the injection speeds and runner settings. Specimen weights for each trial can be found in Appendix B – Test Results for PC.

5.1.1 Low Injection Rate

The average flow rate for the lowest injection rate, as determined by a distance profile, is summarized in Table 5-1. As calculated the average injection rate

of the low injection rate for PC was 14.24 cc/s. All process settings were maintained during the testing process with the low injection rate.

	Time (s)	Position (mm)	Time (s)	Position (mm)	Time (s)	Position (mm)
Point 1	5.04	10.613	4.48	11.569	14.12	11.808
Point 2	5.28	18.214	4.72	18.596	14.32	18.501
Difference	0.24	7.601	0.24	7.027	0.2	6.693
Injection Rate (mm/s)		31.67		29.28		33.46
Area of Barrel (mm^2)		452.39		452.39		452.39
Injection Flow Rate(mm^3/s)		14327.57		13245.60		15139.23
Injection Flow Rate (cc/s)		**14.33**		**13.25**		**15.14**
Average (cc/s)	**14.24**					

Table 5-1: PC Low Flow Rate Calculation

Figure 5.1 shows specimens resulting from the testing. The top left specimen is a representative result obtained with the traditional runner insert. As can be seen, the inner cavities filled first with the traditional runner system with no melt rotation applied. The seven additional product tree specimens included in the figure were obtained with melt rotation settings 0 through 6. Using a traditional runner it is seen that there is a fill imbalance between the inner and outer cavities, with the inner cavities filling first. This was an expected result. Melt rotation levels 0 through 3 then qualitatively appeared to lead to more balanced filling of the four product cavities. Further levels of melt rotation (4, 5, and 6), however, actually generated a "reverse" fill imbalance where the outer cavities actually filled prior to the inner cavities.

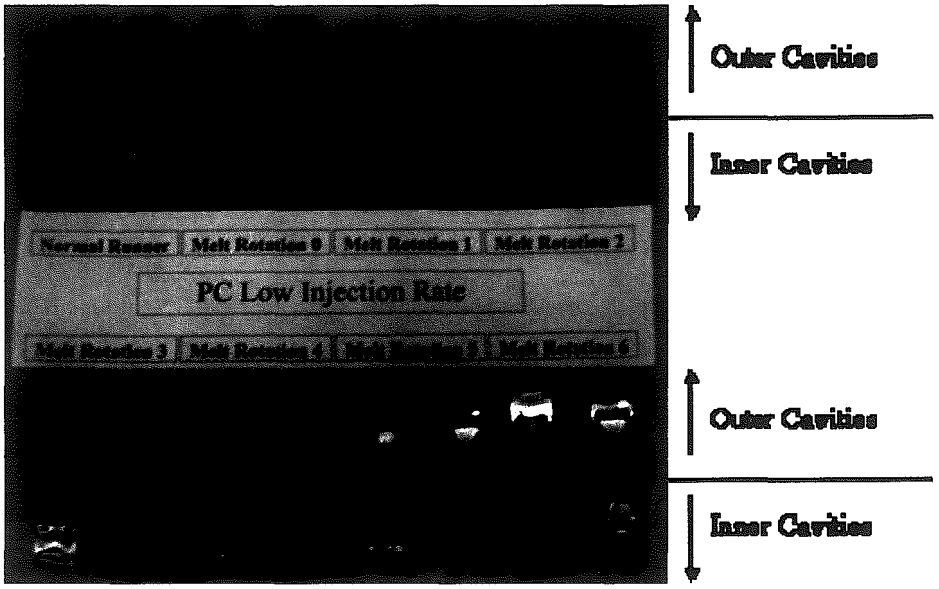

Figure 5.1: PC Test Specimens at Low Injection Rate

	Flow Group A (Inner) Average Weight (g)	Flow Group B (Outer) Average Weight (g)
Traditional Runner	2.965	2.701
Melt Rotation 0	2.630	3.043
Melt Rotation 1	2.551	2.971
Melt Rotation 2	2.480	2.978
Melt Rotation 3	2.512	3.010
Melt Rotation 4	1.878	2.685
Melt Rotation 5	1.788	2.680
Melt Rotation 6	1.513	2.436

Table 5-2: PC Low Injection Rate Flow Groups Average Weights

The quantitative results are presented in Table 5-2. The graph in Figure 5.2 displays the relative difference in the inner vs. outer cavity average product weights for the eight runner systems studied. From the figure it can be seen for the low injection rate the normal runner and melt rotation 0 provides the closest fill balance between the inner and outer cavities. Though the traditional runner had the inner cavities with more fill and melt rotation 0 had the outer cavities with more fill. The

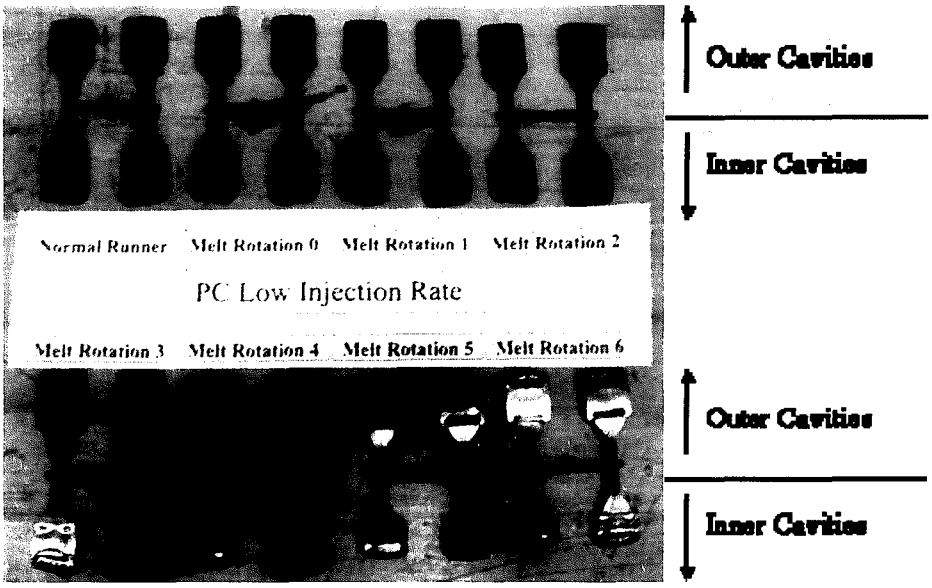

Figure 5.1: PC Test Specimens at Low Injection Rate

	Flow Group A (Inner) Average Weight (g)	Flow Group B (Outer) Average Weight (g)
Traditional Runner	2.965	2.701
Melt Rotation 0	2.630	3.043
Melt Rotation 1	2.551	2.971
Melt Rotation 2	2.480	2.978
Melt Rotation 3	2.512	3.010
Melt Rotation 4	1.878	2.685
Melt Rotation 5	1.788	2.680
Melt Rotation 6	1.513	2.436

Table 5-2: PC Low Injection Rate Flow Groups Average Weights

The quantitative results are presented in Table 5-2. The graph in Figure 5.2 displays the relative difference in the inner vs. outer cavity average product weights for the eight runner systems studied. From the figure it can be seen for the low injection rate the normal runner and melt rotation 0 provides the closest fill balance between the inner and outer cavities. Though the traditional runner had the inner cavities with more fill and melt rotation 0 had the outer cavities with more fill. The

results also show the minimum and maximum values for each runner setting. The standard deviation of the results ranged from 0.41% to 1.06% for each of the Melt Rotation settings.

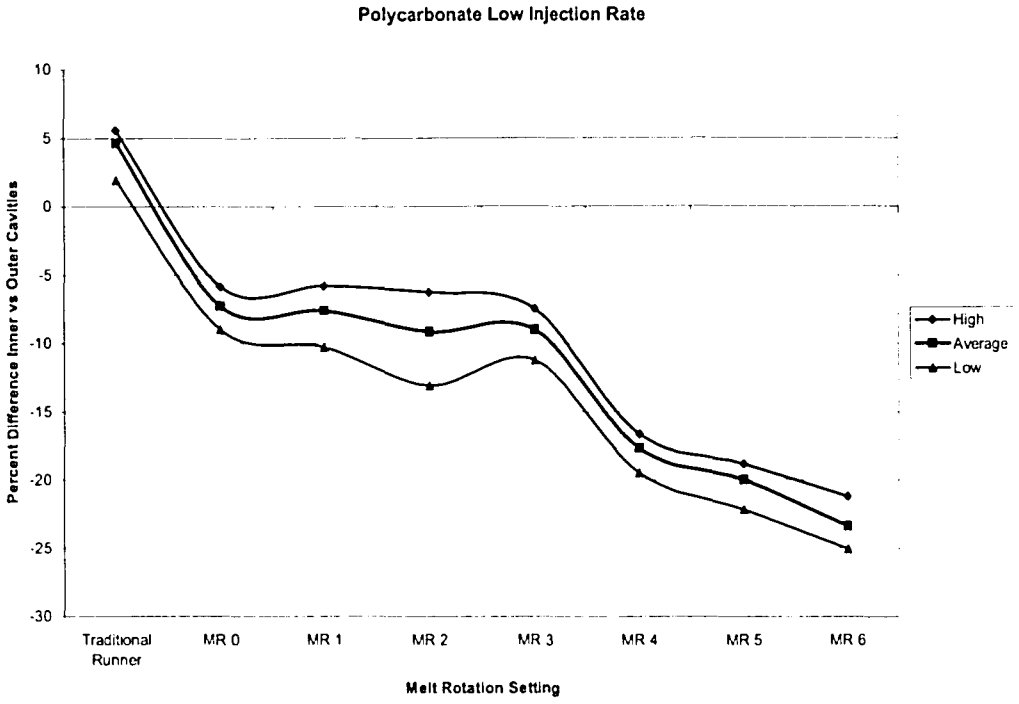

Figure 5.2: PC Test Results; Low Injection Rate

5.1.2 Medium Injection Rate

The average flow rate for the medium injection rate, as determined by a distance time profile, is summarized in Table 5-3. As calculated the average injection rate of the medium injection rate for PC was 19.96 cc/s. Once this was determined, all process settings were maintained at fixed levels throughout the remainder of testing with this medium level injection rate.

	Time (s)	Position (mm)	Time (s)	Position (mm)	Time (s)	Position (mm)
Point 1	4.4	11.808	4.64	10.756	4.4	13.481
Point 2	4.56	18.644	4.8	18.309	4.48	16.875
Difference	0.16	6.836	0.16	7.553	0.08	3.394
Injection Rate (mm/s)		42.73		47.21		42.43
Area of Barrel (mm^2)		452.39		452.39		452.39
Injection Flow Rate(mm^3/s)		19328.36		21355.64		19192.65
Injection Flow Rate (cc/s)		**19.33**		**21.36**		**19.19**
Average (cc/s)	**19.96**					

Table 5-3: PC Medium Flow Rate Calculation

Figure 5.3 shows specimens from testing at the medium injection rate. Using a traditional runner it is seen that there is a fill imbalance between the inner and outer cavities, with the inner cavities filling first. This is a similar result to the low injection rate. Melt rotation 4 through 6 results in fill reversal from a traditional runner, with outer cavities filling first. Melt rotation 1 and 2 appeared to provide filling that is closest to being balanced.

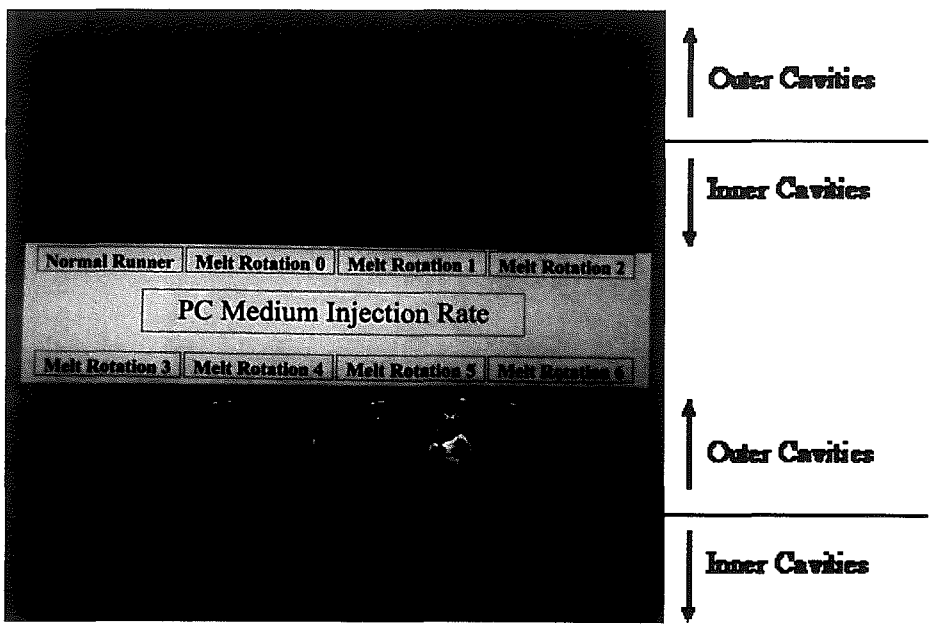

Figure 5.3: PC Test Specimens at Medium Injection Rate

	Time (s)	Position (mm)	Time (s)	Position (mm)	Time (s)	Position (mm)
Point 1	4.4	11.808	4.64	10.756	4.4	13.481
Point 2	4.56	18.644	4.8	18.309	4.48	16.875
Difference	0.16	6.836	0.16	7.553	0.08	3.394
Injection Rate (mm/s)		42.73		47.21		42.43
Area of Barrel (mm^2)		452.39		452.39		452.39
Injection Flow Rate(mm^3/s)		19328.36		21355.64		19192.65
Injection Flow Rate (cc/s)		**19.33**		**21.36**		**19.19**
Average (cc/s)	**19.96**					

Table 5-3: PC Medium Flow Rate Calculation

Figure 5.3 shows specimens from testing at the medium injection rate. Using a traditional runner it is seen that there is a fill imbalance between the inner and outer cavities, with the inner cavities filling first. This is a similar result to the low injection rate. Melt rotation 4 through 6 results in fill reversal from a traditional runner, with outer cavities filling first. Melt rotation 1 and 2 appeared to provide filling that is closest to being balanced.

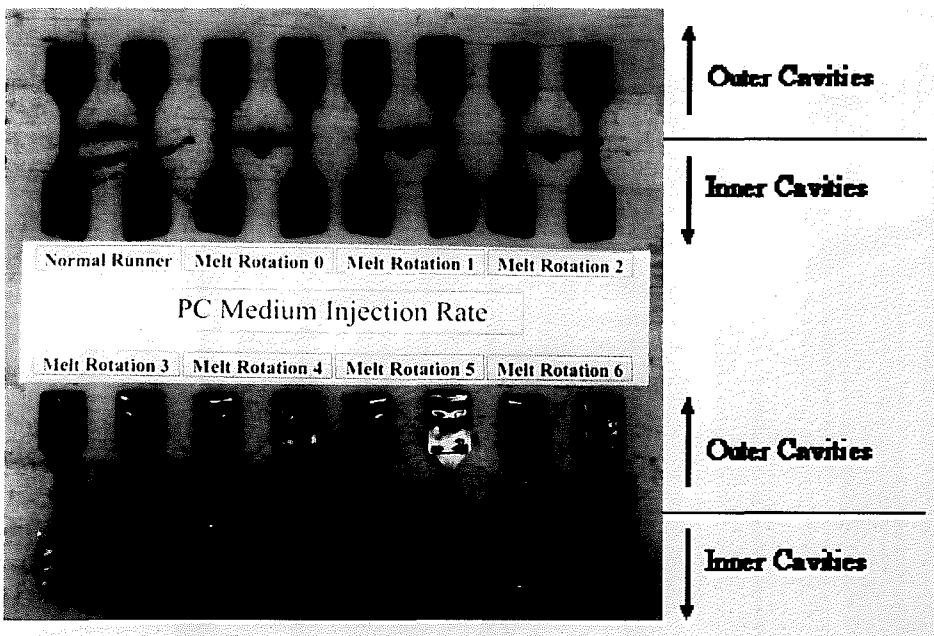

Figure 5.3: PC Test Specimens at Medium Injection Rate

	Flow Group A (Inner) Average Weight (g)	Flow Group B (Outer) Average Weight (g)
Traditional Runner	3.188	2.694
Melt Rotation 0	2.793	3.054
Melt Rotation 1	2.836	3.014
Melt Rotation 2	2.822	3.005
Melt Rotation 3	2.783	3.054
Melt Rotation 4	2.722	3.101
Melt Rotation 5	2.659	3.128
Melt Rotation 6	2.592	3.182

Table 5-4: PC Medium Injection Rate Flow Groups Average Weights

The quantitative results are found in Table 5-4. The graph in Figure 5.4 shows that for the medium injection rate both melt rotation 1 and 2 provided a nearly balanced fill between the inner and outer cavities. The results also show the minimum and maximum values for each runner setting. The standard deviation of the results ranged from 0.16% to 0.36% for each of the melt rotation settings.

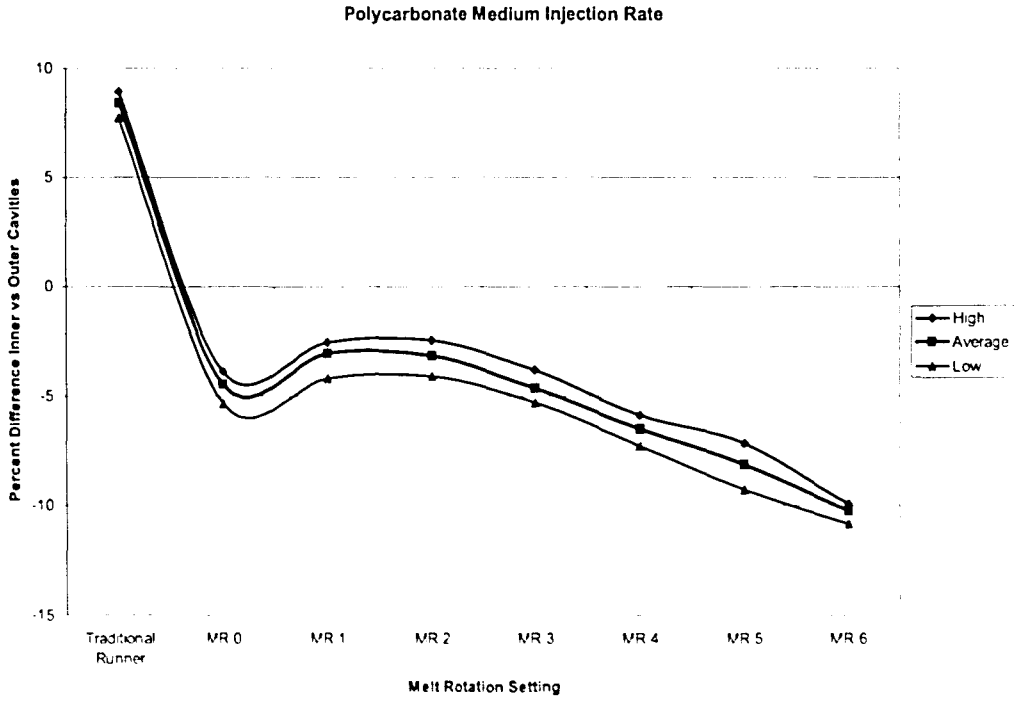

Figure 5.4: PC Test Results; Medium Injection Rate

5.1.3 High Injection Rate

The average flow rate for the highest injection rate, as determined by a distance time profile, is summarized in Table 5-5. As calculated the average injection rate of the high injection rate for PC was 26.13 cc/s. All process settings were kept constant throughout the high injection rate study.

	Time (s)	Position (mm)	Time (s)	Position (mm)	Time (s)	Position (mm)
Point 1	4.48	12.19	4.8	10.135	4.6	12.525
Point 2	4.6	19.074	4.96	19.887	4.72	19.122
Difference	0.12	6.884	0.16	9.752	0.12	6.597
Injection Rate (mm/s)		57.37		60.95		54.97
Area of Barrel (mm^2)		452.39		452.39		452.39
Injection Flow Rate(mm^3/s)		25952.11		27573.17		24870.14
Injection Flow Rate (cc/s)		**25.95**		**27.57**		**24.87**
Average (cc/s)	**26.13**					

Table 5-5: PC High Flow Rate Calculation

Figure 5.5 shows specimens from testing. Much like the previous injection rates, the traditional runner resulted in a fill imbalance between the inner and outer cavities, with the inner cavities filling first. Again there is a slight shift in the ideal Melt Rotation setting with the change in the injection rate. Melt rotation levels 0 through 3 produced a near balance of the flow to the four cavities. Melt rotation level 5 and 6 yielded a reverse imbalance with the outer cavities filling first.

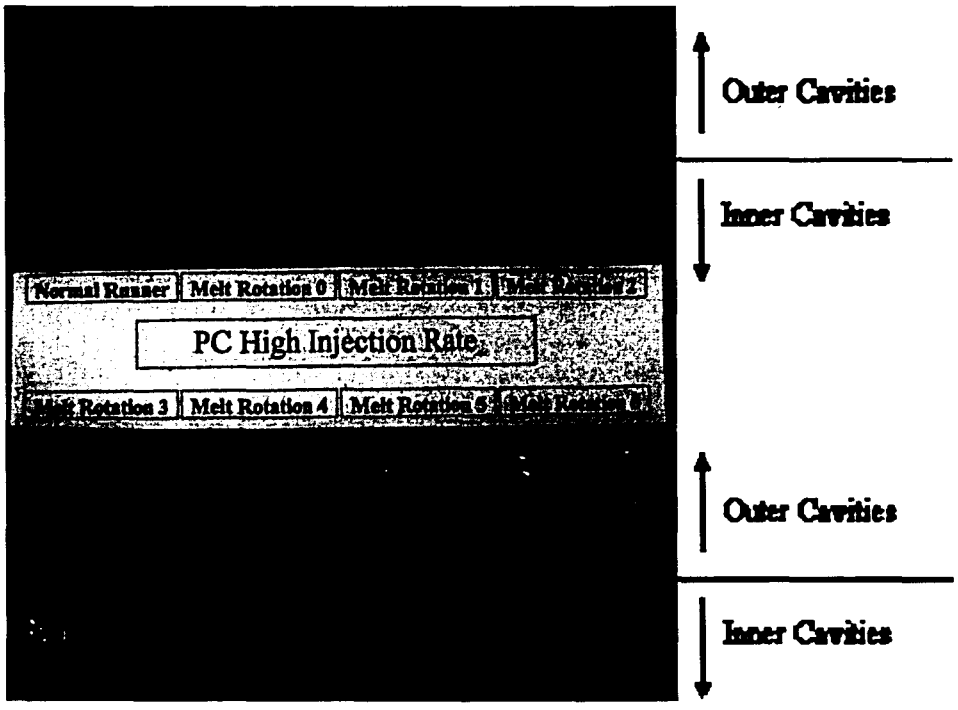

Figure 5.5: PC Test Specimens at High Injection Rate

	Flow Group A (Inner) Average Weight (g)	Flow Group B (Outer) Average Weight (g)
Traditional Runner	3.381	2.773
Melt Rotation 0	2.945	3.128
Melt Rotation 1	2.994	3.098
Melt Rotation 2	3.055	3.103
Melt Rotation 3	2.994	3.162
Melt Rotation 4	2.914	3.234
Melt Rotation 5	2.874	3.268
Melt Rotation 6	2.790	3.278

Table 5-6: PC High Injection Rate Flow Groups Average Weights

The quantitative results are found in Table 5-6. The graph in Figure 5.6 shows that for the high injection rate melt rotation 2 provides a nearly balanced fill between inner and outer cavities. The results also show the minimum and maximum values for each runner setting. The standard deviation of the results ranged from 0.18% to 0.55% for each of the melt rotation settings.

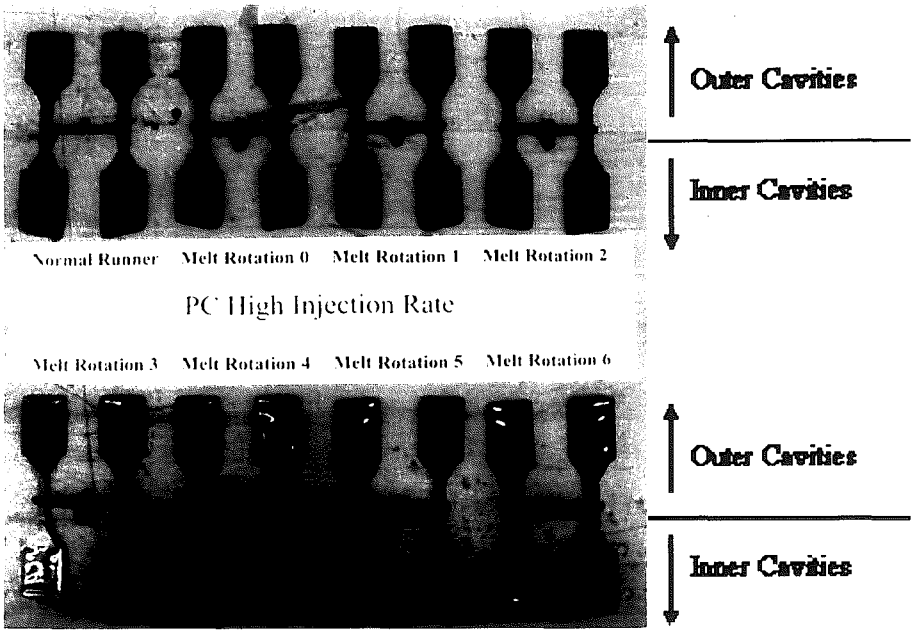

Figure 5.5: PC Test Specimens at High Injection Rate

	Flow Group A (Inner) Average Weight (g)	Flow Group B (Outer) Average Weight (g)
Traditional Runner	3.381	2.773
Melt Rotation 0	2.945	3.128
Melt Rotation 1	2.994	3.098
Melt Rotation 2	3.055	3.103
Melt Rotation 3	2.994	3.162
Melt Rotation 4	2.914	3.234
Melt Rotation 5	2.874	3.268
Melt Rotation 6	2.790	3.278

Table 5-6: PC High Injection Rate Flow Groups Average Weights

The quantitative results are found in Table 5-6. The graph in Figure 5.6 shows that for the high injection rate melt rotation 2 provides a nearly balanced fill between inner and outer cavities. The results also show the minimum and maximum values for each runner setting. The standard deviation of the results ranged from 0.18% to 0.55% for each of the melt rotation settings.

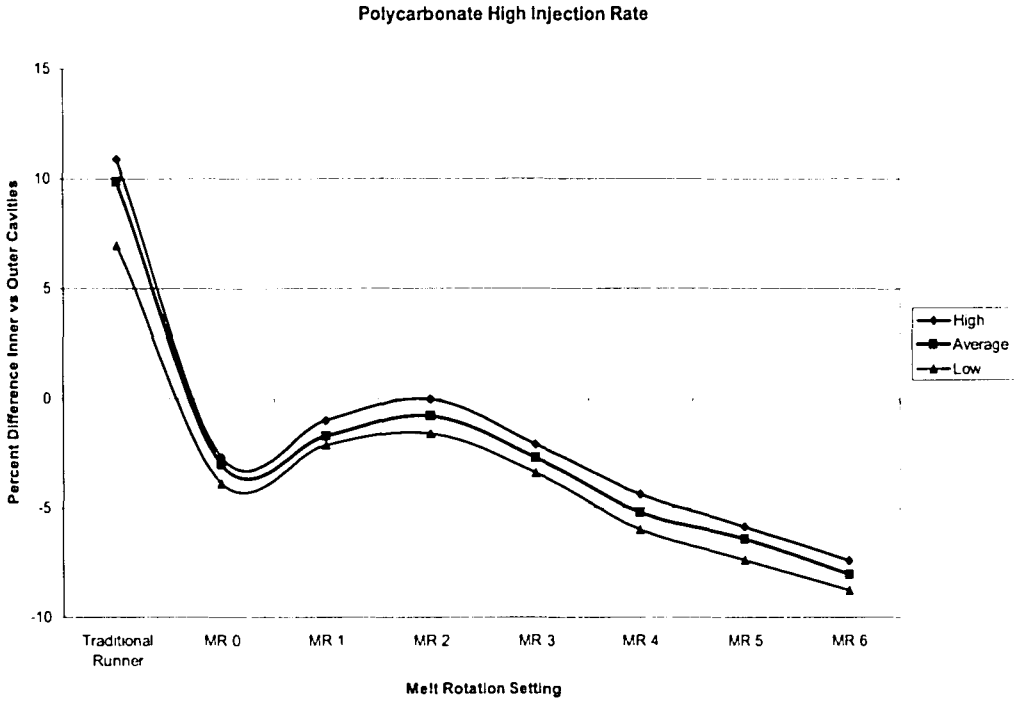

Figure 5.6: PC Test Results; High Injection Rate

5.1.4 Summary of Results for PC

Following an analysis of the collective results for PC at the three different injection rates, it was concluded that a closer filling balance was reached through the use of multiple melt rotation settings. Figure 5.7 graphically compares the average results for the different injection rates. It shows that the trend for each rate follows a similar curve. The higher the injection rate, the higher the curve is shifted up on the y-axis. The shift up with an increase of injection rate would be expected. A shift up on the y-axis is a result of a larger fill imbalance favoring the inner cavities. This is due to the higher shearing of the faster moving melt. Looking solely at the polycarbonate plastic, the test results validate the need for adjustable melt rotation

systems. The results show that even using the same material, a shift in the process settings could require a different degree of rotation to achieve cavity balance.

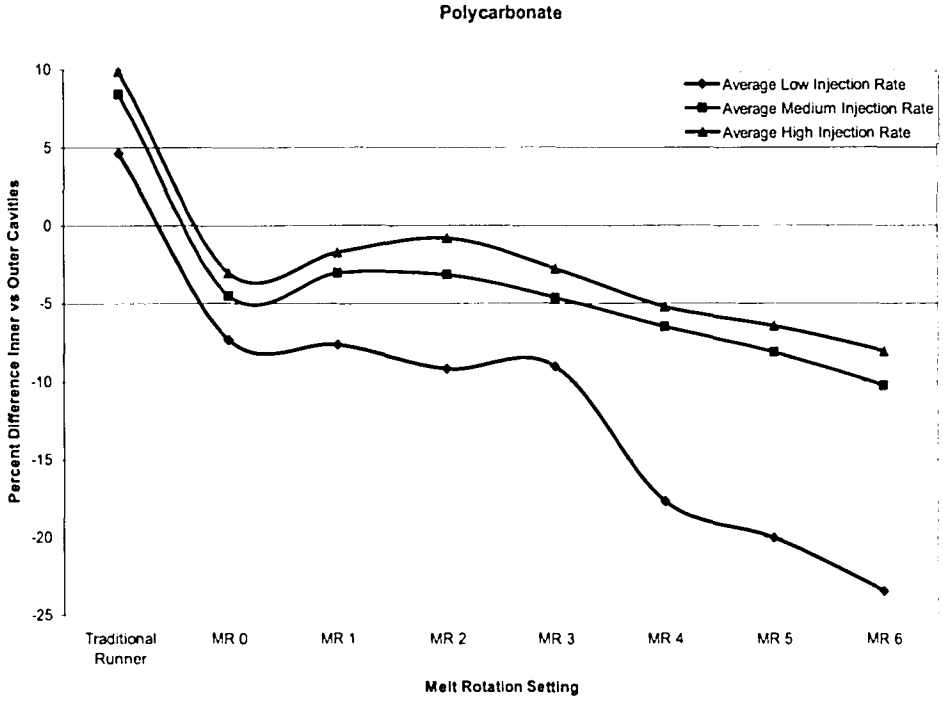

Figure 5.7: PC Test Results Summary

5.2 *Results for Polypropylene (PP)*

For the polypropylene testing the processing conditions were once again adjusted so that the leading cavity was approximately 70-80% filled. The shot size was then held constant during the testing. After the process had stabilized, ten parts were collected for each of the injection speeds with each of the runner systems. Specimen weights for each trial can be found in Appendix C – Test Results for PP.

5.2.1 Low Injection Rate

The average flow rate for the low injection rate, as determined by a distance time profile, is summarized in Table 5-7. As calculated the average injection rate of the low injection rate for PP was 3.99 cc/s. All process settings were maintained during the testing process with the low injection rate.

	Time (s)	Position (mm)	Time (s)	Position (mm)	Time (s)	Position (mm)
Point 1	5.36	10.422	5.2	10.661	4.88	10.326
Point 2	6.24	18.07	6.04	18.07	5.76	18.214
Difference	0.88	7.648	0.84	7.409	0.88	7.888
Injection Rate (mm/s)		8.69		8.82		8.96
Area of Barrel (mm^2)		452.39		452.39		452.39
Injection Flow Rate(mm^3/s)		3931.68		3990.19		4055.06
Injection Flow Rate (cc/s)		**3.93**		**3.99**		**4.06**
Average (cc/s)	**3.99**					

Table 5-7: PP Low Flow Rate Calculation

Figure 5.8 shows specimens resulting from the testing. The top left specimen is that produced with the traditional runner insert. The seven additional specimens as ordered form left to right starting in the top row are for melt rotation 0 through melt rotation 6. Using a traditional runner it is seen that there is a fill imbalance between the inner and outer cavities, with the outer cavities filling first. This is an expected result with PP. As shown melt rotation 0 through 6 are closer to a fill balance then the traditional runner.

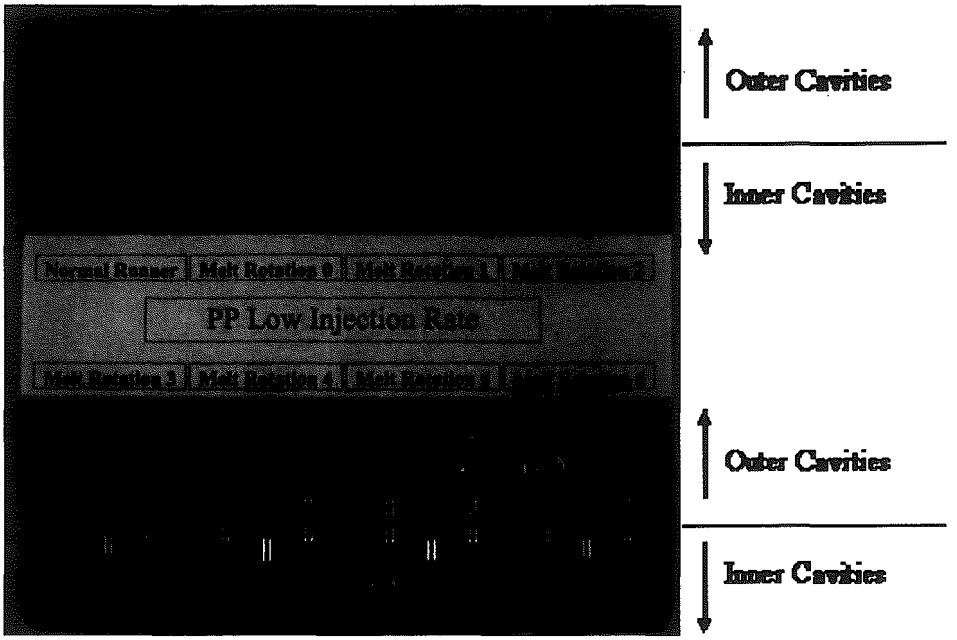

Figure 5.8: PP Test Specimens at Low Injection Rate

	Flow Group A (Inner) Average Weight (g)	Flow Group B (Outer) Average Weight (g)
Traditional Runner	1.663	2.529
Melt Rotation 0	1.816	2.278
Melt Rotation 1	1.832	2.281
Melt Rotation 2	1.806	2.264
Melt Rotation 3	1.852	2.250
Melt Rotation 4	1.834	2.213
Melt Rotation 5	1.815	2.198
Melt Rotation 6	1.829	2.185

Table 5-8: PP Low Injection Rate Flow Groups Average Weights

The quantitative results are presented in Table 5-8. The graph in Figure 5.9 shows that for the low injection rate melt rotation 6 provided the closest fill balance between the inner and outer cavities. The traditional runner had the largest fill imbalance. The results also show the minimum and maximum values for each runner setting. The standard deviation of the results ranged from 0.20% to 1.51% for each of the melt rotation settings.

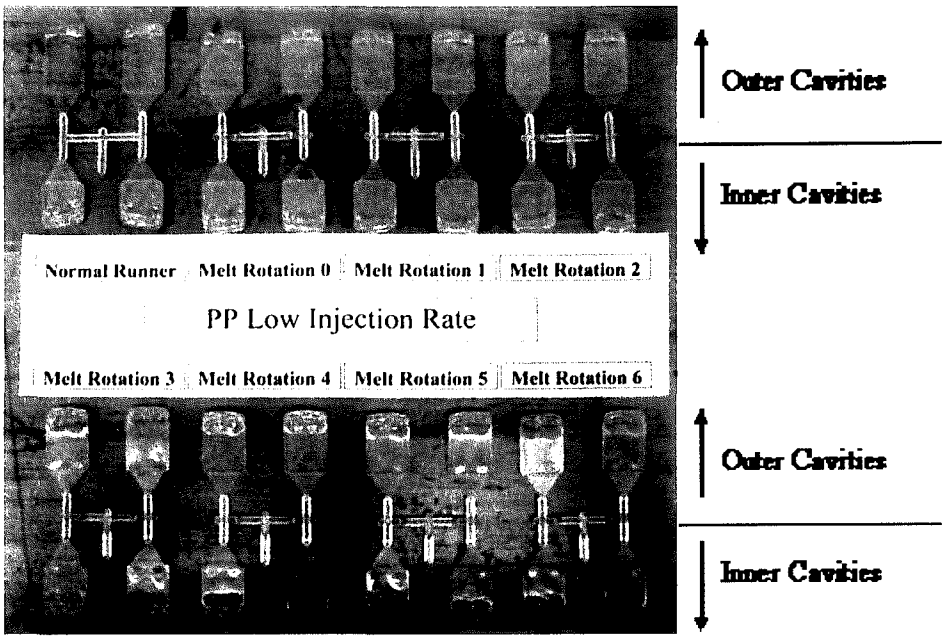

Figure 5.8: PP Test Specimens at Low Injection Rate

	Flow Group A (Inner) Average Weight (g)	Flow Group B (Outer) Average Weight (g)
Traditional Runner	1.663	2.529
Melt Rotation 0	1.816	2.278
Melt Rotation 1	1.832	2.281
Melt Rotation 2	1.806	2.264
Melt Rotation 3	1.852	2.250
Melt Rotation 4	1.834	2.213
Melt Rotation 5	1.815	2.198
Melt Rotation 6	1.829	2.185

Table 5-8: PP Low Injection Rate Flow Groups Average Weights

The quantitative results are presented in Table 5-8. The graph in Figure 5.9 shows that for the low injection rate melt rotation 6 provided the closest fill balance between the inner and outer cavities. The traditional runner had the largest fill imbalance. The results also show the minimum and maximum values for each runner setting. The standard deviation of the results ranged from 0.20% to 1.51% for each of the melt rotation settings.

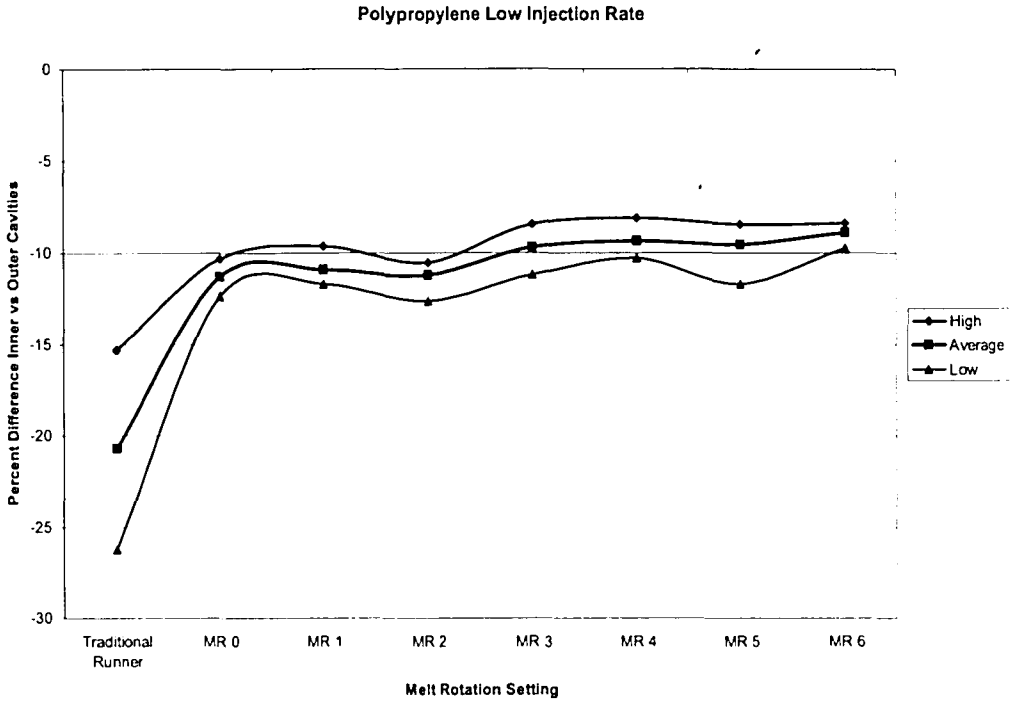

Figure 5.9: PP Test Results; Low Injection Rate

5.2.2 Medium Injection Rate

The average flow rate for the medium injection rate, as determined by a distance time profile, is summarized in Table 5-9. As calculated the average injection rate of the medium injection rate for PP was 52.08 cc/s. All process settings were maintained during the testing process with the medium injection rate.

	Time (s)	Position (mm)	Time (s)	Position (mm)	Time (s)	Position (mm)
Point 1	4.88	10.183	4.92	11.999	4.84	9.657
Point 2	4.96	19.505	5	20.652	4.92	19.313
Difference	0.08	9.322	0.08	8.653	0.08	9.656
Injection Rate (mm/s)		116.53		108.16		120.70
Area of Barrel (mm^2)		452.39		452.39		452.39
Injection Flow Rate(mm^3/s)		52714.74		48931.63		54603.47
Injection Flow Rate (cc/s)		**52.71**		**48.93**		**54.60**
Average (cc/s)	**52.08**					

Table 5-9: PP Medium Flow Rate Calculation

Figure 5.10 shows specimens from testing at the medium injection rate. Using a traditional runner it is seen that there is a fill imbalance between the inner and outer cavities, with the outer cavities filling first. This is a similar result to the low injection rate. All runner trials showed comparable fill imbalances.

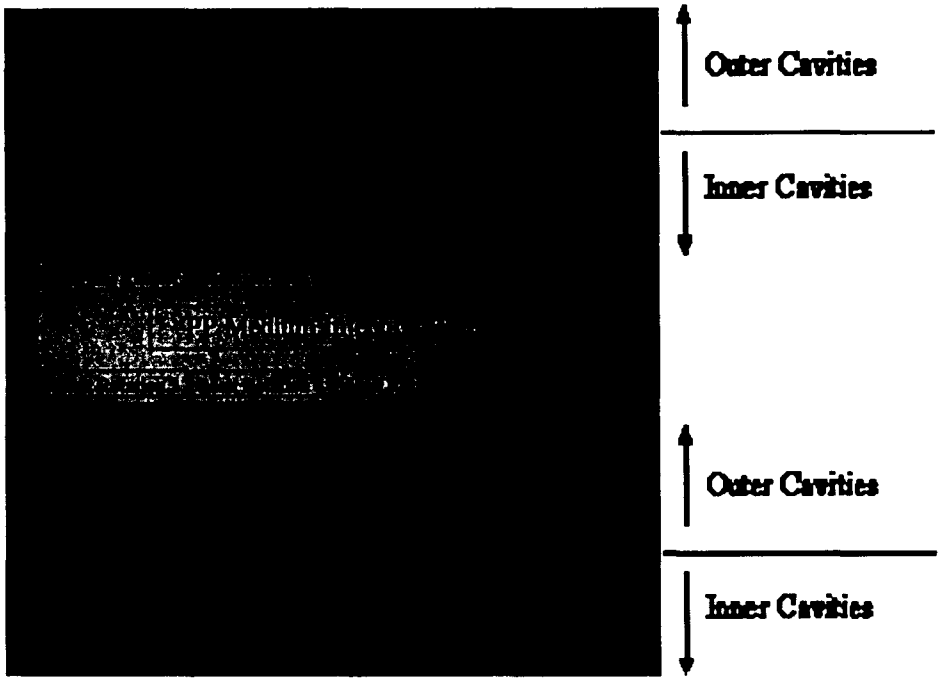

Figure 5.10: PP Test Specimens at Medium Injection Rate

	Flow Group A (Inner) Average Weight (g)	Flow Group B (Outer) Average Weight (g)
Traditional Runner	2.260	2.403
Melt Rotation 0	2.210	2.360
Melt Rotation 1	2.243	2.401
Melt Rotation 2	2.236	2.402
Melt Rotation 3	2.231	2.400
Melt Rotation 4	2.234	2.369
Melt Rotation 5	2.239	2.374
Melt Rotation 6	2.233	2.357

Table 5-10: PP Medium Injection Rate Flow Groups Average Weights

The quantitative results are presented in Table 5-10. The graph in Figure 5.11 shows that for the medium injection rate melt rotation 6 provided the closest fill

Figure 5.10 shows specimens from testing at the medium injection rate. Using a traditional runner it is seen that there is a fill imbalance between the inner and outer cavities, with the outer cavities filling first. This is a similar result to the low injection rate. All runner trials showed comparable fill imbalances.

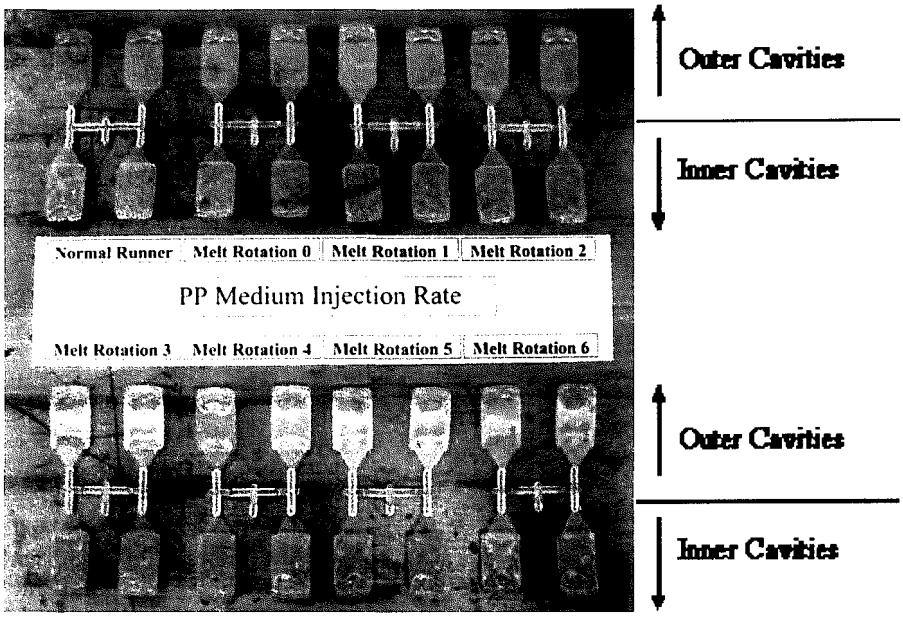

Figure 5.10: PP Test Specimens at Medium Injection Rate

	Flow Group A (Inner) Average Weight (g)	Flow Group B (Outer) Average Weight (g)
Traditional Runner	2.260	2.403
Melt Rotation 0	2.210	2.360
Melt Rotation 1	2.243	2.401
Melt Rotation 2	2.236	2.402
Melt Rotation 3	2.231	2.400
Melt Rotation 4	2.234	2.369
Melt Rotation 5	2.239	2.374
Melt Rotation 6	2.233	2.357

Table 5-10: PP Medium Injection Rate Flow Groups Average Weights

The quantitative results are presented in Table 5-10. The graph in Figure 5.11 shows that for the medium injection rate melt rotation 6 provided the closest fill

balance between the inner and outer cavities. The results also show the minimum and maximum values for each runner setting. The standard deviation of the results ranged from 0.04% to 0.23% for each of the melt rotation settings.

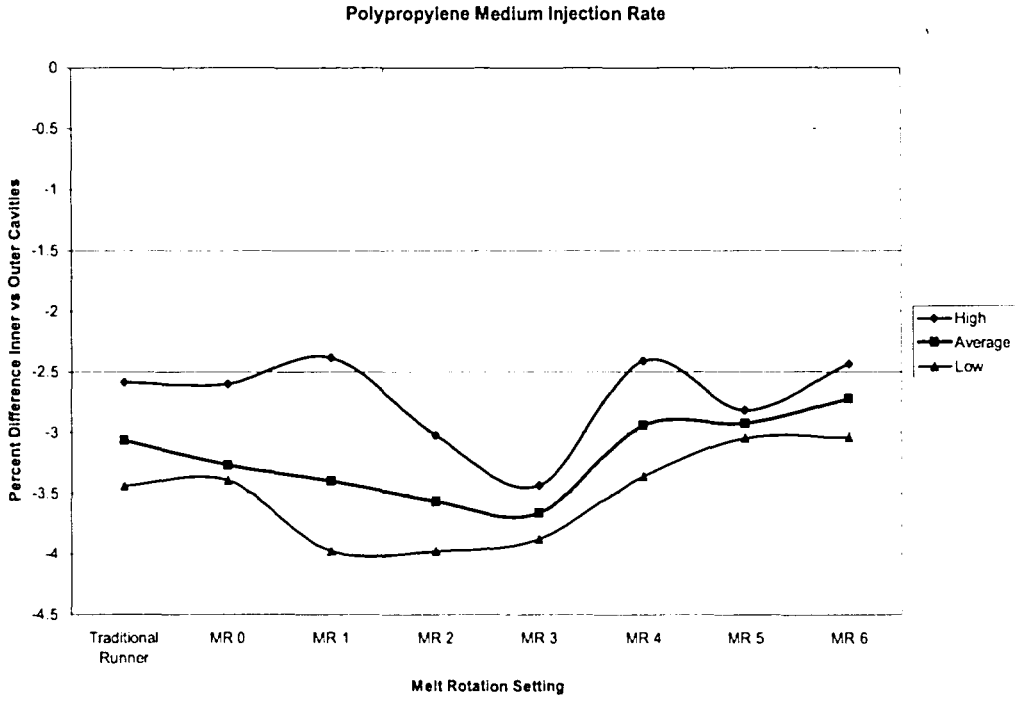

Figure 5.11: PP Test Results; Medium Injection Rate

5.2.3 High Injection Rate

The average flow rate for the highest injection rate, as determined by a distance time profile, is summarized in Table 5-11. As calculated the average injection rate of the high injection rate for PP was 110.84 cc/s. All process settings were maintained during the testing process with the high injection rate.

	Time (s)	Position (mm)	Time (s)	Position (mm)	Time (s)	Position (mm)
Point 1	4.76	8.462	4.64	10.469	4.92	6.741
Point 2	4.8	18.262	4.68	20.317	4.96	16.493
Difference	0.04	9.8	0.04	9.848	0.04	9.752
Injection Rate (mm/s)		245.00		246.20		243.80
Area of Barrel (mm^2)		452.39		452.39		452.39
Injection Flow Rate(mm^3/s)		110835.55		111378.42		110292.68
Injection Flow Rate (cc/s)		**110.84**		**111.38**		**110.29**
Average (cc/s)	**110.84**					

Table 5-11: PP High Flow Rate Calculation

Figure 5.12 shows specimens from testing. Much like the previous injection rates, the traditional runner results in a fill imbalance between the inner and outer cavities, with the outer cavities filling first. Again all trials showed comparable fill imbalance results.

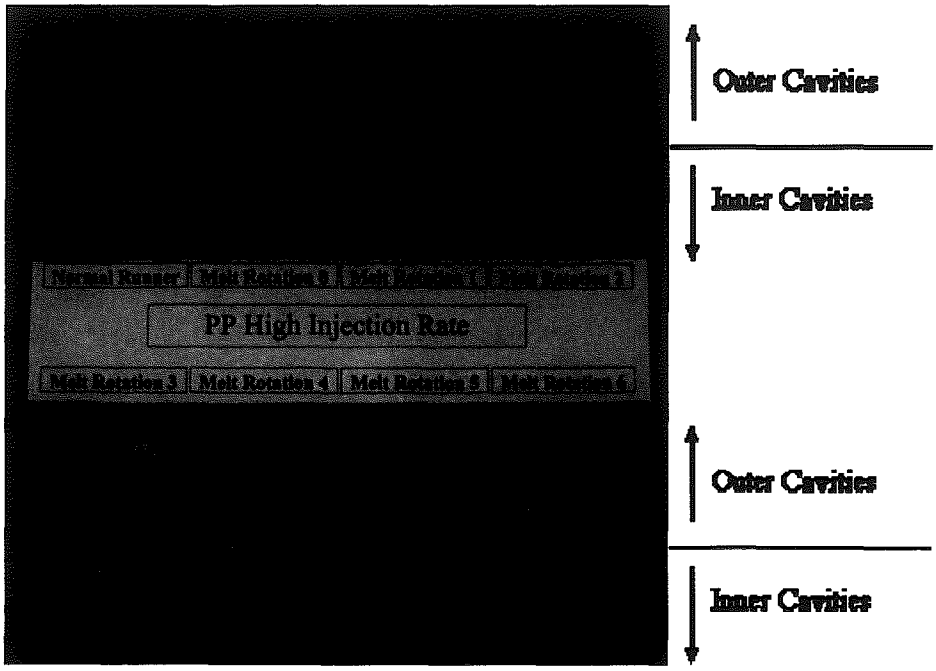

Figure 5.12: PP Test Specimens at High Injection Rate

	Time (s)	Position (mm)	Time (s)	Position (mm)	Time (s)	Position (mm)
Point 1	4.76	8.462	4.64	10.469	4.92	6.741
Point 2	4.8	18.262	4.68	20.317	4.96	16.493
Difference	0.04	9.8	0.04	9.848	0.04	9.752
Injection Rate (mm/s)		245.00		246.20		243.80
Area of Barrel (mm^2)		452.39		452.39		452.39
Injection Flow Rate(mm^3/s)		110835.55		111378.42		110292.68
Injection Flow Rate (cc/s)		**110.84**		**111.38**		**110.29**
Average (cc/s)	**110.84**					

Table 5-11: PP High Flow Rate Calculation

Figure 5.12 shows specimens from testing. Much like the previous injection rates, the traditional runner results in a fill imbalance between the inner and outer cavities, with the outer cavities filling first. Again all trials showed comparable fill imbalance results.

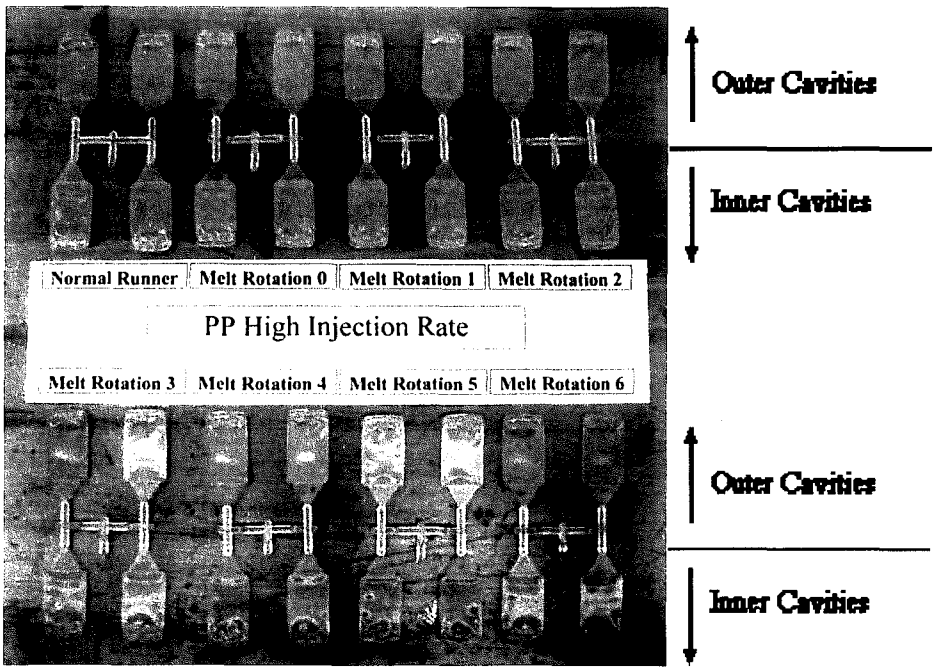

Figure 5.12: PP Test Specimens at High Injection Rate

	Flow Group A (Inner) Average Weight (g)	Flow Group B (Outer) Average Weight (g)
Traditional Runner	2.442	2.541
Melt Rotation 0	2.386	2.521
Melt Rotation 1	2.401	2.544
Melt Rotation 2	2.398	2.540
Melt Rotation 3	2.369	2.508
Melt Rotation 4	2.464	2.618
Melt Rotation 5	2.432	2.564
Melt Rotation 6	2.421	2.536

Table 5-12: PP High Injection Rate Flow Groups Average Weights

The quantitative results are presented in Table 5-12. The graph in Figure 5.13 shows that for the high injection rate the traditional runner and melt rotation 6 provided the closest to a balanced fill between inner and outer cavities. The results also show the minimum and maximum values for each runner setting. The standard deviation of the results ranged from 0.05% to 0.76% for each of the melt rotation settings.

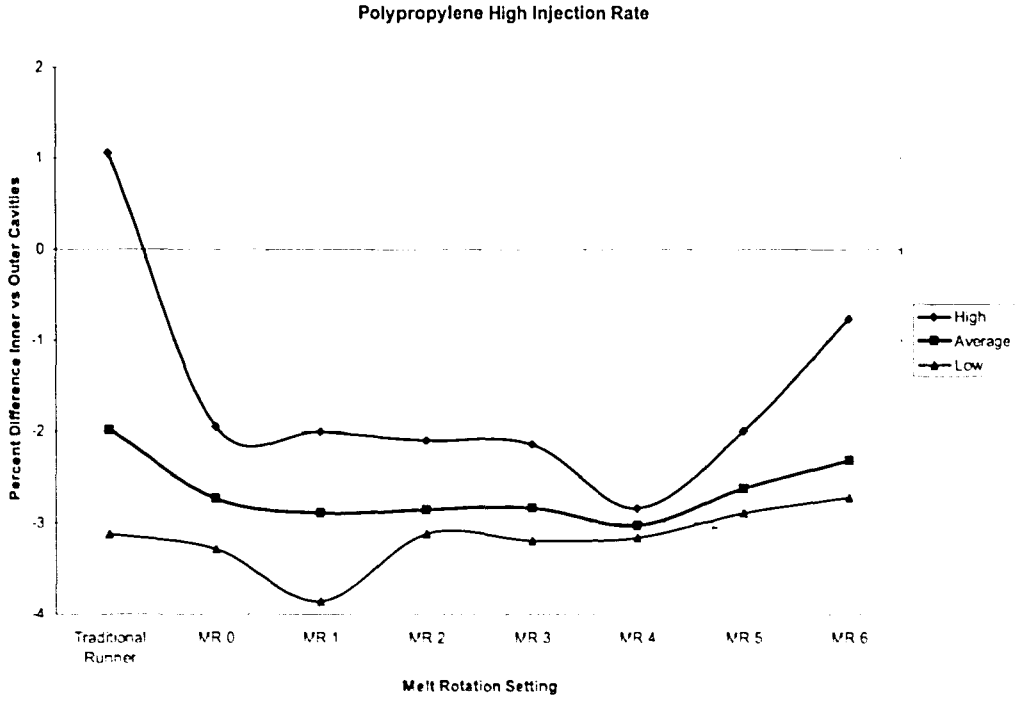

Figure 5.13: PP Test Results: High Injection Rate

5.2.4 Summary of Results for PP

The PP behaved slightly unexpectedly. Only the high and medium injection rates resulted in a similar trend line. The low injection rate behaved very erratically. Figure 5.14 graphically compares the average results of the different injection rates. Fill balance for the all the injection rates was never reached, though the melt rotation did provide a change in the imbalances. The higher the injection rate was the closer the inner and outer cavities were to being balanced.

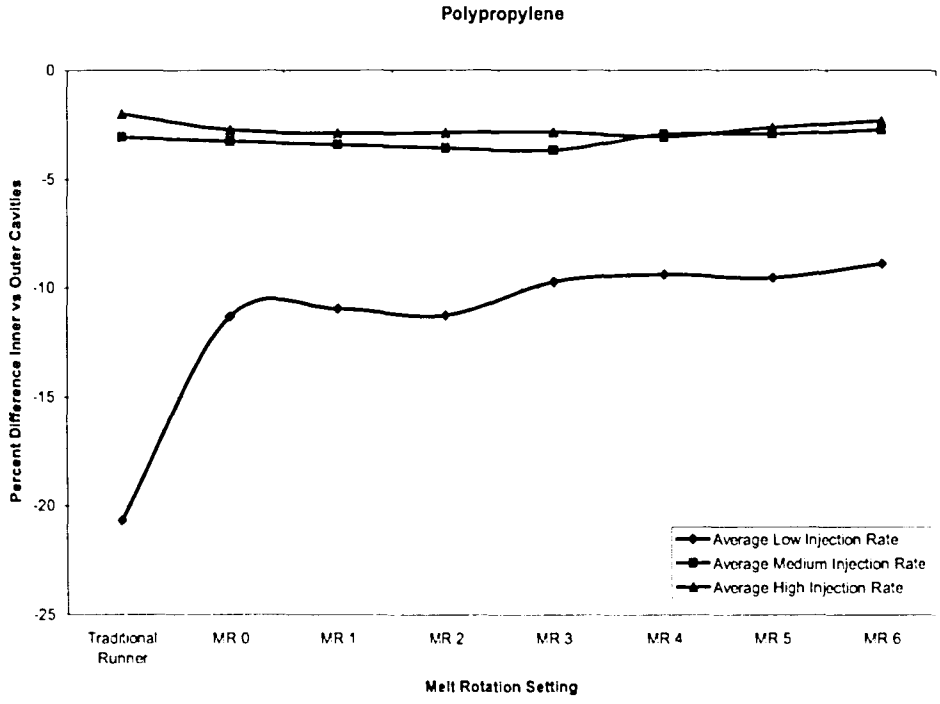

Figure 5.14: PP Test Results Summary

5.3 Results for Polyamide 6 (PA 6)

The mold was injected so that the leading cavity was approximately 70-80% filled. The shot size was then held constant during the testing. After the process had

stabilized, ten parts were collected for each of the injection speeds and runner settings. Specimen weights for each trial can be found in Appendix D – Test Results for PA 6.

5.3.1 Low Injection Rate

The average flow rate for the low injection rate, as determined by a distance time profile, is summarized in Table 5-13. As calculated the average injection rate of the low injection rate for PA 6 was 13.97 cc/s. All process settings were maintained during the testing process with the low injection rate.

	Time (s)	Position (mm)	Time (s)	Position (mm)	Time (s)	Position (mm)
Point 1	3.56	11.354	3.56	12.047	3.52	13.194
Point 2	3.8	18.62	3.76	18.07	3.72	19.648
Difference	0.24	7.266	0.2	6.023	0.2	6.454
Injection Rate (mm/s)		30.28		30.12		32.27
Area of Barrel (mm^2)		452.39		452.39		452.39
Injection Flow Rate(mm^3/s)		13696.11		13623.72		14598.63
Injection Flow Rate (cc/s)		**13.70**		**13.62**		**14.60**
Average (cc/s)	**13.97**					

Table 5-13: PA 6 Low Flow Rate Calculation

Figure 5.15 shows specimens from testing. The top left specimen is the results from the traditional runner insert which shows the outer cavities filling first. The seven additional specimens as ordered form left to right starting in the top row are melt rotation 0 through melt rotation 6. Using a traditional runner it is seen that there is a fill imbalance between the inner and outer cavities, with the outer cavities filling first. This is because the slow injection rate did not allow for enough shear thinning to create the more commonly observed fill imbalance of inner cavities filling before the outer cavities.

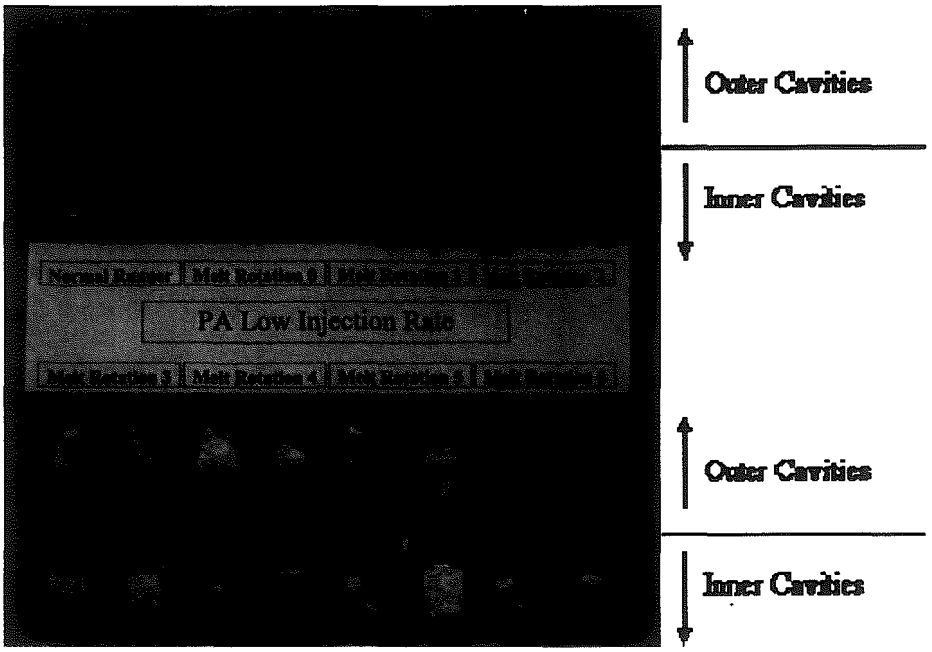

Figure 5.15: PA 6 Test Specimens at Low Injection Rate

	Flow Group A (Inner) Average Weight (g)	Flow Group B (Outer) Average Weight (g)
Traditional Runner	2.701	2.960
Melt Rotation 0	2.717	2.908
Melt Rotation 1	2.722	2.918
Melt Rotation 2	2.701	2.911
Melt Rotation 3	2.705	2.910
Melt Rotation 4	2.708	2.893
Melt Rotation 5	2.713	2.879
Melt Rotation 6	2.689	2.881

Table 5-14: PA 6 Low Injection Rate Flow Groups Average Weights

The quantitative results are presented in Table 5-14. The graph in Figure 5.16 shows that for the low injection rate melt rotation 5 provides the closest fill balance between the inner and outer cavities. The results also show the minimum and maximum values for each runner setting. The standard deviation of the results ranged from 0.10% to 0.33% for each of the melt rotation settings.

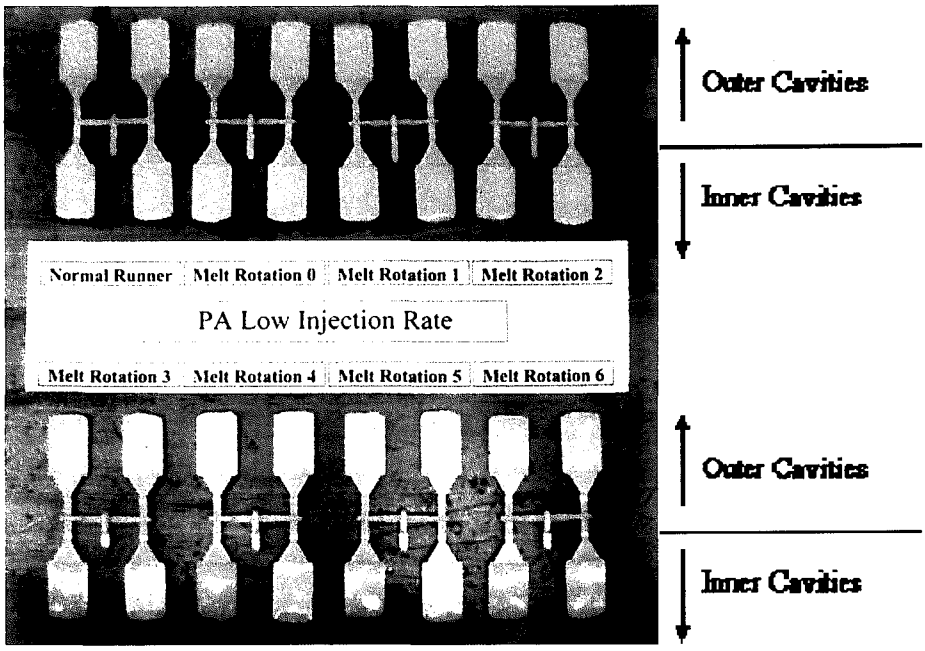

Figure 5.15: PA 6 Test Specimens at Low Injection Rate

	Flow Group A (Inner) Average Weight (g)	Flow Group B (Outer) Average Weight (g)
Traditional Runner	2.701	2.960
Melt Rotation 0	2.717	2.908
Melt Rotation 1	2.722	2.918
Melt Rotation 2	2.701	2.911
Melt Rotation 3	2.705	2.910
Melt Rotation 4	2.708	2.893
Melt Rotation 5	2.713	2.879
Melt Rotation 6	2.689	2.881

Table 5-14: PA 6 Low Injection Rate Flow Groups Average Weights

The quantitative results are presented in Table 5-14. The graph in Figure 5.16 shows that for the low injection rate melt rotation 5 provides the closest fill balance between the inner and outer cavities. The results also show the minimum and maximum values for each runner setting. The standard deviation of the results ranged from 0.10% to 0.33% for each of the melt rotation settings.

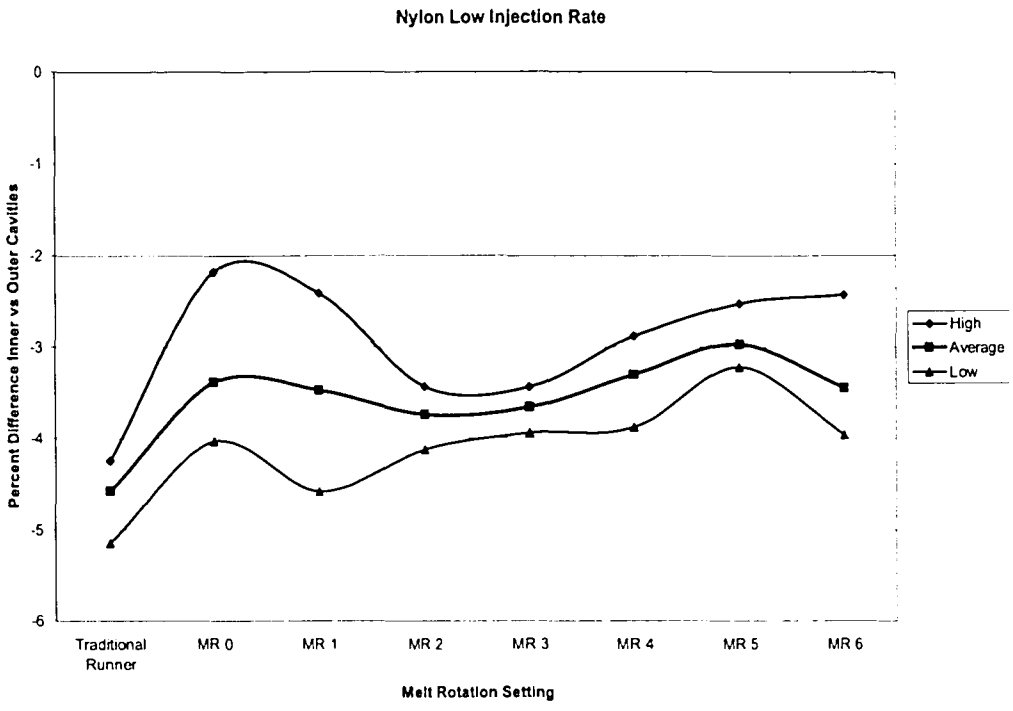

Figure 5.16: PA 6 Test Results; Low Injection Rate

5.3.2 Medium Injection Rate

The average flow rate for the medium injection rate, as determined by a distance time profile, is summarized in Table 5-15. As calculated the average injection rate of the medium injection rate for PA 6 was 35.78 cc/s. All process settings were maintained during the testing process with the medium injection rate.

	Time (s)	Position (mm)	Time (s)	Position (mm)	Time (s)	Position (mm)
Point 1	4	13.242	5	13.959	3.52	13.003
Point 2	4.08	19.505	5.08	20.222	3.6	19.457
Difference	0.08	6.263	0.08	6.263	0.08	6.454
Injection Rate (mm/s)		78.29		78.29		80.67
Area of Barrel (mm^2)		452.39		452.39		452.39
Injection Flow Rate(mm^3/s)		35416.48		35416.48		36496.56
Injection Flow Rate (cc/s)		**35.42**		**35.42**		**36.50**
Average (cc/s)	**35.78**					

Table 5-15: PA 6 Medium Flow Rate Calculation

Figure 5.17 shows specimens from testing at the medium injection rate. Using a traditional runner it is seen that there is a fill imbalance between the inner and outer cavities, with the inner cavities filling first. All of the melt rotation settings results in fill reversal from a traditional runner, with the outer cavities filling first.

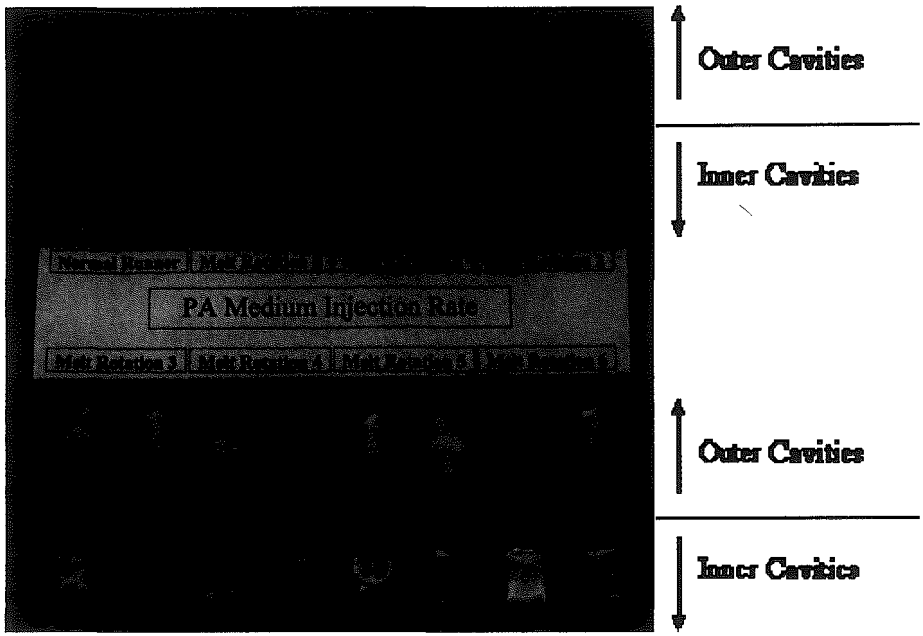

Figure 5.17: PA 6 Test Specimens at Medium Injection Rate

	Flow Group A (Inner) Average Weight (g)	Flow Group B (Outer) Average Weight (g)
Traditional Runner	3.061	3.005
Melt Rotation 0	2.947	3.016
Melt Rotation 1	2.945	3.003
Melt Rotation 2	2.944	2.995
Melt Rotation 3	2.925	3.012
Melt Rotation 4	2.913	3.004
Melt Rotation 5	2.909	2.998
Melt Rotation 6	2.909	3.007

Table 5-16: PA 6 Medium Injection Rate Flow Groups Average Weights

The quantitative results are presented in Table 5-16. The graph in Figure 5.18 shows that for the medium injection rate melt rotation 2 provided the most balanced

Figure 5.17 shows specimens from testing at the medium injection rate. Using a traditional runner it is seen that there is a fill imbalance between the inner and outer cavities, with the inner cavities filling first. All of the melt rotation settings results in fill reversal from a traditional runner, with the outer cavities filling first.

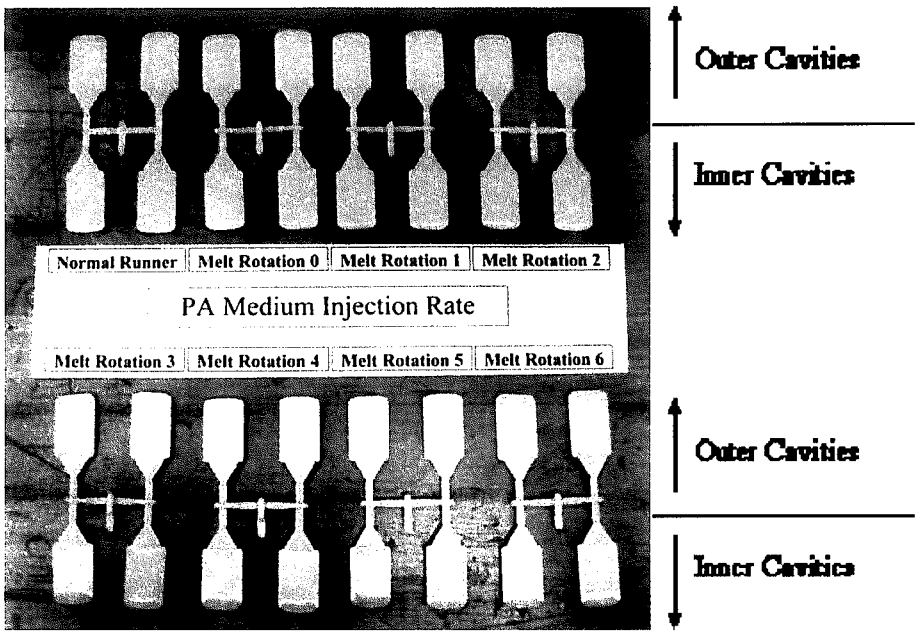

Figure 5.17: PA 6 Test Specimens at Medium Injection Rate

	Flow Group A (Inner) Average Weight (g)	Flow Group B (Outer) Average Weight (g)
Traditional Runner	3.061	3.005
Melt Rotation 0	2.947	3.016
Melt Rotation 1	2.945	3.003
Melt Rotation 2	2.944	2.995
Melt Rotation 3	2.925	3.012
Melt Rotation 4	2.913	3.004
Melt Rotation 5	2.909	2.998
Melt Rotation 6	2.909	3.007

Table 5-16: PA 6 Medium Injection Rate Flow Groups Average Weights

The quantitative results are presented in Table 5-16. The graph in Figure 5.18 shows that for the medium injection rate melt rotation 2 provided the most balanced

fill between the inner and outer cavities. The results also show the minimum and maximum values for each runner setting. The standard deviation of the results ranged from 0.06% to 0.17% for each of the melt rotation settings.

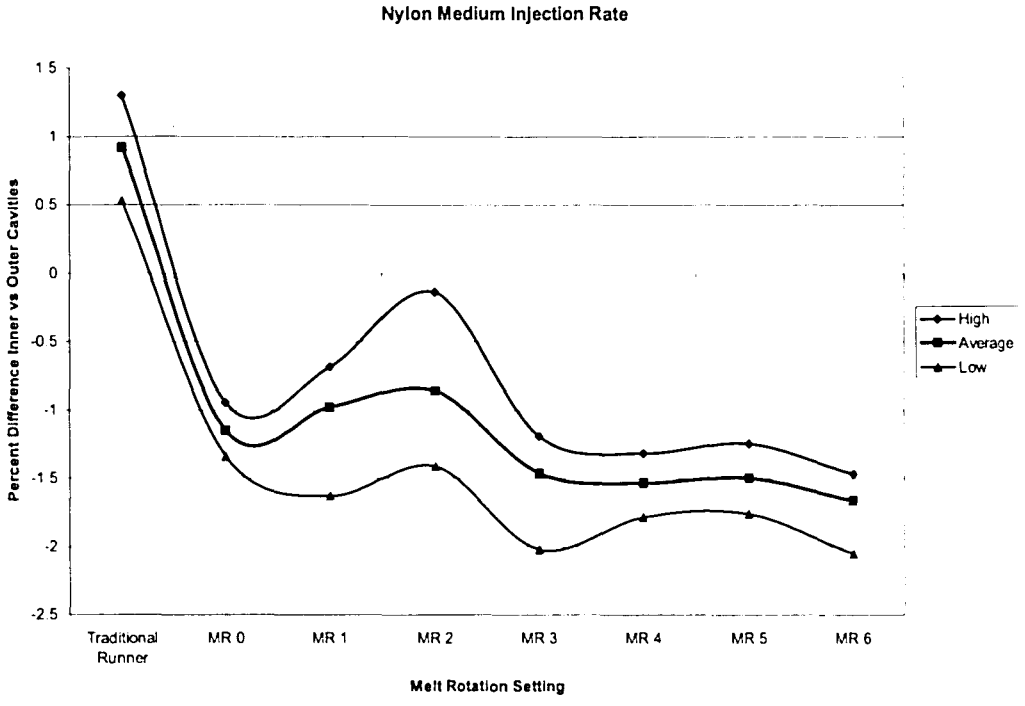

Figure 5.18: PA 6 Test Results; Medium Injection Rate

5.3.3 High Injection Rate

The average flow rate for the highest injection rate, as determined by a distance time profile, is summarized in Table 5-17. As calculated the average injection rate of the high injection rate for PA 6 was 78.76 cc/s. All process settings were maintained during the testing process with the high injection rate.

	Time (s)	Position (mm)	Time (s)	Position (mm)	Time (s)	Position (mm)
Point 1	3.4	13.481	3.64	13.481	3.88	13.003
Point 2	3.44	20.461	3.68	20.317	3.92	20.078
Difference	0.04	6.98	0.04	6.836	0.04	7.075
Injection Rate (mm/s)		174.50		170.90		176.88
Area of Barrel (mm^2)		452.39		452.39		452.39
Injection Flow Rate(mm^3/s)		78942.05		77313.45		80016.48
Injection Flow Rate (cc/s)		**78.94**		**77.31**		**80.02**
Average (cc/s)	**78.76**					

Table 5-17: PA 6 High Flow Rate Calculation

Figure 5.19 shows specimens from testing. Much like the previous injection rates, the traditional runner results in a fill imbalance between the inner and outer cavities, with the inner cavities filling first. Melt rotation 0 also shows the fill imbalance seen with the traditional runner. Melt rotation 1 through 3 appears as if the cavities are nearly balanced. Melt rotation 5 and 6 show reverse imbalance with outer cavities filling first.

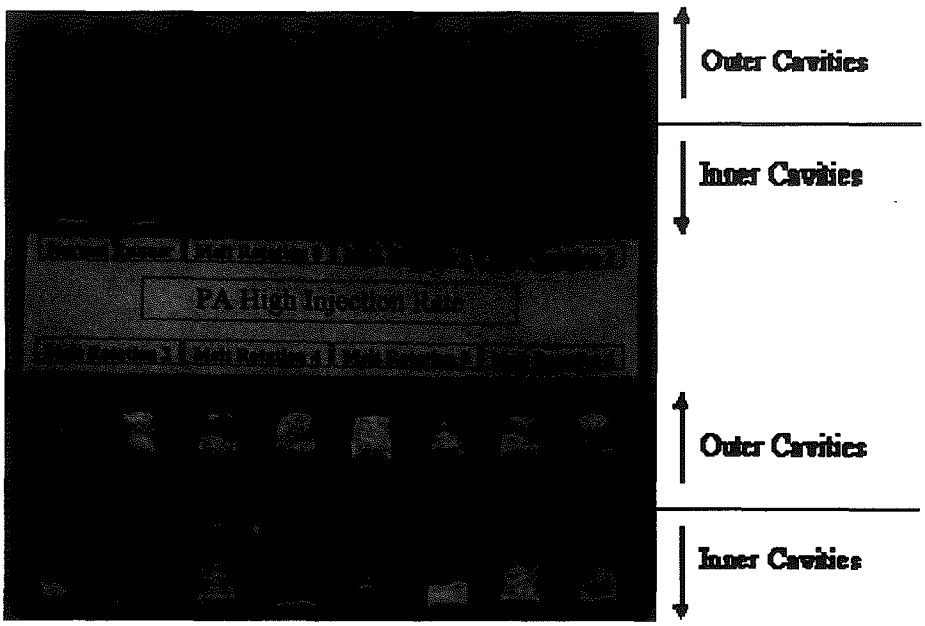

Figure 5.19: PA 6 Test Specimens at High Injection Rate

	Time (s)	Position (mm)	Time (s)	Position (mm)	Time (s)	Position (mm)
Point 1	3.4	13.481	3.64	13.481	3.88	13.003
Point 2	3.44	20.461	3.68	20.317	3.92	20.078
Difference	0.04	6.98	0.04	6.836	0.04	7.075
Injection Rate (mm/s)		174.50		170.90		176.88
Area of Barrel (mm^2)		452.39		452.39		452.39
Injection Flow Rate(mm^3/s)		78942.05		77313.45		80016.48
Injection Flow Rate (cc/s)		**78.94**		**77.31**		**80.02**
Average (cc/s)	**78.76**					

Table 5-17: PA 6 High Flow Rate Calculation

Figure 5.19 shows specimens from testing. Much like the previous injection rates, the traditional runner results in a fill imbalance between the inner and outer cavities, with the inner cavities filling first. Melt rotation 0 also shows the fill imbalance seen with the traditional runner. Melt rotation 1 through 3 appears as if the cavities are nearly balanced. Melt rotation 5 and 6 show reverse imbalance with outer cavities filling first.

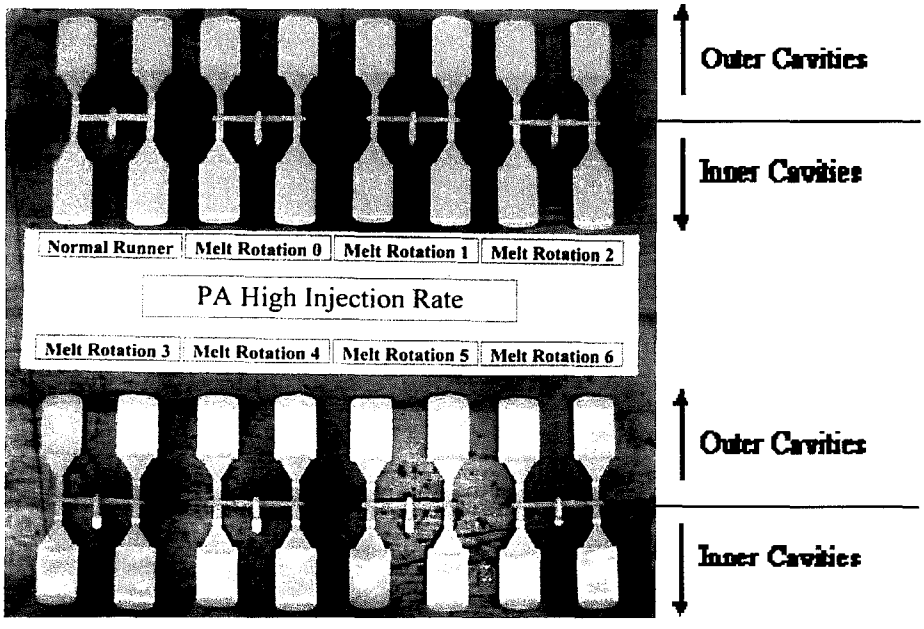

Figure 5.19: PA 6 Test Specimens at High Injection Rate

	Flow Group A (Inner) Average Weight (g)	Flow Group B (Outer) Average Weight (g)
Traditional Runner	3.011	2.868
Melt Rotation 0	2.909	2.888
Melt Rotation 1	2.906	2.863
Melt Rotation 2	2.898	2.853
Melt Rotation 3	2.862	2.865
Melt Rotation 4	2.846	2.873
Melt Rotation 5	2.847	2.880
Melt Rotation 6	2.828	2.886

Table 5-18: PA 6 High Injection Rate Flow Groups Average Weights

The quantitative results are presented in Table 5-18. The graph in Figure 5.20 shows that for the high injection rate melt rotation 3 provides a nearly balanced fill between the inner and outer cavities. The results also show the minimum and maximum values for each runner setting. The standard deviation of the results ranged from 0.05% to 0.19% for each of the melt rotation settings.

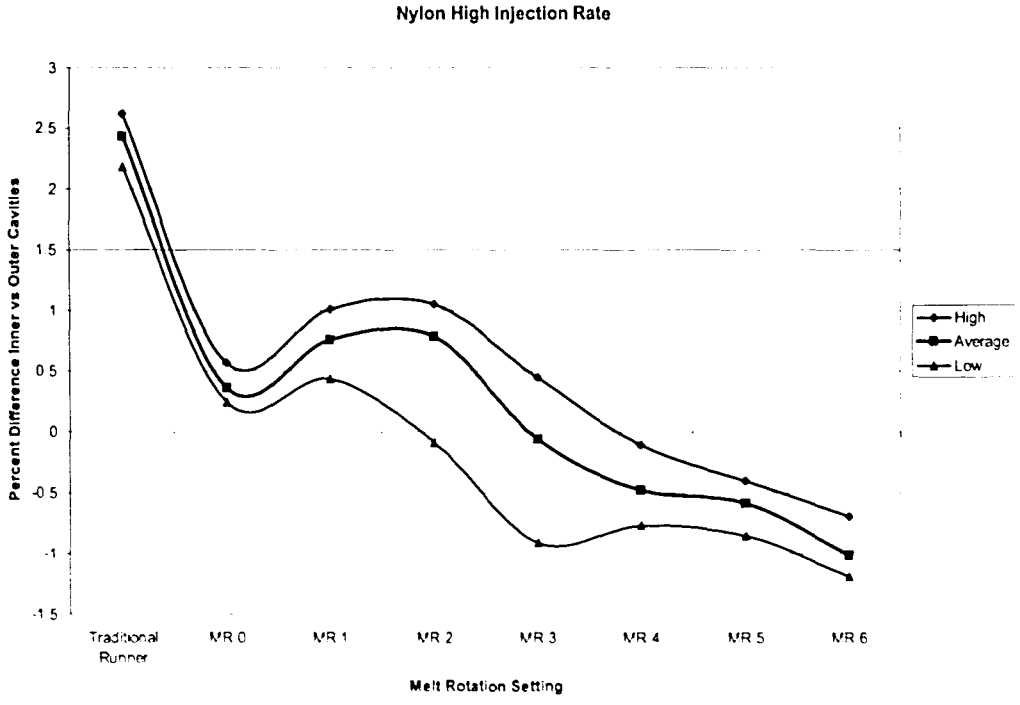

Figure 5.20: PA 6 Test Results: High Injection Rate

5.3.4 Summary of Results for PA 6

The PA 6 behaved slightly unexpectedly. Only the high and medium injection rates resulted in a similar trend line. The low injection rate behaved very erratically. Figure 5.21 graphically compares the average results of the different injection rates Fill imbalance for the low injection and medium injection rates were never reached, though the melt rotation did provide a better balance than the traditional runner. The results of the high injection rate showed that near fill balance was reached using the adjustable melt rotation. The higher the injection rate is shifted up on the y-axis. The shift up with an increase of injection rate would be expected. A shift up on the y-axis is a result of a larger fill imbalance favoring the inner cavities. This is due to the higher shearing of the faster moving melt. The results show need for adjustability to achieve a greater filling balance for a material run at different injection rates.

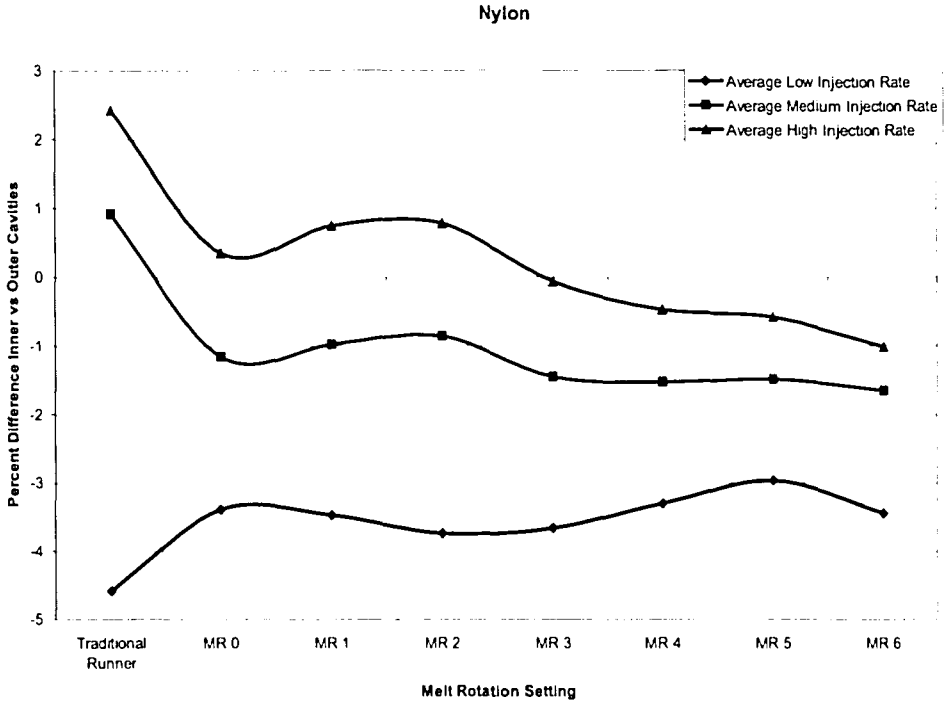

Figure 5.21: PA 6 Test Results Summary

5.4 Results for Polybutylene Terephthalate (PBT)

The mold was injected so that the leading cavity was approximately 70-80% filled. The shot size was then held constant during the testing. After the process had stabilized, ten parts were collected for each of the injection speeds and runner settings. Specimen weights for each trial can be found in Appendix E – Test Results for PBT.

5.4.1 Low Injection Rate

The average flow rate for the low injection rate, as determined by a distance time profile, is summarized in Table 5-19. As calculated the average injection rate of

the low injection rate for PBT was 16.29 cc/s. All process settings were maintained during the testing process with the low injection rate.

	Time (s)	Position (mm)	Time (s)	Position (mm)
Point 1	4	14.915	3.92	13.242
Point 2	4.16	21.082	4.08	18.596
Difference	0.16	6.167	0.16	5.354
Injection Rate (mm/s)		38.54		33.46
Area of Barrel (mm^2)		452.39		452.39
Injection Flow Rate(mm^3/s)		17436.81		15138.10
Injection Flow Rate (cc/s)		**17.44**		**15.14**
Average (cc/s)	**16.29**			

Table 5-19: PBT Low Flow Rate Calculation

Figure 5.22 shows specimens from testing. The top left specimen is the results from the traditional runner insert which shows inner cavities filling first. The seven additional specimens as ordered form left to right starting in the top row are melt rotation 0 through melt rotation 6. Using a traditional runner it is seen that there is a fill imbalance between the inner and outer cavities, with the inner cavities filling first. This is an expected result. All melt rotation settings show a fill imbalance of the outer cavities filling before the inner cavities.

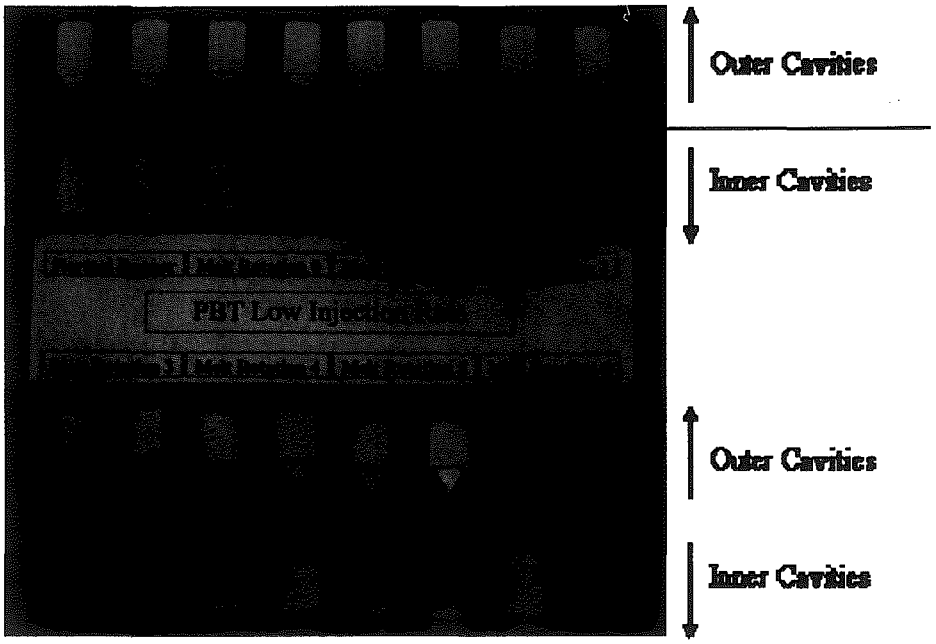

Figure 5.22: PBT Test Specimens at Low Injection Rate

	Flow Group A (Inner) Average Weight (g)	Flow Group B (Outer) Average Weight (g)
Traditional Runner	4.128	4.026
Melt Rotation 0	3.875	4.038
Melt Rotation 1	3.874	4.032
Melt Rotation 2	3.872	4.044
Melt Rotation 3	3.820	4.025
Melt Rotation 4	3.814	4.023
Melt Rotation 5	3.779	4.012
Melt Rotation 6	3.764	4.013

Table 5-20: PBT Low Injection Rate Flow Groups Average Weights

The quantitative results are presented in Table 5-20. The graph in Figure 5.23 shows that for the low injection rate the traditional runner and melt rotation 0 provides the closest fill balance between the inner and outer cavities. Though the traditional runner had the inner cavities with more fill and melt rotation 0 had the outer cavities with more fill. The results also show the minimum and maximum

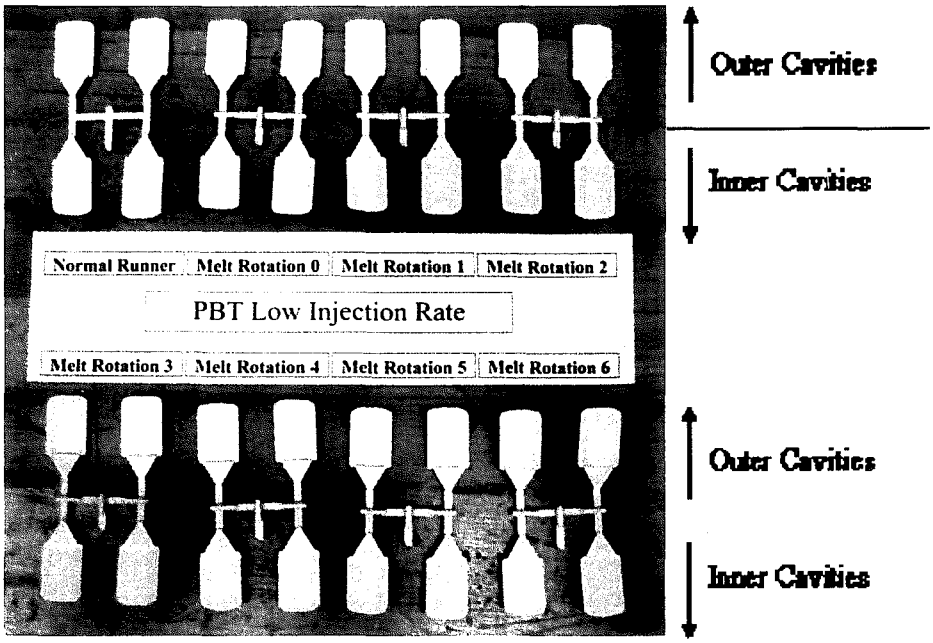

Figure 5.22: PBT Test Specimens at Low Injection Rate

	Flow Group A (Inner) Average Weight (g)	Flow Group B (Outer) Average Weight (g)
Traditional Runner	4.128	4.026
Melt Rotation 0	3.875	4.038
Melt Rotation 1	3.874	4.032
Melt Rotation 2	3.872	4.044
Melt Rotation 3	3.820	4.025
Melt Rotation 4	3.814	4.023
Melt Rotation 5	3.779	4.012
Melt Rotation 6	3.764	4.013

Table 5-20: PBT Low Injection Rate Flow Groups Average Weights

The quantitative results are presented in Table 5-20. The graph in Figure 5.23 shows that for the low injection rate the traditional runner and melt rotation 0 provides the closest fill balance between the inner and outer cavities. Though the traditional runner had the inner cavities with more fill and melt rotation 0 had the outer cavities with more fill. The results also show the minimum and maximum

values for each runner setting. The standard deviation of the results ranged from 0.19% to 0.52% for each of the melt rotation settings.

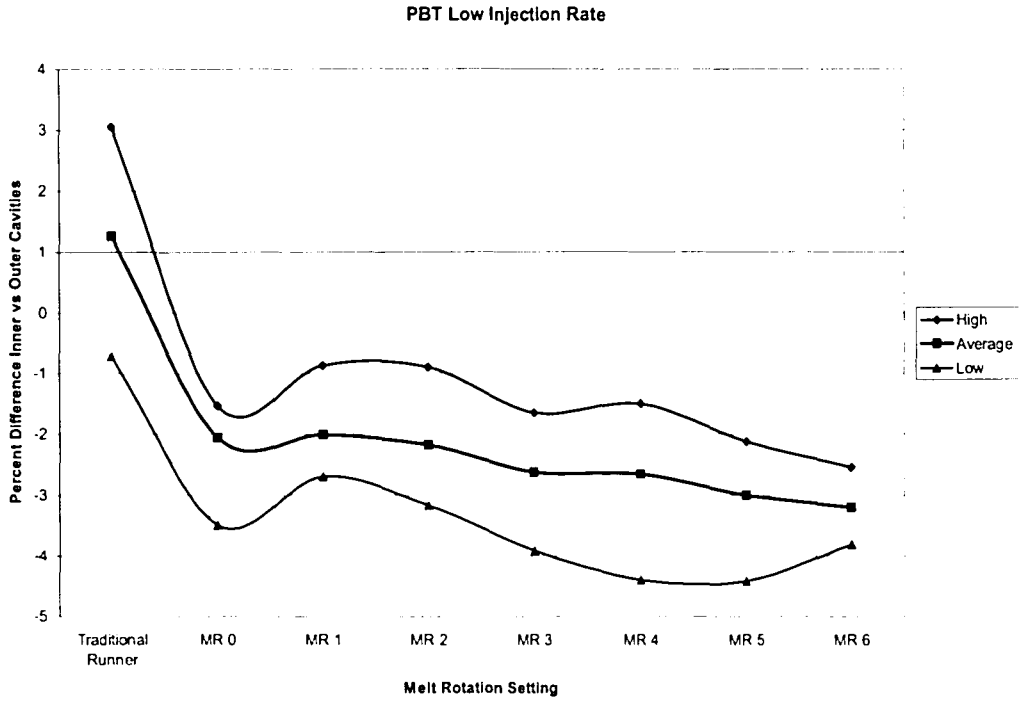

Figure 5.23: PBT Test Results; Low Injection Rate

5.4.2 Medium Injection Rate

The average flow rate for the medium injection rate, as determined by a distance time profile, is summarized in Table 5-21. As calculated the average injection rate of the medium injection rate for PBT was 44.61 cc/s. All process settings were maintained during the testing process with the medium injection rate.

	Time (s)	Position (mm)	Time (s)	Position (mm)	Time (s)	Position (mm)
Point 1	3.84	13.338	4.36	14.15	3.72	13.864
Point 2	3.92	21.465	4.44	21.608	3.8	21.943
Difference	0.08	8.127	0.08	7.458	0.08	8.079
Injection Rate (mm/s)		101.59		93.22		100.99
Area of Barrel (mm^2)		452.39		452.39		452.39
Injection Flow Rate(mm^3/s)		45957.17		42174.06		45685.74
Injection Flow Rate (cc/s)		**45.96**		**42.17**		**45.69**
Average (cc/s)	**44.61**					

Table 5-21: PBT Medium Flow Rate Calculation

Figure 5.24 shows specimens from testing at the medium injection rate. Using a traditional runner it is seen that there is a fill imbalance between the inner and outer cavities, with the inner cavities filling first. This is a similar result to the low injection rate. Melt rotation 4 and 5 appear to provide filling that is close to being balanced.

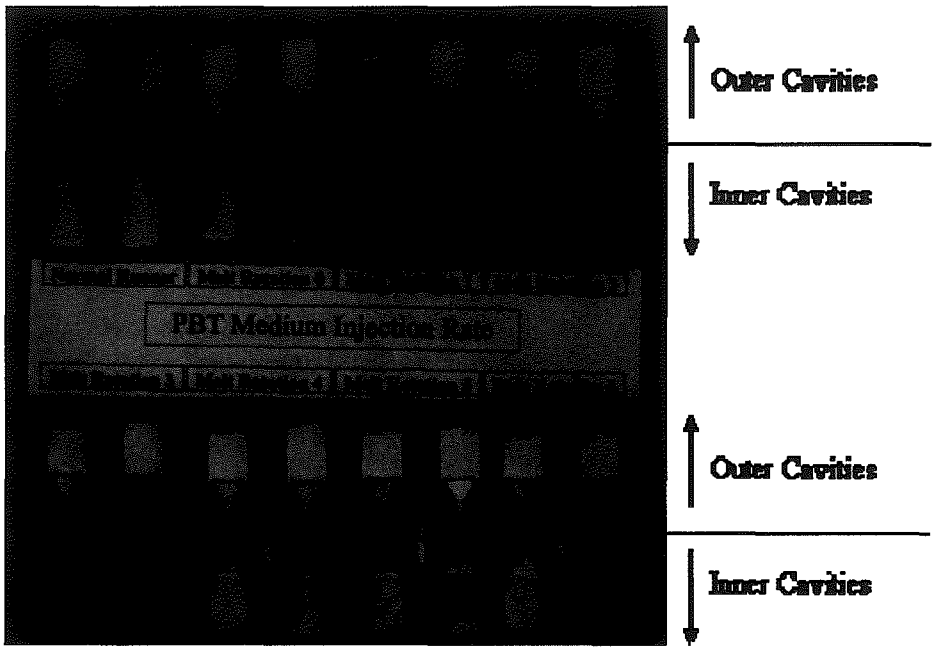

Figure 5.24: PBT Test Specimens at Medium Injection Rate

	Time (s)	Position (mm)	Time (s)	Position (mm)	Time (s)	Position (mm)
Point 1	3.84	13.338	4.36	14.15	3.72	13.864
Point 2	3.92	21.465	4.44	21.608	3.8	21.943
Difference	0.08	8.127	0.08	7.458	0.08	8.079
Injection Rate (mm/s)		101.59		93.22		100.99
Area of Barrel (mm^2)		452.39		452.39		452.39
Injection Flow Rate(mm^3/s)		45957.17		42174.06		45685.74
Injection Flow Rate (cc/s)		**45.96**		**42.17**		**45.69**
Average (cc/s)	**44.61**					

Table 5-21: PBT Medium Flow Rate Calculation

Figure 5.24 shows specimens from testing at the medium injection rate. Using a traditional runner it is seen that there is a fill imbalance between the inner and outer cavities, with the inner cavities filling first. This is a similar result to the low injection rate. Melt rotation 4 and 5 appear to provide filling that is close to being balanced.

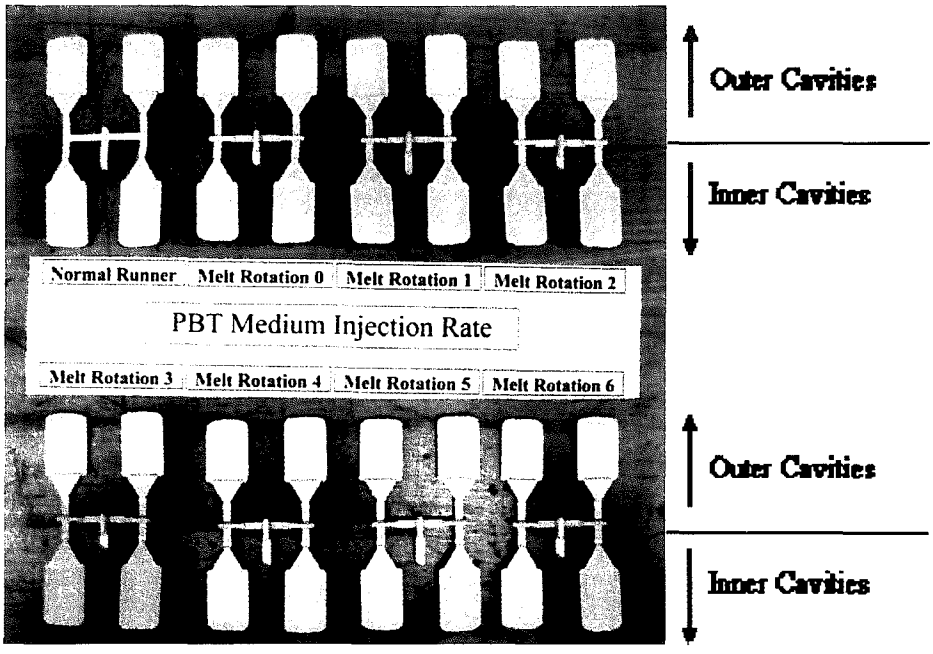

Figure 5.24: PBT Test Specimens at Medium Injection Rate

	Flow Group A (Inner) Average Weight (g)	Flow Group B (Outer) Average Weight (g)
Traditional Runner	4.302	4.040
Melt Rotation 0	4.004	4.156
Melt Rotation 1	4.049	4.162
Melt Rotation 2	4.061	4.153
Melt Rotation 3	4.079	4.144
Melt Rotation 4	4.079	4.129
Melt Rotation 5	4.064	4.119
Melt Rotation 6	4.005	4.117

Table 5-22: PBT Medium Injection Rate Flow Groups Average Weights

The quantitative results presented in Table 5-22. The graph in Figure 5.25 shows that for the medium injection rate both melt rotation 4 and 5 provides a nearly balanced fill between the inner and outer cavities. The results also show the minimum and maximum values for each runner setting. The standard deviation of the results ranged from 0.11% to 0.42% for each of the melt rotation settings.

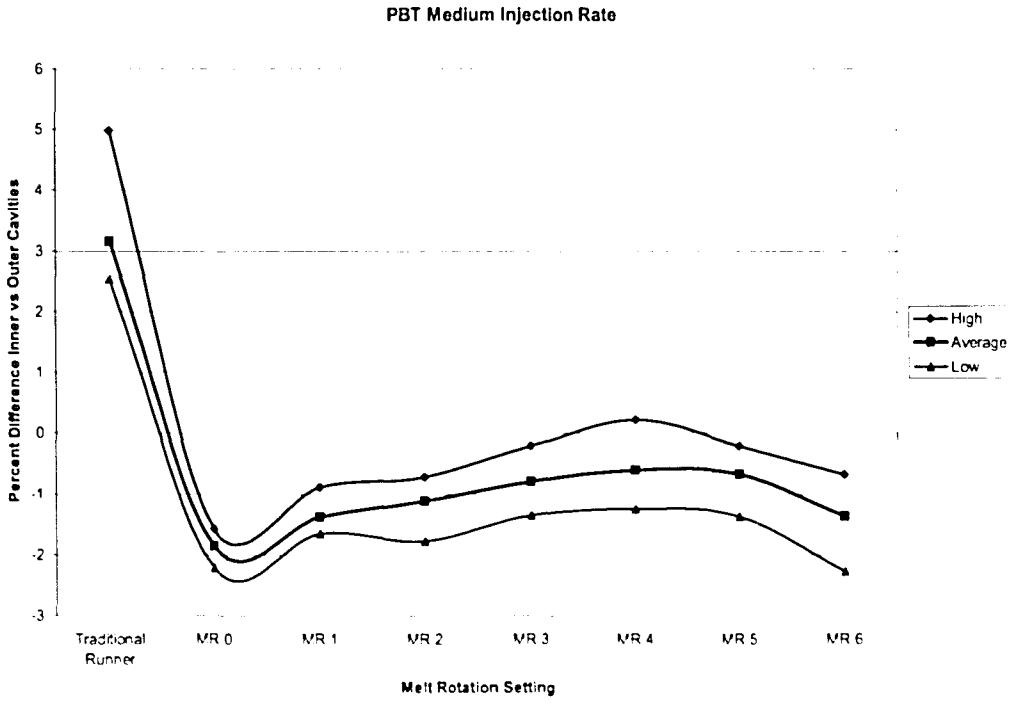

Figure 5.25: PBT Test Results: Medium Injection Rate

5.4.3 High Injection Rate

The average flow rate for the highest injection rate, as determined by a distance time profile, is summarized in Table 5-23. As calculated the average injection rate of the high injection rate for PBT was 83.62 cc/s. All process settings were maintained during the testing process with the high injection rate.

	Time (s)	Position (mm)	Time (s)	Position (mm)	Time (s)	Position (mm)
Point 1	3.88	11.425	3.52	13.051	0.84	13.29
Point 2	3.92	18.309	3.56	20.7	0.88	20.939
Difference	0.04	6.884	0.04	7.649	0.04	7.649
Injection Rate (mm/s)		172.10		191.23		191.23
Area of Barrel (mm^2)		452.39		452.39		452.39
Injection Flow Rate(mm^3/s)		77856.32		86508.28		86508.28
Injection Flow Rate (cc/s)		**77.86**		**86.51**		**86.51**
Average (cc/s)	**83.62**					

Table 5-23: PBT High Flow Rate Calculation

Figure 5.26 shows specimens from testing. Much like the previous injection rates, the traditional runner results in a fill imbalance between the inner and outer cavities, with the inner cavities filling first. Melt rotation settings 3, 4 and 5 appear to be the closest to a filling balance.

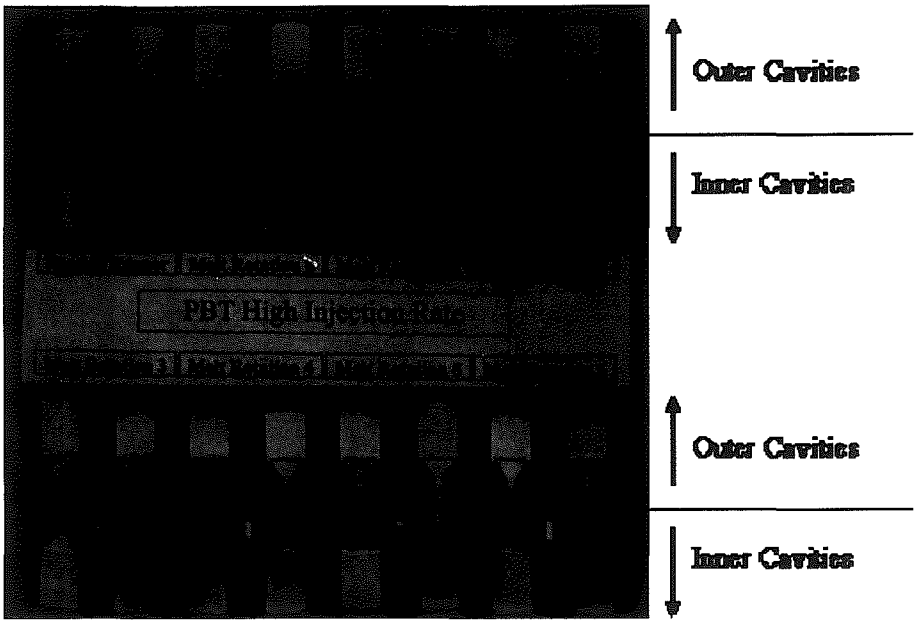

Figure 5.26: PBT Test Specimens at High Injection Rate

	Flow Group A (Inner) Average Weight (g)	Flow Group B (Outer) Average Weight (g)
Traditional Runner	4.324	3.959
Melt Rotation 0	4.001	4.030
Melt Rotation 1	4.008	4.037
Melt Rotation 2	3.987	4.025
Melt Rotation 3	4.000	4.000
Melt Rotation 4	3.989	3.973
Melt Rotation 5	3.972	3.965
Melt Rotation 6	3.943	3.989

Table 5-24: PBT High Injection Rate Flow Groups Average Weights

The quantitative results are presented in Table 5-24. The graph in Figure 5.27 shows that for the high injection rate melt rotation 3 provides a nearly balanced fill between inner and outer cavities. Melt rotation 5 also provides a nearly balanced filling. The results also show the minimum and maximum values for each runner setting. The standard deviation of the results ranged from 0.23% to 0.55% for each of the melt rotation settings.

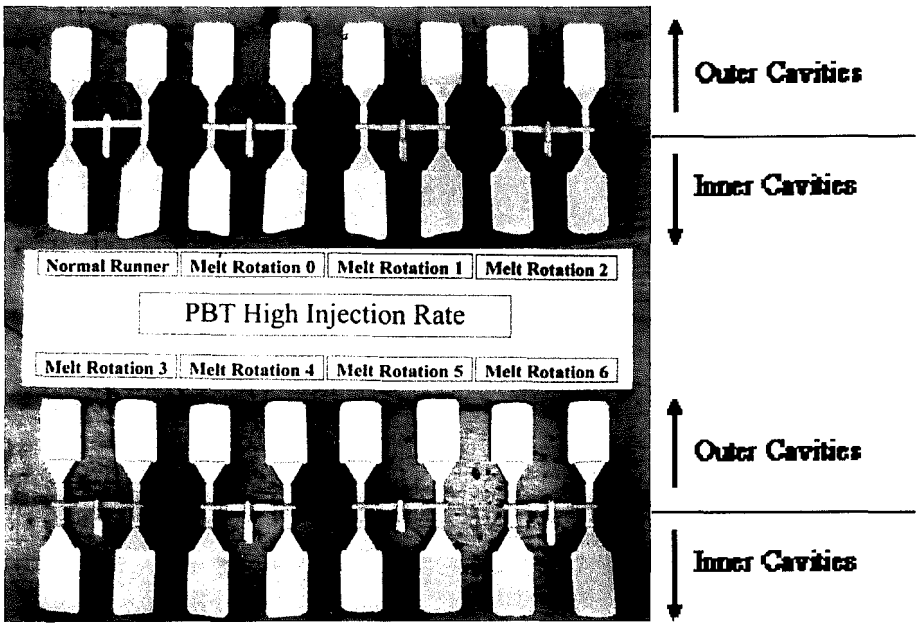

Figure 5.26: PBT Test Specimens at High Injection Rate

	Flow Group A (Inner) Average Weight (g)	Flow Group B (Outer) Average Weight (g)
Traditional Runner	4.324	3.959
Melt Rotation 0	4.001	4.030
Melt Rotation 1	4.008	4.037
Melt Rotation 2	3.987	4.025
Melt Rotation 3	4.000	4.000
Melt Rotation 4	3.989	3.973
Melt Rotation 5	3.972	3.965
Melt Rotation 6	3.943	3.989

Table 5-24: PBT High Injection Rate Flow Groups Average Weights

The quantitative results are presented in Table 5-24. The graph in Figure 5.27 shows that for the high injection rate melt rotation 3 provides a nearly balanced fill between inner and outer cavities. Melt rotation 5 also provides a nearly balanced filling. The results also show the minimum and maximum values for each runner setting. The standard deviation of the results ranged from 0.23% to 0.55% for each of the melt rotation settings.

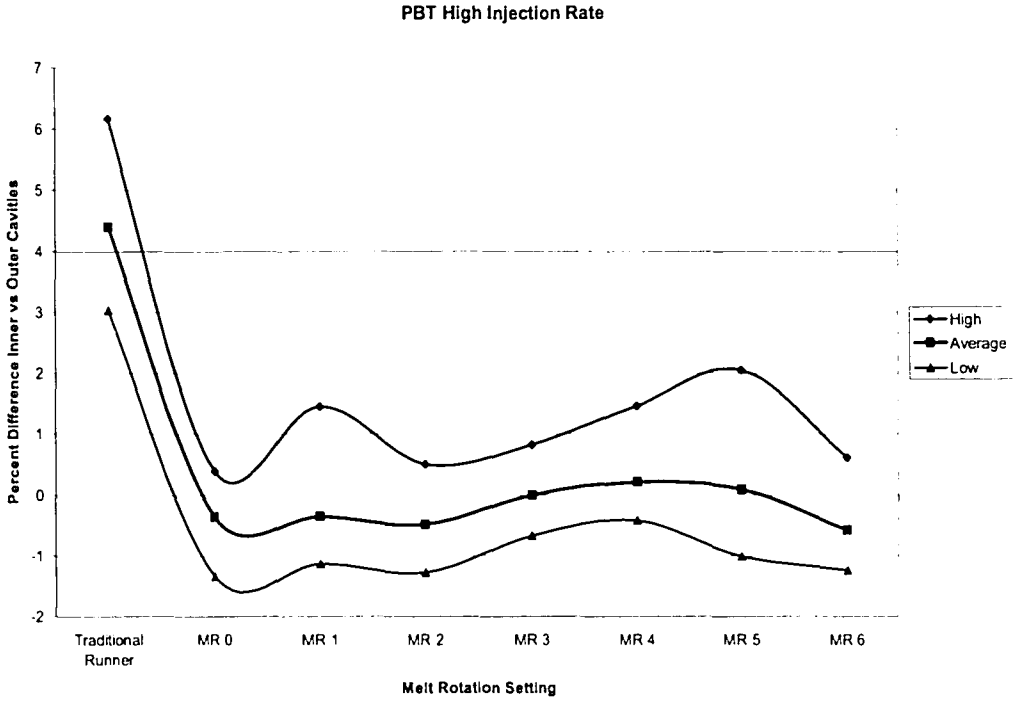

Figure 5.27: PBT Test Results; High Injection Rate

5.4.4 Summary of Results for PBT

In the investigation of the results from three different injection rates, it was seen that a closer filling balance was reached through the use of multiple melt rotation settings. Figure 5.28 graphically compares the average results of the different injection rates. It shows that the trend for each rate follows a similar curve. The higher the injection rate, the higher the curve is shifted up on the y-axis. The shift up with an increase of injection rate would be expected. A shift up on the y-axis is a result of a larger fill imbalance favoring the inner cavities. This is due to the higher shearing of the faster moving melt. Looking solely at the PBT, the test results validate the need for an adjustable melt rotation. The results show that even using the same

material, a shift in the process settings could require a different degree of rotation to achieve cavity balance.

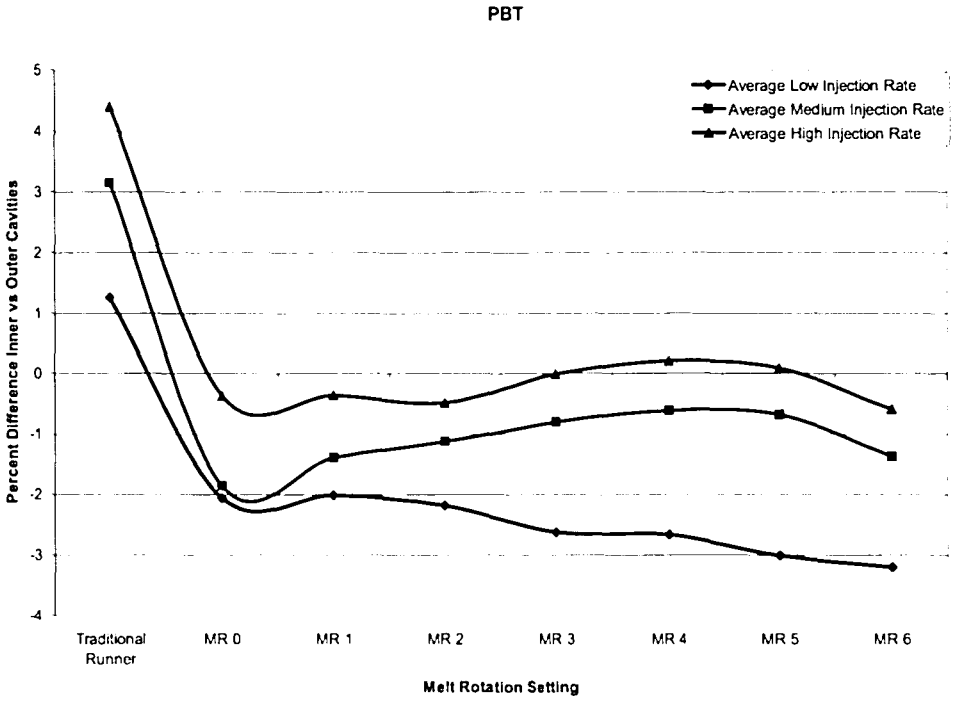

Figure 5.28: PBT Test Results Summary

5.4.5 Summary of Results for all Materials

The overall results of the melt rotation at the lower injection velocity are somewhat sporadic. As shown in Figure 5.29 the melt rotation helped to create a closer fill balance for the Nylon and Polypropylene. As for the Polycarbonate and PBT the melt rotation was able to change the imbalance from the inner cavities for the normal runner to the outer cavities for the melt rotation.

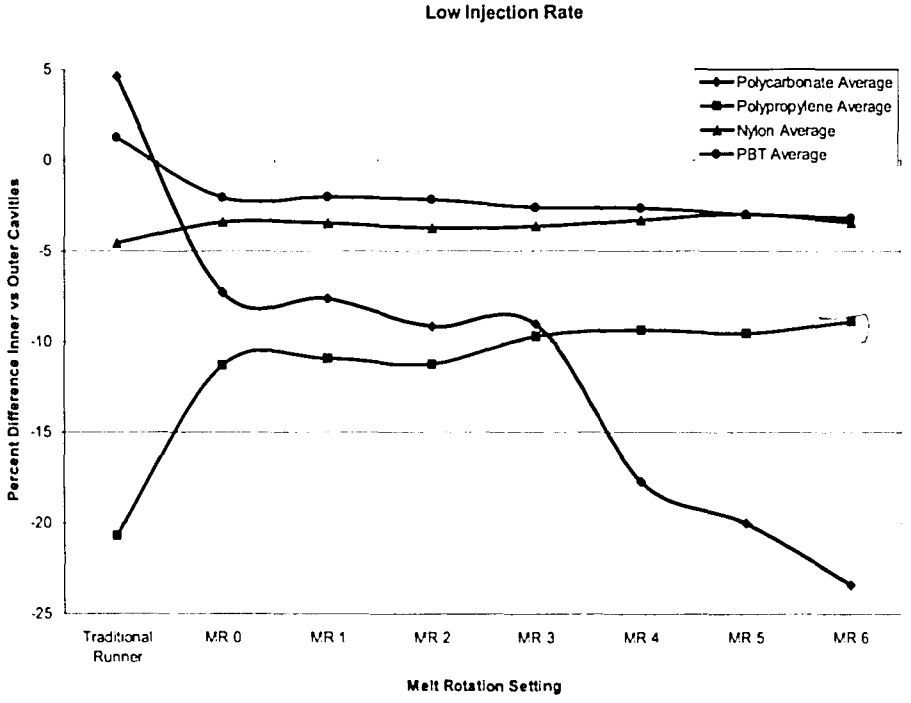

Figure 5.29: Overall Results for Four Materials at Low Injection Rate

The results of the melt rotation at the medium injection velocity are closer to what is expected. As shown in Figure 5.30 the melt rotation helped to create a closer fill balance for the PBT, Polycarbonate, and Polypropylene. As for the Polycarbonate, Nylon, and PBT the melt rotation was able to change the imbalance from the inner cavities for the traditional runner to the outer cavities for the melt rotation.

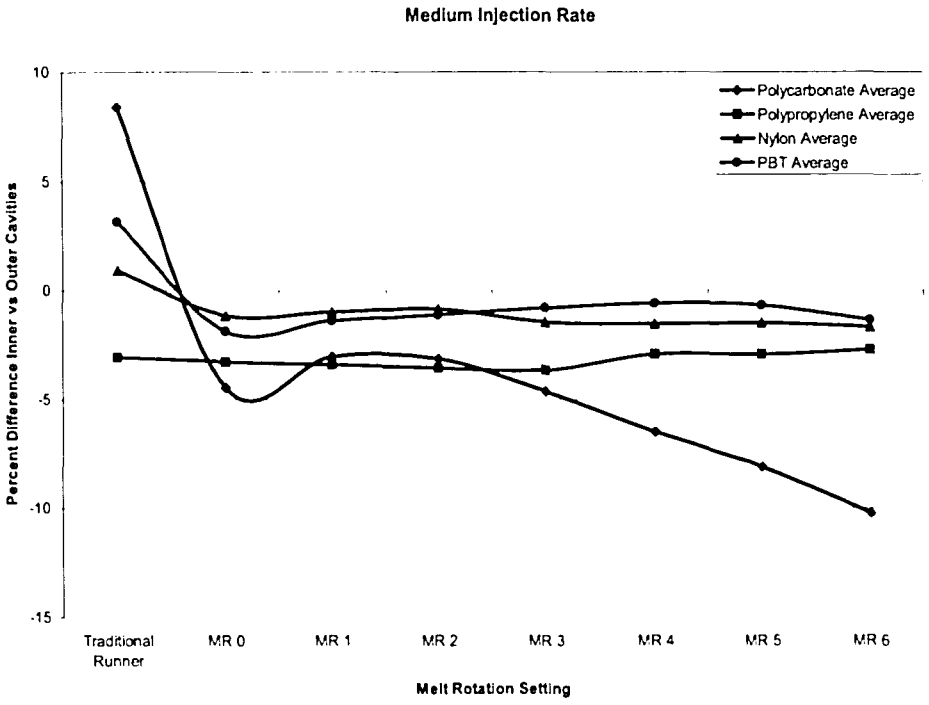

Figure 5.30: Overall Results for Four Materials at Medium Injection Rate

The results of the melt rotation at the high injection velocity are for the most part what were expected. As shown in Figure 5.31 the melt rotation helped to create a closer fill balance for the PBT, Polycarbonate, and Polypropylene. As for the Polycarbonate, Nylon, and PBT the melt rotation was able to change the imbalance from the inner cavities for the normal runner to the outer cavities for the melt rotation. In fact melt rotation was able to create a perfect filling balance for Nylon and PBT using melt rotation 3. It also greatly reduced the fill imbalance of Polycarbonate with the use of melt Rotation 2.

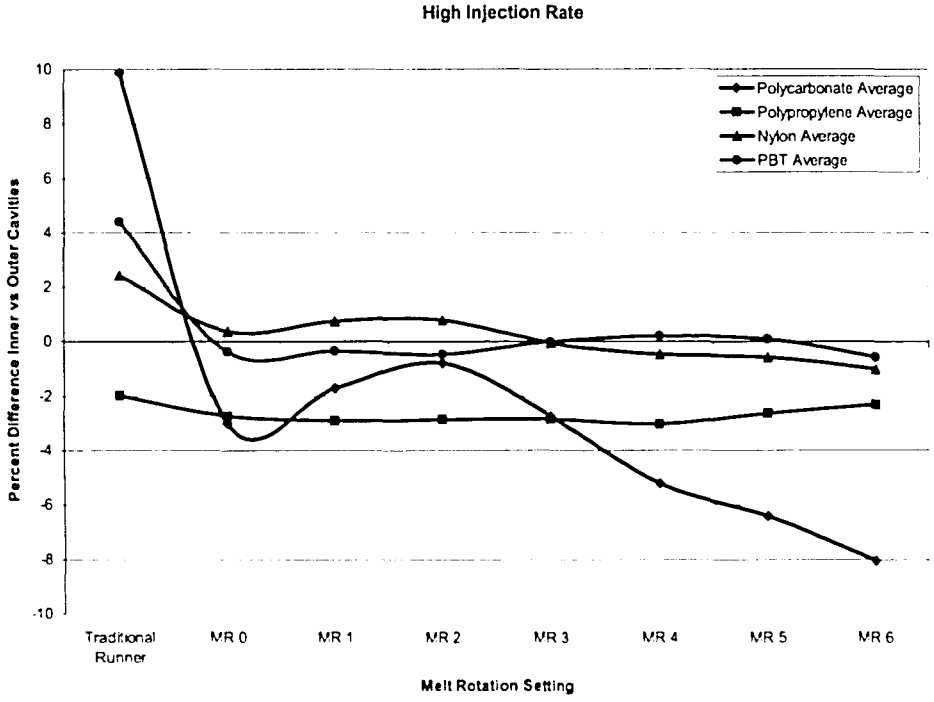

Figure 5.31: Overall Results for Four Materials at High Injection Rate

The results from the trail adjustable melt rotation runs for all four materials are full of important information that will help in the development of adjustable melt rotation technology. The next chapter will cover the conclusions that have come from

this experiment and the studies that need to be performed in the future to continue to help with the understanding of melt rotation.

6 Conclusions and Recommendations

6.1 Conclusions

Unfortunately the use of Polyflow to quantitatively predict the shear induced imbalances created in the runner systems of cold runner molds did not work out as planned. The partial results that were obtained from the simulations do not show enough promise for the feasibility of Polyflow being used as software to aid in the design of runner systems and melt rotation technology.

The results obtained using the adjustable melt rotation technology are much more promising. The trials of all four materials showed the need for adjustable melt rotation. The study shows that adjustable melt rotation can be used to obtain fill balance or near fill balance for different materials as well as the same material at different injection rates. Previously this was only accomplished through the machining of melt rotation tailored to a specific material and specific processing parameters. The use of adjustable melt rotation allows for a single mold to be designed to run multiple materials at multiple processing conditions. This can not be accomplished with standard melt rotation, only with adjustable melt rotation. This would allow for less design time. A standard adjustable melt rotation insert could be designed to fit at the intersections in the runner. The melt rotation then would be adjusted accordingly for the material and process being ran. This eliminates the extra design time and mold re-work needed to create melt rotation for a specific material and process.

6.2 Future Work

Although this research project made considerable progress in melt rotation related to material, injection velocity, and degree of melt rotation, the tests conducted only covered a small scope and have left room for more research. There are still numerous uncertainties involved with fill imbalances and melt rotation. These stem from the complexity of polymers and their properties.

Though these experiments have validated the capabilities of adjustable melt rotation technology to correct fill imbalances or at least lessen the imbalance, there are some things that need to be investigated. First area of investigation is with the use of the LVDT to determine the injection velocity. The data obtained from the LVDT would have multiple positions recorded at the same time step; this is illustrated in Table 6-1. For some times, there would be up to four position points for a single time increment. All steps were taken to use the data in order to get the most unbiased results.

	Position (mm)	Time (sec)
Point 1	11.856	3.6
Point 2	16.206	3.6

Table 6-1: Same Time, Multiple Positions

Another problem associated with these experiments is a combination of the LVDT and controlling injection velocity through injection pressure. If the filling cycle is controlled by injection pressure then the more material that is injection the slower the material is being injection. Therefore there was not one actual injection velocity. It was an average velocity. At the beginning of fill the material was moving

at a faster velocity then that of the velocity at the end of the fill. This is shown in Table 6-2 which is from a single set of data obtained during one injection cycle. It shows the injection rate varied greatly during injection, which means the shear created during injection, would be greatly affected by the change in velocity.

	Time (s)	Position (mm)	Time (s)	Position (mm)	Time (s)	Position (mm)
Point 1	4.48	11.569	4.52	14.533	4.56	15.68
Point 2	4.56	15.68	4.6	16.541	4.64	17.305
Difference	0.08	4.111	0.08	2.008	0.08	1.625
Injection Rate (mm/s)		51.39		25.1		20.31
Area of Barrel (mm^2)		452.39		452.39		452.39
Injection Flow Rate(mm^3/s)		23247.19		11354.99		9189.17
Injection Flow Rate (cc/s)		**23.25**		**11.35**		**9.19**

Table 6-2: Different Injection Rates, Same Data

Since the injection rate was controlled by the injection pressure this means as the melt rotation increased, the average injection velocity decreased. This is due to the fact that the melt rotation and extra bends associated with it, cause for more pressure to be needed during injection in order to achieve the same injection velocity as a geometrically balanced runner. This is shown in Table 6-3 and Table 6-4 where the average injection velocity for the normal runner was 14.24 cc/s and for melt rotation 6 was 12.07 cc/s. This means there was less shear created when melt rotation 6 was used, lessening the affect of fill balancing the melt rotation creates.

	Time (s)	Position (mm)	Time (s)	Position (mm)	Time (s)	Position (mm)
Point 1	5.04	10.613	4.48	11.569	14.12	11.808
Point 2	5.28	18.214	4.72	18.596	14.32	18.501
Difference	0.24	7.601	0.24	7.027	0.2	6.693
Injection Rate (mm/s)		31.67		29.28		33.46
Area of Barrel (mm^2)		452.39		452.39		452.39
Injection Flow Rate(mm^3/s)		14327.57		13245.6		15139.23
Injection Flow Rate (cc/s)		**14.33**		**13.25**		**15.14**
Average (cc/s)	**14.24**					

Table 6-3: PC Normal Runner Low Injection Rate

	Time (s)	Position (mm)	Time (s)	Position (mm)	Time (s)	Position (mm)
Point 1	4.44	10.23	4.24	9.37	4.2	11.33
Point 2	4.72	18.023	4.56	18.118	4.44	17.305
Difference	0.28	7.793	0.32	8.748	0.24	5.975
Injection Rate (mm/s)		27.83		27.34		24.9
Area of Barrel (mm^2)		452.39		452.39		452.39
Injection Flow Rate(mm^3/s)		12590.98		12367.21		11262.63
Injection Flow Rate (cc/s)		**12.59**		**12.37**		**11.26**
Average (cc/s)	**12.07**					

Table 6-4: PC Melt Rotation 6 Low Injection Rate

Another area that needs investigated is the reason that the traditional runner fill imbalance and the melt rotation 0 fill imbalance were not the same. Most of the time the normal runner imbalance was the opposite of the melt rotation 0 imbalance, when it is expected that they should roughly be the same. The reason for this most likely lies in the used of a half melt rotation at the intersection of the secondary runner and the tertiary runner. To investigate this, adjustable melt rotation inserts should be used that have no melt rotation at the intersection of the secondary and tertiary runners.

All of these experimental projects would not have to occur though if a proper simulation program that can quantitatively predict fill imbalances was created. The program would be able to predict the flow imbalances and melt rotation geometry

needed for a mold to create uniform parts long before any steel was cut. Until then experiments are needed to better understand the shear induced fill imbalance phenomenon and the use of adjustable melt rotation technology to help with the fill imbalance problems.

Overall, the present research project provided a contribution to the development and understanding of melt rotation technology. It was found that the concept of adjustable melt rotation is extremely promising, and in fact necessary in many cases. With further development, this innovative concept is likely to solve many injection molding flow balance problems in the future.

References

1. Bishop, R., Shearing of Plastic Runner Causes Property Differences in Parts: ANTEC, 2000
2. Beaumont, J., Young, J., and Jaworski, M., Solving Mold Filling Imbalances in Multi-Cavity Injection Molds: Journal of Injection Molding Technology, 1998, 2(2): p.47-58.
3. Selden, R., Thin Wall Molding of Engineering Plastics – A Literature Survey: Journal of Injection Molding Technology, 2000, 4(4): p.159-166.
4. Salamon, B., and Donal, R., Characterizing and Controlling Secondary Flows in Injection Molds: Journal of Injection Molding Technology, 1997, 1(1): p.36-43.
5. Gupta, Rakesh, Polymer and Composite Rheology, Hudgen, D.E., Editor, Marcel Dekker, Inc: New York
6. Beaumont, K., Young, J., Mold Filling Imbalances in Geometrically Balanced Runner Systems: Journal of Injection Molding Technology, 1997, 1(3): p.133-143.
7. Beaumont Technologies, Inc. Website, http://www.beaumontinc.com
8. Haylett, R., Rhoades, D., True 3D Flow Analysis for Designing Hot and Cold Runners in Injection Molds: ANTEC 2001.
9. Cook, P., Yu, H., Kietzmann, C., Costa, F., Prediction of Flow Imbalance in Geometrically Balanced Feed Systems: ANTEC 2005.
10. Chien, C., Chiang, C., Yang, W., Tsai, V., Hsu, D., True 3D CAE visualization of filling imbalance in geometry-balanced runners: ANTEC 2005.
11. Reifschneider, L., Documentation and Simulating Flow Segregation in Geometrically Balanced Runners: Journal of Injection Molding Technology, 2001, 5(4): p. 208-233.
12. Beaumont, J., Stewart, C., Ezzo, M., Controlling Intra-Cavity Melt Flow and Weld Strength Through New Runner Design Technology: ANTEC 2005.
13. Beaumont, J., Boell, K., Controlling Balanced Molding Through New Hot Runner Manifold Designs: ANTEC 2001.
14. Beaumont, J., Nagel, R., Sherman, R., Successful Injection Molding – Process, Design, and Simulation, Hanser Publishers: Munich, Germany.
15. Dropik, M., Isolation of True Runner System Behavior in Simulation Tools for Injection Molding: ANTEC 2006
16. Takarada, K., Coulter, J., Myers, M., Beaumont, J., The Effect Of Primary Runner Length on Fill-Imbalance in a Geometrically Balanced Eight Cavity Polymer Injected Mold: ANTEC 2006.

Appendices

Appendix A – Mold and Insert Drawings

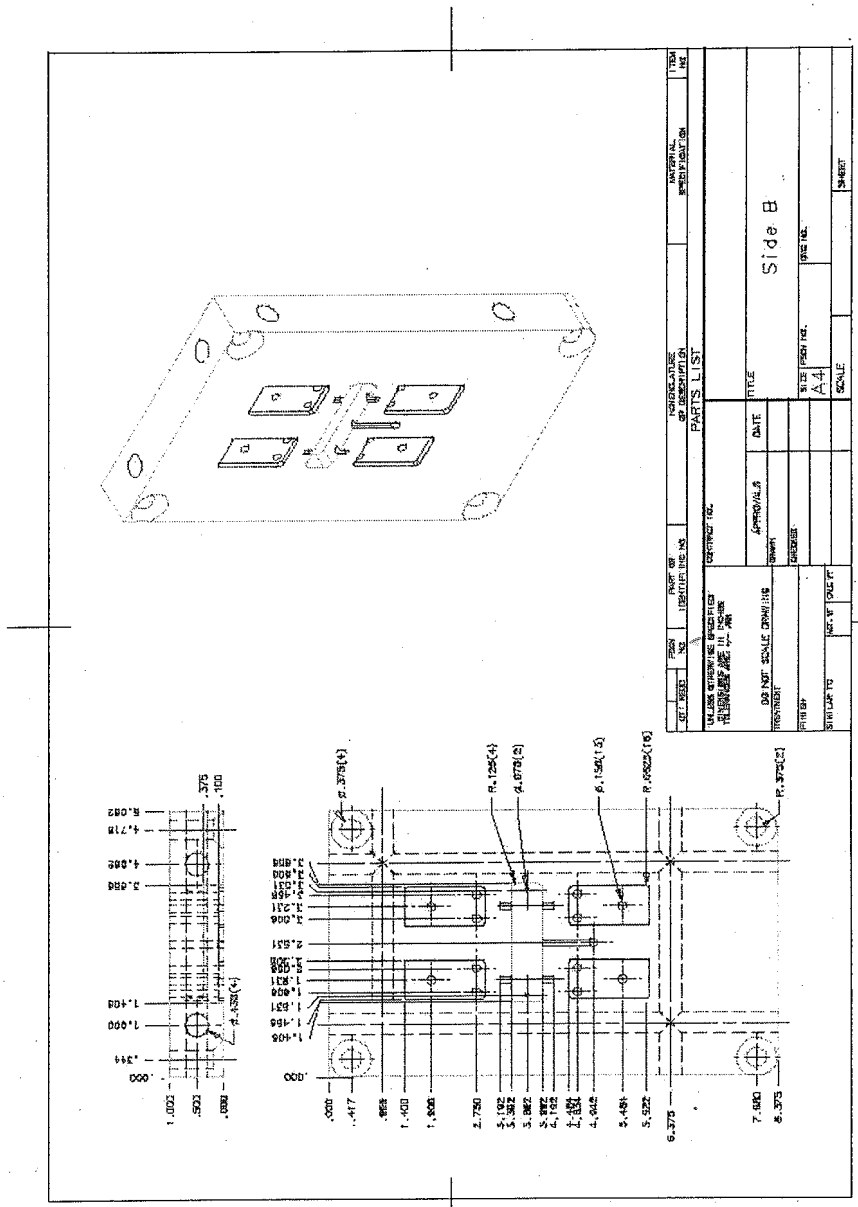

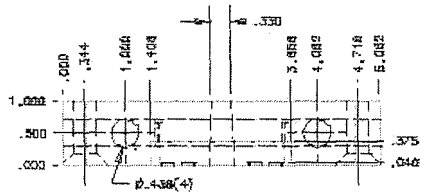

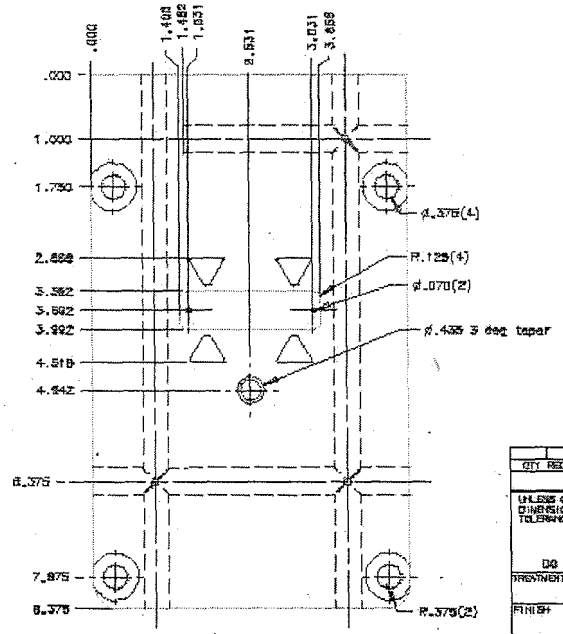

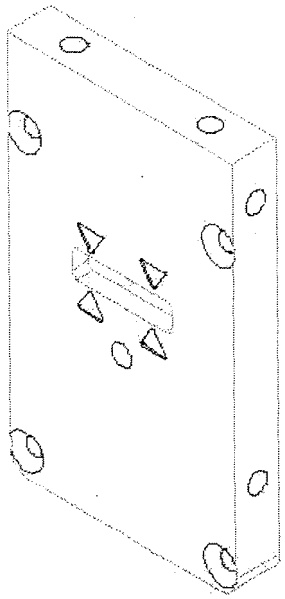

QTY REQD	PSN NO	PART OR IDENTIFYING NO	NOMENCLATURE OR DESCRIPTION	MATERIAL SPECIFICATION	ITEM NO
			PARTS LIST		

UNLESS OTHERWISE SPECIFIED DIMENSIONS ARE IN INCHES TOLERANCES ARE: +/- .001

DO NOT SCALE DRAWING

CONTRACT NO.

APPROVALS	DATE
DRAWN	
CHECKED	

FINISH

SIMILAR TO | MAT'L | CALC'T

TITLE: Side A

SIZE A4 | PSN NO. | DWG NO.

SCALE | SHEET

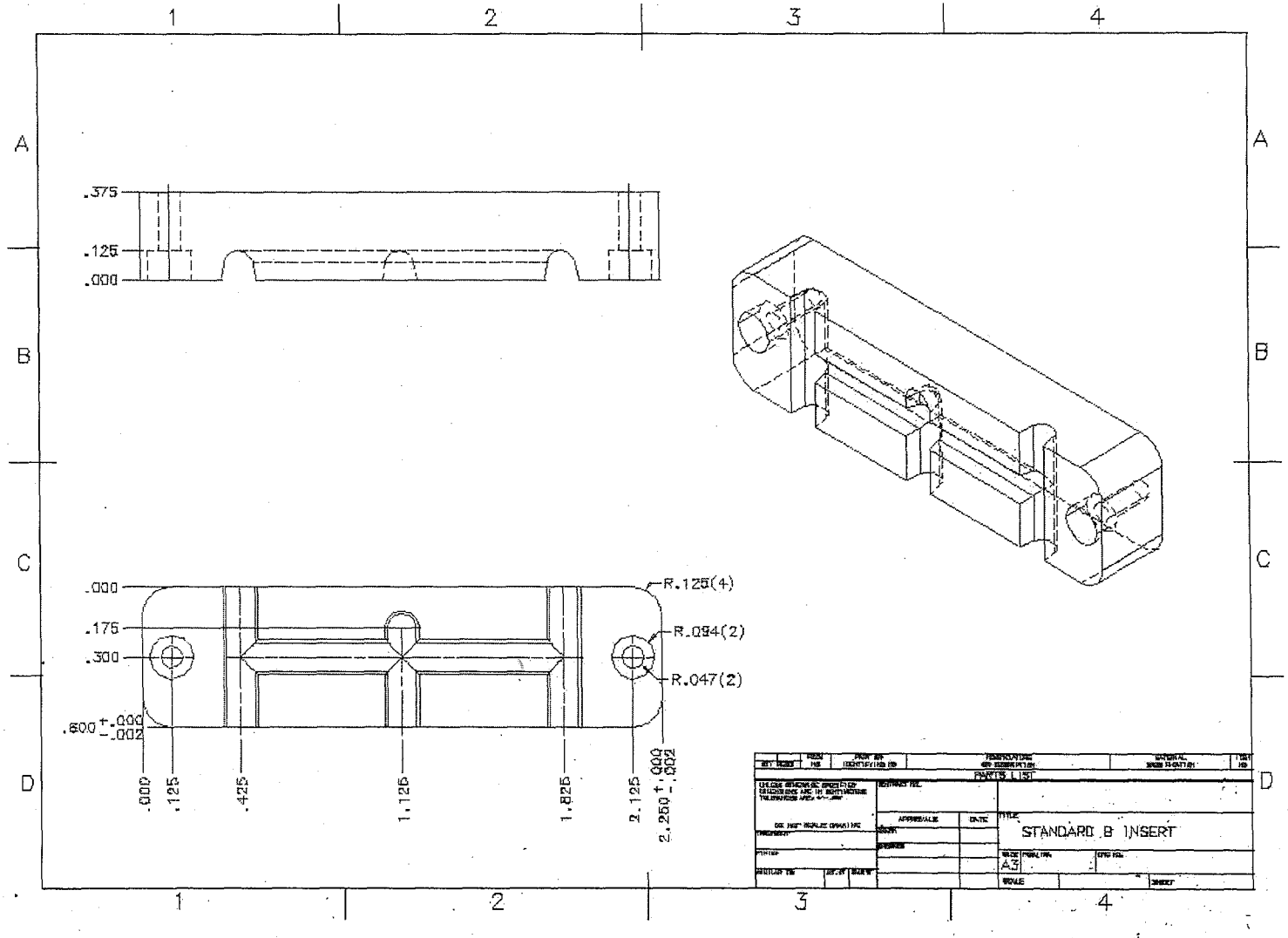
1
2
3
4
A
B
C
D
.375
.125
.000
.000
.175
.300
.600 +.000 -.002
R.125(4)
R.094(2)
R.047(2)
.000
.125
.425
1.125
1.825
2.125
2.250 +.000 -.002
PARTS LIST
STANDARD B INSERT
A3

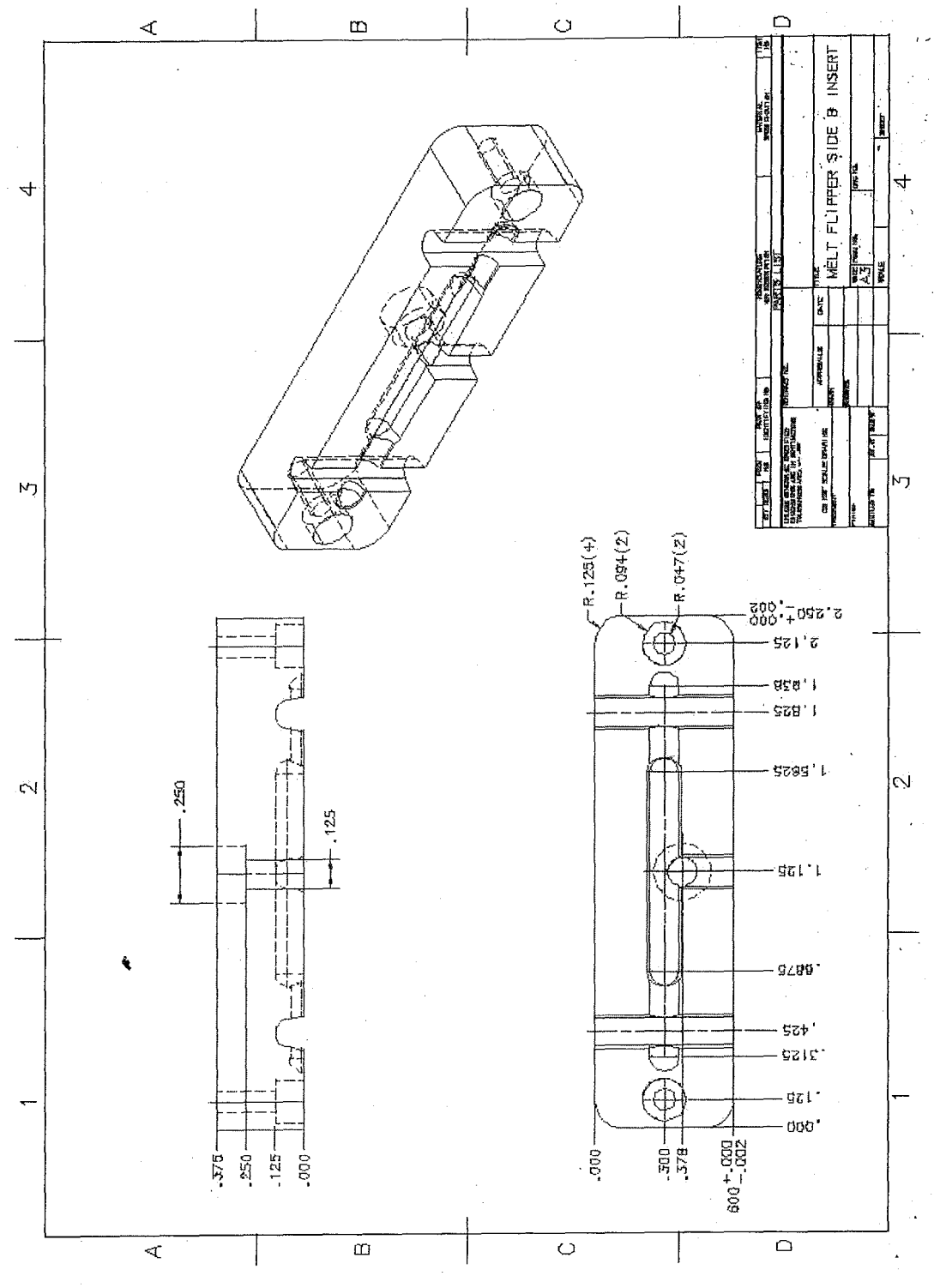
MELT FLIPPER SIDE B INSERT
R.125(4)
R.094(2)
R.047(2)
2.250+.000 -.002
2.125
1.858
1.825
1.5625
1.125
.6875
.425
.3125
.125
.000
.000
.300
.378
.600+.000 -.002
.250
.125
.376
.250
.125
.000

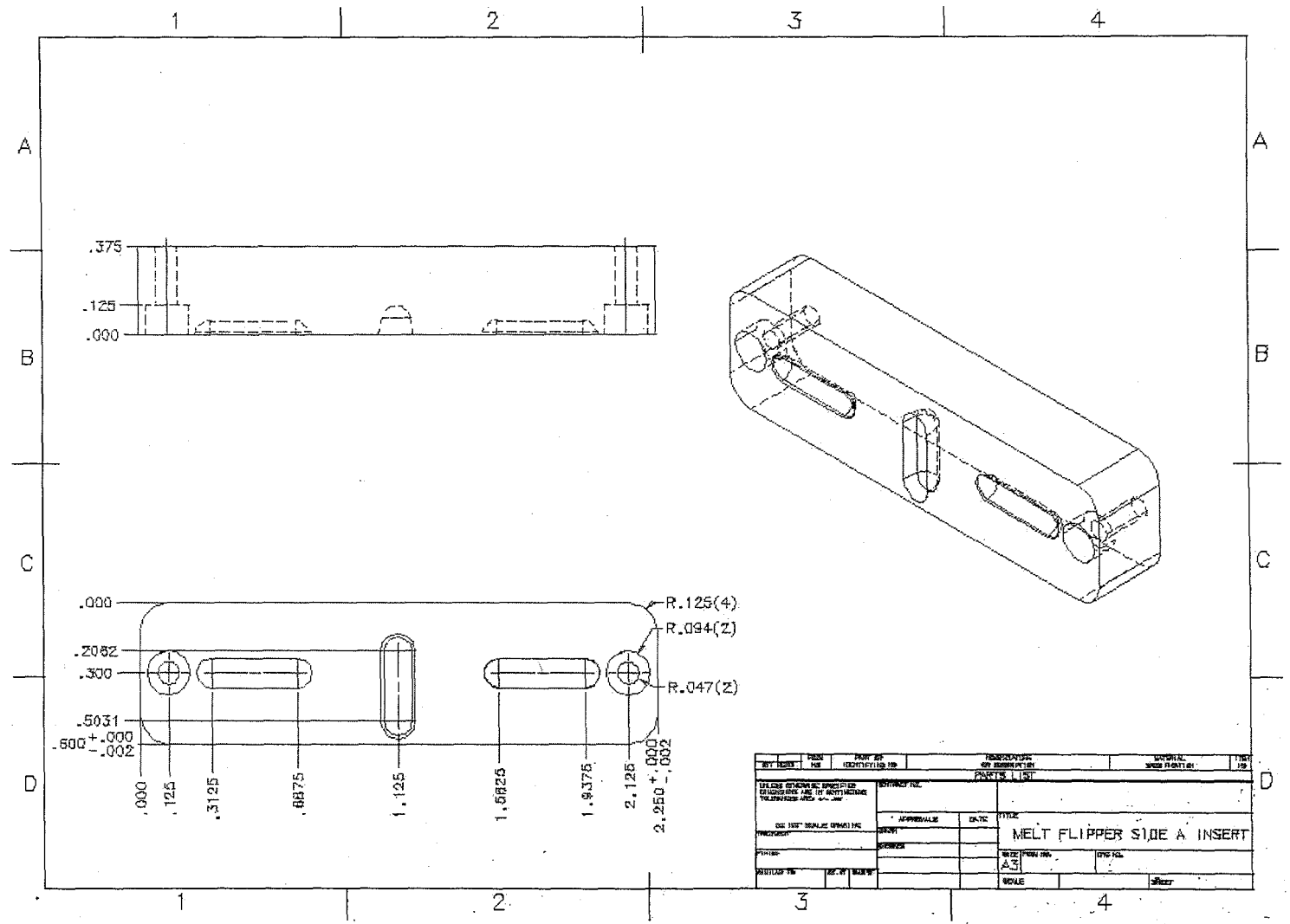
1
2
3
4
A
B
C
D
.375
.125
.000
.000
.2082
.300
.5031
.600 +.000 -.002
R.125(4)
R.094(2)
R.047(2)
.000
.125
.3125
.8875
1.125
1.5825
1.9375
2.126
2.250 +.000 -.002
MELT FLIPPER SIDE A INSERT

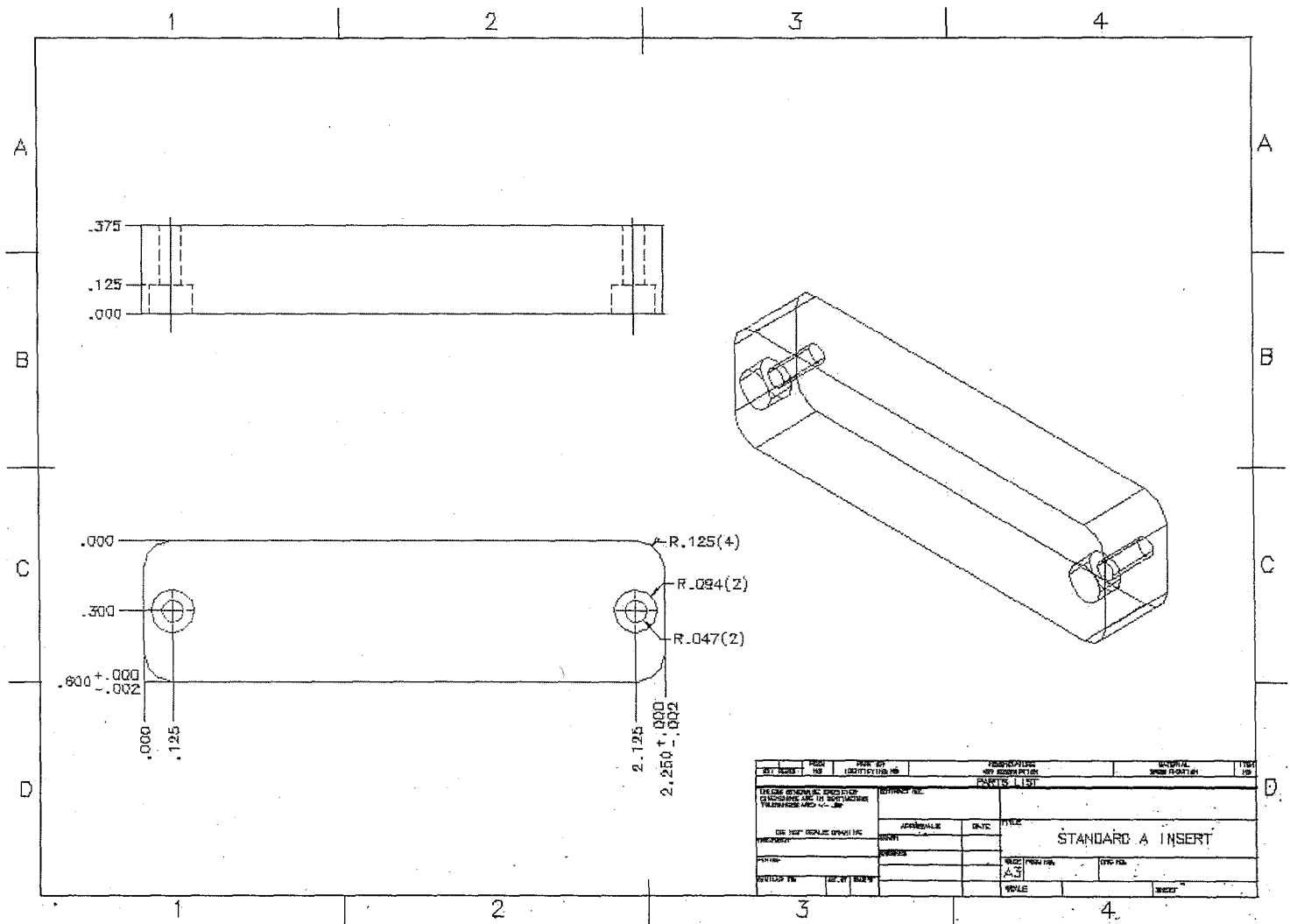
1
2
3
4
A
B
C
D
.375
.125
.000
.000
.300
.600 +.000 -.002
.000
.125
R.125(4)
R.094(2)
R.047(2)
2.125
2.250 +.000 -.002
PARTS LIST
STANDARD A INSERT
A3

Appendix B – Test Results for PC

Polycarbonate Low Injection Velocity

Normal Runner

	Cavities Weight							
Trial	1A	1B	2A	2B	Total Weight	Flow Group A	Flow Group B	Difference
1	1.455	1.373	1.557	1.349	5.734	0.525	0.475	0.051
2	1.488	1.383	1.578	1.373	5.822	0.527	0.473	0.053
3	1.491	1.375	1.561	1.356	5.783	0.528	0.472	0.056
4	1.468	1.367	1.561	1.346	5.742	0.528	0.472	0.055
5	1.436	1.373	1.538	1.333	5.680	0.524	0.476	0.047
6	1.464	1.376	1.558	1.354	5.752	0.525	0.475	0.051
7	1.445	1.353	1.519	1.343	5.660	0.524	0.476	0.047
8	1.387	1.345	1.497	1.332	5.561	0.519	0.481	0.037
9	1.279	1.330	1.425	1.272	5.306	0.510	0.490	0.019
10	1.418	1.353	1.523	1.323	5.617	0.524	0.476	0.047
					Average	0.523	0.477	0.046
					High	0.528	0.490	0.056
					Low	0.510	0.472	0.019
					Std Dev	0.005	0.005	

Melt Rotation 0

	Cavities Weight							
Trial	1A	1B	2A	2B	Total Weight	Flow Group A	Flow Group B	Difference
1	1.325	1.538	1.405	1.533	5.801	0.471	0.529	-0.059
2	1.296	1.536	1.391	1.526	5.749	0.467	0.533	-0.065
3	1.283	1.527	1.393	1.526	5.729	0.467	0.533	-0.066
4	1.307	1.525	1.384	1.519	5.735	0.469	0.531	-0.062
5	1.264	1.521	1.401	1.528	5.714	0.466	0.534	-0.067
6	1.262	1.537	1.354	1.521	5.674	0.461	0.539	-0.078
7	1.203	1.514	1.322	1.510	5.549	0.455	0.545	-0.090
8	1.228	1.516	1.332	1.498	5.574	0.459	0.541	-0.081
9	1.262	1.523	1.361	1.516	5.662	0.463	0.537	-0.073
10	1.199	1.507	1.329	1.506	5.541	0.456	0.544	-0.088
					Average	0.464	0.536	-0.073
					High	0.471	0.545	-0.059
					Low	0.455	0.529	-0.090
					Std Dev	0.005	0.005	

Melt Rotation 1

	Cavities Weight							
Trial	1A	1B	2A	2B	Total Weight	Flow Group A	Flow Group B	Difference
1	1.236	1.505	1.325	1.482	5.548	0.462	0.538	-0.077
2	1.268	1.483	1.369	1.492	5.612	0.470	0.530	-0.060
3	1.262	1.476	1.368	1.480	5.586	0.471	0.529	-0.058
4	1.261	1.491	1.362	1.489	5.603	0.468	0.532	-0.064
5	1.197	1.482	1.294	1.469	5.442	0.458	0.542	-0.085
6	1.186	1.485	1.321	1.480	5.472	0.458	0.542	-0.084
7	1.132	1.482	1.274	1.476	5.364	0.449	0.551	-0.103
8	1.185	1.497	1.284	1.482	5.448	0.453	0.547	-0.094
9	1.273	1.488	1.360	1.496	5.617	0.469	0.531	-0.062
10	1.228	1.489	1.328	1.481	5.526	0.463	0.537	-0.075
					Average	0.462	0.538	-0.076
					High	0.471	0.551	-0.058
					Low	0.449	0.529	-0.103
					Std Dev	0.008	0.008	

Melt Rotation 2

	Cavities Weight							
Trial	1A	1B	2A	2B	Total Weight	Flow Group A	Flow Group B	Difference
1	1.043	1.447	1.156	1.415	5.061	0.434	0.566	-0.131
2	1.147	1.509	1.267	1.480	5.403	0.447	0.553	-0.106
3	1.262	1.499	1.379	1.496	5.636	0.469	0.531	-0.063
4	1.184	1.514	1.290	1.491	5.479	0.452	0.548	-0.097
5	1.254	1.505	1.376	1.511	5.646	0.466	0.534	-0.068
6	1.209	1.498	1.323	1.477	5.507	0.460	0.540	-0.080
7	1.201	1.511	1.318	1.496	5.526	0.456	0.544	-0.088
8	1.203	1.482	1.329	1.477	5.491	0.461	0.539	-0.078
9	1.188	1.506	1.303	1.475	5.472	0.455	0.545	-0.090
10	1.114	1.505	1.258	1.482	5.359	0.443	0.557	-0.115
					Average	0.454	0.546	-0.092
					High	0.469	0.566	-0.063
					Low	0.434	0.531	-0.131
					Std Dev	0.011	0.011	

Melt Rotation 3

	Cavities Weight							
Trial	1A	1B	2A	2B	Total Weight	Flow Group A	Flow Group B	Difference
1	1.150	1.516	1.271	1.519	5.456	0.444	0.556	-0.113
2	1.255	1.519	1.355	1.514	5.643	0.463	0.537	-0.075
3	1.232	1.501	1.351	1.504	5.588	0.462	0.538	-0.076
4	1.224	1.500	1.345	1.503	5.572	0.461	0.539	-0.078
5	1.222	1.522	1.308	1.499	5.551	0.456	0.544	-0.088
6	1.168	1.497	1.280	1.475	5.420	0.452	0.548	-0.097
7	1.225	1.516	1.316	1.503	5.560	0.457	0.543	-0.086
8	1.208	1.499	1.307	1.496	5.510	0.456	0.544	-0.087
9	1.178	1.500	1.304	1.503	5.485	0.453	0.547	-0.095
10	1.147	1.516	1.272	1.495	5.430	0.445	0.555	-0.109
					Average	0.455	0.545	-0.090
					High	0.463	0.556	-0.075
					Low	0.444	0.537	-0.113
					Std Dev	0.007	0.007	

Melt Rotation 4

	Cavities Weight							
Trial	1A	1B	2A	2B	Total Weight	Flow Group A	Flow Group B	Difference
1	0.936	1.443	1.043	1.399	4.821	0.410	0.590	-0.179
2	0.882	1.372	1.010	1.367	4.631	0.409	0.591	-0.183
3	0.958	1.476	1.090	1.465	4.989	0.411	0.589	-0.179
4	0.906	1.376	1.031	1.367	4.680	0.414	0.586	-0.172
5	0.879	1.349	0.987	1.310	4.525	0.412	0.588	-0.175
6	0.735	1.186	0.853	1.172	3.946	0.402	0.598	-0.195
7	0.964	1.454	1.097	1.430	4.945	0.417	0.583	-0.166
8	0.809	1.229	0.918	1.203	4.159	0.415	0.585	-0.170
9	0.839	1.303	0.963	1.287	4.392	0.410	0.590	-0.179
10	0.883	1.343	1.000	1.322	4.548	0.414	0.586	-0.172
					Average	0.411	0.589	-0.177
					High	0.417	0.598	-0.166
					Low	0.402	0.583	-0.195
					Std Dev	0.004	0.004	

Melt Rotation 5

Cavities Weight

Trial	1A	1B	2A	2B	Total Weight	Flow Group A	Flow Group B	Difference
1	0.786	1.304	0.895	1.279	4.264	0.394	0.606	-0.212
2	0.736	1.247	0.833	1.216	4.032	0.389	0.611	-0.222
3	0.794	1.272	0.903	1.254	4.223	0.402	0.598	-0.196
4	0.907	1.447	1.036	1.425	4.815	0.404	0.596	-0.193
5	0.927	1.455	1.046	1.433	4.861	0.406	0.594	-0.188
6	0.806	1.299	0.914	1.279	4.298	0.400	0.600	-0.200
7	0.854	1.367	0.952	1.326	4.499	0.401	0.599	-0.197
8	0.844	1.369	0.961	1.354	4.528	0.399	0.601	-0.203
9	0.831	1.329	0.930	1.302	4.392	0.401	0.599	-0.198
10	0.903	1.429	1.025	1.417	4.774	0.404	0.596	-0.192
					Average	0.400	0.600	-0.200
					High	0.406	0.611	-0.188
					Low	0.389	0.594	-0.222
					Std Dev	0.005	0.005	

Melt Rotation 6

Cavities Weight

Trial	1A	1B	2A	2B	Total Weight	Flow Group A	Flow Group B	Difference
1	0.781	1.297	0.868	1.272	4.218	0.391	0.609	-0.218
2	0.711	1.250	0.811	1.225	3.997	0.381	0.619	-0.238
3	0.624	1.128	0.701	1.084	3.537	0.375	0.625	-0.251
4	0.767	1.310	0.851	1.259	4.187	0.386	0.614	-0.227
5	0.633	1.141	0.714	1.096	3.584	0.376	0.624	-0.248
6	0.696	1.226	0.799	1.207	3.928	0.381	0.619	-0.239
7	0.676	1.111	0.757	1.093	3.637	0.394	0.606	-0.212
8	0.762	1.307	0.852	1.275	4.196	0.385	0.615	-0.231
9	0.771	1.324	0.874	1.305	4.274	0.385	0.615	-0.230
10	0.696	1.234	0.783	1.211	3.924	0.377	0.623	-0.246
					Average	0.383	0.617	-0.234
					High	0.394	0.625	-0.212
					Low	0.375	0.606	-0.251
					Std Dev	0.006	0.006	

Polycarbonate Medium Injection Velocity

Normal Runner

	Cavities Weight							
Trial	1A	1B	2A	2B	Total Weight	Flow Group A	Flow Group B	Difference
1	1.591	1.354	1.644	1.358	5.947	0.544	0.456	0.088
2	1.561	1.349	1.618	1.341	5.869	0.542	0.458	0.083
3	1.579	1.357	1.618	1.340	5.894	0.542	0.458	0.085
4	1.583	1.348	1.648	1.353	5.932	0.545	0.455	0.089
5	1.562	1.328	1.597	1.328	5.815	0.543	0.457	0.087
6	1.562	1.348	1.626	1.355	5.891	0.541	0.459	0.082
7	1.560	1.366	1.621	1.359	5.906	0.539	0.461	0.077
8	1.545	1.329	1.586	1.332	5.792	0.541	0.459	0.081
9	1.550	1.352	1.642	1.352	5.896	0.541	0.459	0.083
10	1.559	1.345	1.631	1.344	5.879	0.543	0.457	0.085
					Average	0.542	0.458	0.084
					High	0.545	0.461	0.089
					Low	0.539	0.455	0.077
					Std Dev	0.002	0.002	

Melt Rotation 0

	Cavities Weight							
Trial	1A	1B	2A	2B	Total Weight	Flow Group A	Flow Group B	Difference
1	1.372	1.539	1.443	1.530	5.884	0.478	0.522	-0.043
2	1.344	1.511	1.460	1.537	5.852	0.479	0.521	-0.042
3	1.373	1.531	1.458	1.529	5.891	0.481	0.519	-0.039
4	1.359	1.531	1.424	1.527	5.841	0.476	0.524	-0.047
5	1.378	1.531	1.458	1.544	5.911	0.480	0.520	-0.040
6	1.369	1.531	1.435	1.519	5.854	0.479	0.521	-0.042
7	1.328	1.527	1.431	1.544	5.830	0.473	0.527	-0.054
8	1.325	1.507	1.434	1.524	5.790	0.477	0.523	-0.047
9	1.347	1.522	1.435	1.521	5.825	0.478	0.522	-0.045
10	1.331	1.515	1.426	1.521	5.793	0.476	0.524	-0.048
					Average	0.478	0.522	-0.045
					High	0.481	0.527	-0.039
					Low	0.473	0.519	-0.054
					Std Dev	0.002	0.002	

Melt Rotation 1

	Cavities Weight							
Trial	1A	1B	2A	2B	Total Weight	Flow Group A	Flow Group B	Difference
1	1.392	1.513	1.465	1.516	5.886	0.485	0.515	-0.029
2	1.399	1.508	1.484	1.528	5.919	0.487	0.513	-0.026
3	1.405	1.517	1.481	1.522	5.925	0.487	0.513	-0.026
4	1.397	1.508	1.474	1.513	5.892	0.487	0.513	-0.025
5	1.365	1.488	1.478	1.521	5.852	0.486	0.514	-0.028
6	1.358	1.495	1.463	1.505	5.821	0.485	0.515	-0.031
7	1.339	1.507	1.424	1.498	5.768	0.479	0.521	-0.042
8	1.342	1.499	1.454	1.507	5.802	0.482	0.518	-0.036
9	1.354	1.484	1.451	1.492	5.781	0.485	0.515	-0.030
10	1.368	1.500	1.469	1.516	5.853	0.485	0.515	-0.031
					Average	0.485	0.515	-0.030
					High	0.487	0.521	-0.025
					Low	0.479	0.513	-0.042
					Std Dev	0.003	0.003	

Melt Rotation 2

	Cavities Weight							
Trial	1A	1B	2A	2B	Total Weight	Flow Group A	Flow Group B	Difference
1	1.370	1.499	1.482	1.528	5.879	0.485	0.515	-0.030
2	1.391	1.495	1.474	1.517	5.877	0.487	0.513	-0.025
3	1.371	1.489	1.482	1.530	5.872	0.486	0.514	-0.028
4	1.337	1.506	1.448	1.517	5.808	0.480	0.520	-0.041
5	1.371	1.506	1.459	1.510	5.846	0.484	0.516	-0.032
6	1.380	1.495	1.476	1.505	5.856	0.488	0.512	-0.025
7	1.341	1.486	1.445	1.503	5.775	0.482	0.518	-0.035
8	1.351	1.484	1.446	1.486	5.767	0.485	0.515	-0.030
9	1.340	1.493	1.430	1.493	5.756	0.481	0.519	-0.038
10	1.362	1.493	1.462	1.515	5.832	0.484	0.516	-0.032
					Average	0.484	0.516	-0.031
					High	0.488	0.520	-0.025
					Low	0.480	0.512	-0.041
					Std Dev	0.003	0.003	

Melt Rotation 3

	Cavities Weight							
Trial	1A	1B	2A	2B	Total Weight	Flow Group A	Flow Group B	Difference
1	1.371	1.551	1.451	1.547	5.920	0.477	0.523	-0.047
2	1.354	1.527	1.449	1.525	5.855	0.479	0.521	-0.043
3	1.363	1.528	1.436	1.523	5.850	0.478	0.522	-0.043
4	1.371	1.525	1.464	1.535	5.895	0.481	0.519	-0.038
5	1.364	1.528	1.452	1.528	5.872	0.480	0.520	-0.041
6	1.346	1.535	1.424	1.533	5.838	0.474	0.526	-0.051
7	1.311	1.506	1.412	1.521	5.750	0.474	0.526	-0.053
8	1.318	1.509	1.401	1.515	5.743	0.473	0.527	-0.053
9	1.328	1.520	1.432	1.522	5.802	0.476	0.524	-0.049
10	1.349	1.529	1.437	1.529	5.844	0.477	0.523	-0.047
					Average	0.477	0.523	-0.046
					High	0.481	0.527	-0.038
					Low	0.473	0.519	-0.053
					Std Dev	0.003	0.003	

Melt Rotation 4

	Cavities Weight							
Trial	1A	1B	2A	2B	Total Weight	Flow Group A	Flow Group B	Difference
1	1.334	1.559	1.420	1.562	5.875	0.469	0.531	-0.062
2	1.321	1.561	1.413	1.554	5.849	0.467	0.533	-0.065
3	1.348	1.560	1.438	1.574	5.920	0.471	0.529	-0.059
4	1.322	1.556	1.411	1.563	5.852	0.467	0.533	-0.066
5	1.320	1.541	1.398	1.535	5.794	0.469	0.531	-0.062
6	1.311	1.540	1.399	1.539	5.789	0.468	0.532	-0.064
7	1.298	1.531	1.397	1.545	5.771	0.467	0.533	-0.066
8	1.287	1.538	1.368	1.534	5.727	0.464	0.536	-0.073
9	1.321	1.556	1.420	1.558	5.855	0.468	0.532	-0.064
10	1.299	1.543	1.396	1.556	5.794	0.465	0.535	-0.070
					Average	0.467	0.533	-0.065
					High	0.471	0.536	-0.059
					Low	0.464	0.529	-0.073
					Std Dev	0.002	0.002	

Melt Rotation 5

	Cavities Weight							
Trial	1A	1B	2A	2B	Total Weight	Flow Group A	Flow Group B	Difference
1	1.314	1.573	1.391	1.551	5.829	0.464	0.536	-0.072
2	1.307	1.580	1.388	1.583	5.858	0.460	0.540	-0.080
3	1.308	1.550	1.399	1.574	5.831	0.464	0.536	-0.072
4	1.294	1.557	1.395	1.588	5.834	0.461	0.539	-0.078
5	1.300	1.559	1.370	1.554	5.783	0.462	0.538	-0.077
6	1.297	1.569	1.386	1.569	5.821	0.461	0.539	-0.078
7	1.269	1.563	1.366	1.572	5.770	0.457	0.543	-0.087
8	1.249	1.553	1.331	1.554	5.687	0.454	0.546	-0.093
9	1.260	1.559	1.352	1.563	5.734	0.456	0.544	-0.089
10	1.258	1.550	1.353	1.557	5.718	0.457	0.543	-0.087
					Average	0.459	0.541	-0.081
					High	0.464	0.546	-0.072
					Low	0.454	0.536	-0.093
					Std Dev	0.004	0.004	

Melt Rotation 6

	Cavities Weight							
Trial	1A	1B	2A	2B	Total Weight	Flow Group A	Flow Group B	Difference
1	1.256	1.595	1.355	1.598	5.804	0.450	0.550	-0.100
2	1.261	1.601	1.361	1.602	5.825	0.450	0.550	-0.100
3	1.244	1.586	1.359	1.610	5.799	0.449	0.551	-0.102
4	1.247	1.592	1.331	1.598	5.768	0.447	0.553	-0.106
5	1.252	1.587	1.344	1.582	5.765	0.450	0.550	-0.099
6	1.241	1.578	1.353	1.599	5.771	0.449	0.551	-0.101
7	1.258	1.598	1.344	1.590	5.790	0.449	0.551	-0.101
8	1.246	1.579	1.350	1.591	5.766	0.450	0.550	-0.100
9	1.241	1.589	1.331	1.589	5.750	0.447	0.553	-0.105
10	1.221	1.579	1.321	1.581	5.702	0.446	0.554	-0.108
					Average	0.449	0.551	-0.102
					High	0.450	0.554	-0.099
					Low	0.446	0.550	-0.108
					Std Dev	0.002	0.002	

Polycarbonate High Injection Velocity

Normal Runner

	Cavities Weight							
Trial	1A	1B	2A	2B	Total Weight	Flow Group A	Flow Group B	Difference
1	1.661	1.359	1.715	1.371	6.106	0.553	0.447	0.106
2	1.684	1.388	1.727	1.389	6.188	0.551	0.449	0.102
3	1.695	1.389	1.708	1.383	6.175	0.551	0.449	0.102
4	1.662	1.383	1.718	1.395	6.158	0.549	0.451	0.098
5	1.676	1.394	1.698	1.378	6.146	0.549	0.451	0.098
6	1.549	1.434	1.748	1.433	6.164	0.535	0.465	0.070
7	1.668	1.354	1.711	1.361	6.094	0.554	0.446	0.109
8	1.656	1.356	1.714	1.368	6.094	0.553	0.447	0.106
9	1.641	1.369	1.745	1.403	6.158	0.550	0.450	0.100
10	1.689	1.410	1.743	1.415	6.257	0.549	0.451	0.097
					Average	0.549	0.451	0.099
					High	0.554	0.465	0.109
					Low	0.535	0.446	0.070
					Std Dev	0.005	0.005	

Melt Rotation 0

	Cavities Weight							
Trial	1A	1B	2A	2B	Total Weight	Flow Group A	Flow Group B	Difference
1	1.444	1.568	1.522	1.565	6.099	0.486	0.514	-0.027
2	1.418	1.540	1.520	1.574	6.052	0.485	0.515	-0.029
3	1.442	1.564	1.508	1.554	6.068	0.486	0.514	-0.028
4	1.453	1.579	1.506	1.572	6.110	0.484	0.516	-0.031
5	1.390	1.557	1.493	1.559	5.999	0.481	0.519	-0.039
6	1.439	1.576	1.514	1.577	6.106	0.484	0.516	-0.033
7	1.433	1.551	1.503	1.563	6.050	0.485	0.515	-0.029
8	1.435	1.556	1.504	1.552	6.047	0.486	0.514	-0.028
9	1.437	1.572	1.525	1.573	6.107	0.485	0.515	-0.030
10	1.441	1.561	1.525	1.568	6.095	0.487	0.513	-0.027
					Average	0.485	0.515	-0.030
					High	0.487	0.519	-0.027
					Low	0.481	0.513	-0.039
					Std Dev	0.002	0.002	

Melt Rotation 1

	Cavities Weight							
Trial	1A	1B	2A	2B	Total Weight	Flow Group A	Flow Group B	Difference
1	1.466	1.535	1.555	1.548	6.104	0.495	0.505	-0.010
2	1.464	1.540	1.543	1.558	6.105	0.493	0.507	-0.015
3	1.462	1.559	1.537	1.554	6.112	0.491	0.509	-0.019
4	1.467	1.537	1.545	1.546	6.095	0.494	0.506	-0.012
5	1.471	1.560	1.531	1.556	6.118	0.491	0.509	-0.019
6	1.479	1.568	1.545	1.562	6.154	0.491	0.509	-0.017
7	1.433	1.536	1.531	1.549	6.049	0.490	0.510	-0.020
8	1.433	1.532	1.537	1.549	6.051	0.491	0.509	-0.018
9	1.434	1.535	1.521	1.539	6.029	0.490	0.510	-0.020
10	1.462	1.553	1.523	1.562	6.100	0.489	0.511	-0.021
					Average	0.491	0.509	-0.017
					High	0.495	0.511	-0.010
					Low	0.489	0.505	-0.021
					Std Dev	0.002	0.002	

Melt Rotation 2

	Cavities Weight							
Trial	1A	1B	2A	2B	Total Weight	Flow Group A	Flow Group B	Difference
1	1.492	1.535	1.586	1.546	6.159	0.500	0.500	0.000
2	1.505	1.553	1.573	1.544	6.175	0.498	0.502	-0.003
3	1.488	1.562	1.576	1.562	6.188	0.495	0.505	-0.010
4	1.490	1.545	1.594	1.555	6.184	0.499	0.501	-0.003
5	1.495	1.567	1.580	1.573	6.215	0.495	0.505	-0.010
6	1.511	1.568	1.574	1.559	6.212	0.497	0.503	-0.007
7	1.435	1.514	1.533	1.511	5.993	0.495	0.505	-0.010
8	1.451	1.540	1.541	1.549	6.081	0.492	0.508	-0.016
9	1.484	1.557	1.570	1.570	6.181	0.494	0.506	-0.012
10	1.489	1.549	1.581	1.570	6.189	0.496	0.504	-0.008
					Average	0.496	0.504	-0.008
					High	0.500	0.508	0.000
					Low	0.492	0.500	-0.016
					Std Dev	0.002	0.002	

Melt Rotation 3

	Cavities Weight							
Trial	1A	1B	2A	2B	Total Weight	Flow Group A	Flow Group B	Difference
1	1.443	1.566	1.541	1.589	6.139	0.486	0.514	-0.028
2	1.445	1.563	1.529	1.591	6.128	0.485	0.515	-0.029
3	1.488	1.591	1.551	1.608	6.238	0.487	0.513	-0.026
4	1.462	1.585	1.566	1.603	6.216	0.487	0.513	-0.026
5	1.452	1.561	1.557	1.589	6.159	0.489	0.511	-0.023
6	1.444	1.545	1.535	1.562	6.086	0.489	0.511	-0.021
7	1.432	1.565	1.524	1.585	6.106	0.484	0.516	-0.032
8	1.459	1.585	1.529	1.577	6.150	0.486	0.514	-0.028
9	1.471	1.583	1.543	1.593	6.190	0.487	0.513	-0.026
10	1.437	1.574	1.528	1.601	6.140	0.483	0.517	-0.034
					Average	0.486	0.514	-0.027
					High	0.489	0.517	-0.021
					Low	0.483	0.511	-0.034
					Std Dev	0.002	0.002	

Melt Rotation 4

	Cavities Weight							
Trial	1A	1B	2A	2B	Total Weight	Flow Group A	Flow Group B	Difference
1	1.427	1.609	1.516	1.637	6.189	0.476	0.524	-0.049
2	1.431	1.599	1.509	1.627	6.166	0.477	0.523	-0.046
3	1.442	1.598	1.511	1.625	6.176	0.478	0.522	-0.044
4	1.434	1.618	1.523	1.641	6.216	0.476	0.524	-0.049
5	1.393	1.591	1.465	1.611	6.060	0.472	0.528	-0.057
6	1.390	1.605	1.482	1.633	6.110	0.470	0.530	-0.060
7	1.389	1.594	1.472	1.619	6.074	0.471	0.529	-0.058
8	1.409	1.611	1.488	1.639	6.147	0.471	0.529	-0.057
9	1.421	1.615	1.498	1.615	6.149	0.475	0.525	-0.051
10	1.434	1.624	1.504	1.631	6.193	0.474	0.526	-0.051
					Average	0.474	0.526	-0.052
					High	0.478	0.530	-0.044
					Low	0.470	0.522	-0.060
					Std Dev	0.003	0.003	

Melt Rotation 5

	Cavities Weight							
Trial	1A	1B	2A	2B	Total Weight	Flow Group A	Flow Group B	Difference
1	1.385	1.611	1.474	1.636	6.106	0.468	0.532	-0.064
2	1.404	1.618	1.472	1.616	6.110	0.471	0.529	-0.059
3	1.410	1.630	1.472	1.647	6.159	0.468	0.532	-0.064
4	1.405	1.625	1.485	1.652	6.167	0.469	0.531	-0.063
5	1.411	1.631	1.475	1.648	6.165	0.468	0.532	-0.064
6	1.396	1.624	1.467	1.639	6.126	0.467	0.533	-0.065
7	1.369	1.624	1.443	1.636	6.072	0.463	0.537	-0.074
8	1.408	1.637	1.492	1.663	6.200	0.468	0.532	-0.065
9	1.398	1.642	1.483	1.643	6.166	0.467	0.533	-0.066
10	1.409	1.621	1.485	1.637	6.152	0.470	0.530	-0.059
					Average	0.468	0.532	-0.064
					High	0.471	0.537	-0.059
					Low	0.463	0.529	-0.074
					Std Dev	0.002	0.002	

Melt Rotation 6

	Cavities Weight							
Trial	1A	1B	2A	2B	Total Weight	Flow Group A	Flow Group B	Difference
1	1.390	1.646	1.442	1.657	6.135	0.462	0.538	-0.077
2	1.379	1.650	1.442	1.652	6.123	0.461	0.539	-0.079
3	1.372	1.639	1.450	1.663	6.124	0.461	0.539	-0.078
4	1.337	1.621	1.401	1.634	5.993	0.457	0.543	-0.086
5	1.370	1.624	1.449	1.647	6.090	0.463	0.537	-0.074
6	1.357	1.617	1.422	1.634	6.030	0.461	0.539	-0.078
7	1.344	1.638	1.421	1.658	6.061	0.456	0.544	-0.088
8	1.341	1.620	1.401	1.638	6.000	0.457	0.543	-0.086
9	1.376	1.636	1.429	1.649	6.090	0.461	0.539	-0.079
10	1.351	1.618	1.421	1.636	6.026	0.460	0.540	-0.080
					Average	0.460	0.540	-0.080
					High	0.463	0.544	-0.074
					Low	0.456	0.537	-0.088
					Std Dev	0.002	0.002	

Appendix C – Test Results for PP

Polypropylene Low Injection Rate

Normal Runner

	Cavities Weight							
Trial	1A	1B	2A	2B	Total Weight	Flow Group A	Flow Group B	Difference
1	0.828	1.250	0.864	1.261	4.203	0.403	0.597	-0.195
2	0.819	1.221	0.849	1.233	4.122	0.405	0.595	-0.191
3	0.884	1.224	0.939	1.258	4.305	0.423	0.577	-0.153
4	0.839	1.237	0.874	1.245	4.195	0.408	0.592	-0.183
5	0.810	1.263	0.844	1.271	4.188	0.395	0.605	-0.210
6	0.821	1.249	0.865	1.259	4.194	0.402	0.598	-0.196
7	0.800	1.299	0.836	1.311	4.246	0.385	0.615	-0.229
8	0.790	1.275	0.827	1.291	4.183	0.387	0.613	-0.227
9	0.793	1.268	0.828	1.276	4.165	0.389	0.611	-0.222
10	0.794	1.309	0.726	1.293	4.122	0.369	0.631	-0.262
					Average	0.397	0.603	-0.207
					High	0.423	0.631	-0.153
					Low	0.369	0.577	-0.262
					Std Dev	0.015	0.015	

Melt Rotation 0

	Cavities Weight							
Trial	1A	1B	2A	2B	Total Weight	Flow Group A	Flow Group B	Difference
1	0.887	1.123	0.943	1.128	4.081	0.448	0.552	-0.103
2	0.883	1.141	0.939	1.147	4.110	0.443	0.557	-0.113
3	0.889	1.140	0.952	1.146	4.127	0.446	0.554	-0.108
4	0.890	1.143	0.942	1.147	4.122	0.444	0.556	-0.111
5	0.881	1.126	0.939	1.132	4.078	0.446	0.554	-0.107
6	0.874	1.148	0.921	1.153	4.096	0.438	0.562	-0.124
7	0.863	1.149	0.938	1.158	4.108	0.438	0.562	-0.123
8	0.873	1.136	0.930	1.143	4.082	0.442	0.558	-0.117
9	0.881	1.130	0.932	1.138	4.081	0.444	0.556	-0.111
10	0.874	1.125	0.927	1.129	4.055	0.444	0.556	-0.112
					Average	0.444	0.556	-0.113
					High	0.448	0.562	-0.103
					Low	0.438	0.552	-0.124
					Std Dev	0.003	0.003	

Melt Rotation 1

	Cavities Weight							
Trial	1A	1B	2A	2B	Total Weight	Flow Group A	Flow Group B	Difference
1	0.880	1.126	0.933	1.134	4.073	0.445	0.555	-0.110
2	0.905	1.158	0.963	1.162	4.188	0.446	0.554	-0.108
3	0.880	1.146	0.943	1.154	4.123	0.442	0.558	-0.116
4	0.904	1.122	0.951	1.128	4.105	0.452	0.548	-0.096
5	0.899	1.142	0.949	1.148	4.138	0.447	0.553	-0.107
6	0.873	1.134	0.929	1.141	4.077	0.442	0.558	-0.116
7	0.882	1.132	0.937	1.143	4.094	0.444	0.556	-0.111
8	0.888	1.154	0.940	1.159	4.141	0.441	0.559	-0.117
9	0.884	1.110	0.935	1.119	4.048	0.449	0.551	-0.101
10	0.892	1.144	0.949	1.155	4.140	0.445	0.555	-0.111
					Average	0.445	0.555	-0.109
					High	0.452	0.559	-0.096
					Low	0.441	0.548	-0.117
					Std Dev	0.003	0.003	

Melt Rotation 2

	Cavities Weight							
Trial	1A	1B	2A	2B	Total Weight	Flow Group A	Flow Group B	Difference
1	0.900	1.139	0.952	1.149	4.140	0.447	0.553	-0.105
2	0.891	1.132	0.945	1.144	4.112	0.446	0.554	-0.107
3	0.880	1.132	0.929	1.142	4.083	0.443	0.557	-0.114
4	0.886	1.130	0.935	1.139	4.090	0.445	0.555	-0.110
5	0.884	1.125	0.936	1.136	4.081	0.446	0.554	-0.108
6	0.879	1.131	0.929	1.141	4.080	0.443	0.557	-0.114
7	0.879	1.115	0.931	1.126	4.051	0.447	0.553	-0.106
8	0.850	1.108	0.898	1.117	3.973	0.440	0.560	-0.120
9	0.867	1.120	0.917	1.125	4.029	0.443	0.557	-0.114
10	0.858	1.138	0.913	1.146	4.055	0.437	0.563	-0.127
					Average	0.444	0.556	-0.112
					High	0.447	0.563	-0.105
					Low	0.437	0.553	-0.127
					Std Dev	0.003	0.003	

Melt Rotation 3

	Cavities Weight							
Trial	1A	1B	2A	2B	Total Weight	Flow Group A	Flow Group B	Difference
1	0.905	1.095	0.952	1.105	4.057	0.458	0.542	-0.085
2	0.903	1.117	0.955	1.132	4.107	0.452	0.548	-0.095
3	0.909	1.115	0.960	1.129	4.113	0.454	0.546	-0.091
4	0.909	1.115	0.959	1.132	4.115	0.454	0.546	-0.092
5	0.914	1.129	0.962	1.147	4.152	0.452	0.548	-0.096
6	0.903	1.123	0.955	1.140	4.121	0.451	0.549	-0.098
7	0.890	1.122	0.941	1.137	4.090	0.448	0.552	-0.105
8	0.875	1.120	0.921	1.129	4.045	0.444	0.556	-0.112
9	0.902	1.127	0.954	1.141	4.124	0.450	0.550	-0.100
10	0.901	1.117	0.948	1.129	4.095	0.452	0.548	-0.097
					Average	0.451	0.549	-0.097
					High	0.458	0.556	-0.085
					Low	0.444	0.542	-0.112
					Std Dev	0.004	0.004	

Melt Rotation 4

	Cavities Weight							
Trial	1A	1B	2A	2B	Total Weight	Flow Group A	Flow Group B	Difference
1	0.892	1.089	0.942	1.116	4.039	0.454	0.546	-0.092
2	0.897	1.101	0.951	1.127	4.076	0.453	0.547	-0.093
3	0.900	1.103	0.952	1.123	4.078	0.454	0.546	-0.092
4	0.886	1.091	0.937	1.113	4.027	0.453	0.547	-0.095
5	0.889	1.092	0.943	1.108	4.032	0.454	0.546	-0.091
6	0.889	1.095	0.939	1.116	4.039	0.453	0.547	-0.095
7	0.884	1.092	0.935	1.114	4.025	0.452	0.548	-0.096
8	0.887	1.102	0.938	1.122	4.049	0.451	0.549	-0.099
9	0.880	1.101	0.930	1.125	4.036	0.448	0.552	-0.103
10	0.909	1.090	0.962	1.110	4.071	0.460	0.540	-0.081
					Average	0.453	0.547	-0.094
					High	0.460	0.552	-0.081
					Low	0.448	0.540	-0.103
					Std Dev	0.003	0.003	

Melt Rotation 5

	Cavities Weight							
Trial	1A	1B	2A	2B	Total Weight	Flow Group A	Flow Group B	Difference
1	0.886	1.091	0.939	1.119	4.035	0.452	0.548	-0.095
2	0.897	1.083	0.949	1.113	4.042	0.457	0.543	-0.087
3	0.885	1.077	0.931	1.109	4.002	0.454	0.546	-0.092
4	0.899	1.080	0.948	1.108	4.035	0.458	0.542	-0.085
5	0.872	1.077	0.927	1.113	3.989	0.451	0.549	-0.098
6	0.891	1.100	0.945	1.131	4.067	0.451	0.549	-0.097
7	0.888	1.082	0.938	1.112	4.020	0.454	0.546	-0.092
8	0.842	1.083	0.894	1.113	3.932	0.442	0.558	-0.117
9	0.886	1.075	0.933	1.105	3.999	0.455	0.545	-0.090
10	0.876	1.085	0.927	1.120	4.008	0.450	0.550	-0.100
					Average	0.452	0.548	-0.095
					High	0.458	0.558	-0.085
					Low	0.442	0.542	-0.117
					Std Dev	0.005	0.005	

Melt Rotation 6

	Cavities Weight							
Trial	1A	1B	2A	2B	Total Weight	Flow Group A	Flow Group B	Difference
1	0.898	1.086	0.945	1.123	4.052	0.455	0.545	-0.090
2	0.898	1.079	0.948	1.118	4.043	0.457	0.543	-0.087
3	0.894	1.068	0.941	1.103	4.006	0.458	0.542	-0.084
4	0.897	1.072	0.944	1.111	4.024	0.458	0.542	-0.085
5	0.900	1.081	0.950	1.114	4.045	0.457	0.543	-0.085
6	0.882	1.084	0.935	1.125	4.026	0.451	0.549	-0.097
7	0.874	1.055	0.923	1.097	3.949	0.455	0.545	-0.090
8	0.880	1.065	0.929	1.099	3.973	0.455	0.545	-0.089
9	0.894	1.074	0.946	1.116	4.030	0.457	0.543	-0.087
10	0.882	1.073	0.932	1.109	3.996	0.454	0.546	-0.092
					Average	0.456	0.544	-0.089
					High	0.458	0.549	-0.084
					Low	0.451	0.542	-0.097
					Std Dev	0.002	0.002	

Polypropylene Medium Injection Rate

Normal Runner

Cavities Weight

Trial	1A	1B	2A	2B	Total Weight	Flow Group A	Flow Group B	Difference
1	1.143	1.217	1.165	1.228	4.753	0.486	0.514	-0.029
2	1.126	1.207	1.155	1.216	4.704	0.485	0.515	-0.030
3	1.102	1.167	1.124	1.177	4.570	0.487	0.513	-0.026
4	1.115	1.197	1.146	1.209	4.667	0.484	0.516	-0.031
5	1.113	1.196	1.140	1.207	4.656	0.484	0.516	-0.032
6	1.112	1.197	1.135	1.204	4.648	0.483	0.517	-0.033
7	1.109	1.197	1.136	1.208	4.650	0.483	0.517	-0.034
8	1.120	1.198	1.149	1.214	4.681	0.485	0.515	-0.031
9	1.124	1.205	1.151	1.218	4.698	0.484	0.516	-0.032
10	1.108	1.181	1.130	1.189	4.608	0.486	0.514	-0.029
					Average	0.485	0.515	-0.031
					High	0.487	0.517	-0.026
					Low	0.483	0.513	-0.034
					Std Dev	0.001	0.001	

Melt Rotation 0

Cavities Weight

Trial	1A	1B	2A	2B	Total Weight	Flow Group A	Flow Group B	Difference
1	1.101	1.192	1.146	1.212	4.651	0.483	0.517	-0.034
2	1.088	1.178	1.131	1.197	4.594	0.483	0.517	-0.034
3	1.088	1.177	1.130	1.196	4.591	0.483	0.517	-0.034
4	1.094	1.181	1.132	1.197	4.604	0.483	0.517	-0.033
5	1.107	1.195	1.148	1.215	4.665	0.483	0.517	-0.033
6	1.084	1.169	1.122	1.188	4.563	0.483	0.517	-0.033
7	1.094	1.182	1.132	1.200	4.608	0.483	0.517	-0.034
8	1.081	1.166	1.125	1.187	4.559	0.484	0.516	-0.032
9	1.045	1.105	1.073	1.126	4.349	0.487	0.513	-0.026
10	1.071	1.158	1.111	1.176	4.516	0.483	0.517	-0.034
					Average	0.484	0.516	-0.033
					High	0.487	0.517	-0.026
					Low	0.483	0.513	-0.034
					Std Dev	0.001	0.001	

Melt Rotation 1

Cavities Weight

Trial	1A	1B	2A	2B	Total Weight	Flow Group A	Flow Group B	Difference
1	1.138	1.217	1.163	1.231	4.749	0.485	0.515	-0.031
2	1.089	1.143	1.104	1.157	4.493	0.488	0.512	-0.024
3	1.078	1.176	1.119	1.195	4.568	0.481	0.519	-0.038
4	1.108	1.193	1.148	1.212	4.661	0.484	0.516	-0.032
5	1.098	1.183	1.138	1.207	4.626	0.483	0.517	-0.033
6	1.097	1.188	1.136	1.206	4.627	0.483	0.517	-0.035
7	1.111	1.209	1.152	1.228	4.700	0.481	0.519	-0.037
8	1.117	1.216	1.141	1.229	4.703	0.480	0.520	-0.040
9	1.119	1.210	1.153	1.234	4.716	0.482	0.518	-0.036
10	1.096	1.182	1.126	1.196	4.600	0.483	0.517	-0.034
					Average	0.483	0.517	-0.034
					High	0.488	0.520	-0.024
					Low	0.480	0.512	-0.040
					Std Dev	0.002	0.002	

Melt Rotation 2

	Cavities Weight							
Trial	1A	1B	2A	2B	Total Weight	Flow Group A	Flow Group B	Difference
1	1.114	1.202	1.151	1.221	4.688	0.483	0.517	-0.034
2	1.091	1.184	1.124	1.199	4.598	0.482	0.518	-0.037
3	1.113	1.211	1.151	1.225	4.700	0.482	0.518	-0.037
4	1.123	1.219	1.163	1.237	4.742	0.482	0.518	-0.036
5	1.078	1.161	1.106	1.178	4.523	0.483	0.517	-0.034
6	1.100	1.197	1.136	1.210	4.643	0.482	0.518	-0.037
7	1.106	1.199	1.142	1.215	4.662	0.482	0.518	-0.036
8	1.109	1.206	1.149	1.227	4.691	0.481	0.519	-0.037
9	1.095	1.195	1.127	1.211	4.628	0.480	0.520	-0.040
10	1.073	1.149	1.109	1.169	4.500	0.485	0.515	-0.030
					Average	0.482	0.518	-0.036
					High	0.485	0.520	-0.030
					Low	0.480	0.515	-0.040
					Std Dev	0.001	0.001	

Melt Rotation 3

	Cavities Weight							
Trial	1A	1B	2A	2B	Total Weight	Flow Group A	Flow Group B	Difference
1	1.086	1.186	1.124	1.202	4.598	0.481	0.519	-0.039
2	1.104	1.192	1.144	1.216	4.656	0.483	0.517	-0.034
3	1.099	1.192	1.132	1.211	4.634	0.481	0.519	-0.037
4	1.114	1.205	1.155	1.227	4.701	0.483	0.517	-0.035
5	1.081	1.167	1.115	1.186	4.549	0.483	0.517	-0.035
6	1.099	1.190	1.140	1.211	4.640	0.483	0.517	-0.035
7	1.091	1.187	1.126	1.205	4.609	0.481	0.519	-0.038
8	1.099	1.194	1.132	1.211	4.636	0.481	0.519	-0.038
9	1.104	1.203	1.140	1.222	4.669	0.481	0.519	-0.039
10	1.093	1.187	1.129	1.208	4.617	0.481	0.519	-0.037
					Average	0.482	0.518	-0.037
					High	0.483	0.519	-0.034
					Low	0.481	0.517	-0.039
					Std Dev	0.001	0.001	

Melt Rotation 4

	Cavities Weight							
Trial	1A	1B	2A	2B	Total Weight	Flow Group A	Flow Group B	Difference
1	1.110	1.190	1.151	1.214	4.665	0.485	0.515	-0.031
2	1.066	1.126	1.100	1.147	4.439	0.488	0.512	-0.024
3	1.106	1.183	1.149	1.209	4.647	0.485	0.515	-0.029
4	1.122	1.200	1.156	1.220	4.698	0.485	0.515	-0.030
5	1.085	1.153	1.123	1.177	4.538	0.487	0.513	-0.027
6	1.086	1.148	1.122	1.171	4.527	0.488	0.512	-0.025
7	1.087	1.165	1.126	1.187	4.565	0.485	0.515	-0.030
8	1.101	1.190	1.141	1.208	4.640	0.483	0.517	-0.034
9	1.099	1.184	1.141	1.207	4.631	0.484	0.516	-0.033
10	1.110	1.195	1.154	1.218	4.677	0.484	0.516	-0.032
					Average	0.485	0.515	-0.029
					High	0.488	0.517	-0.024
					Low	0.483	0.512	-0.034
					Std Dev	0.002	0.002	

Melt Rotation 5

Cavities Weight

Trial	1A	1B	2A	2B	Total Weight	Flow Group A	Flow Group B	Difference
1	1.111	1.185	1.149	1.206	4.651	0.486	0.514	-0.028
2	1.094	1.167	1.131	1.188	4.580	0.486	0.514	-0.028
3	1.094	1.168	1.129	1.187	4.578	0.486	0.514	-0.029
4	1.093	1.167	1.129	1.188	4.577	0.485	0.515	-0.029
5	1.104	1.183	1.139	1.199	4.625	0.485	0.515	-0.030
6	1.093	1.168	1.132	1.189	4.582	0.486	0.514	-0.029
7	1.103	1.183	1.140	1.201	4.627	0.485	0.515	-0.030
8	1.112	1.193	1.152	1.212	4.669	0.485	0.515	-0.030
9	1.108	1.184	1.140	1.202	4.634	0.485	0.515	-0.030
10	1.102	1.176	1.137	1.194	4.609	0.486	0.514	-0.028
					Average	0.485	0.515	-0.029
					High	0.486	0.515	-0.028
					Low	0.485	0.514	-0.030
					Std Dev	0.000	0.000	

Melt Rotation 6

Cavities Weight

Trial	1A	1B	2A	2B	Total Weight	Flow Group A	Flow Group B	Difference
1	1.097	1.171	1.137	1.192	4.597	0.486	0.514	-0.028
2	1.090	1.162	1.133	1.187	4.572	0.486	0.514	-0.028
3	1.105	1.175	1.147	1.199	4.626	0.487	0.513	-0.026
4	1.125	1.208	1.162	1.211	4.706	0.486	0.514	-0.028
5	1.076	1.139	1.113	1.164	4.492	0.487	0.513	-0.025
6	1.093	1.156	1.132	1.180	4.561	0.488	0.512	-0.024
7	1.096	1.175	1.137	1.198	4.606	0.485	0.515	-0.030
8	1.089	1.161	1.130	1.186	4.566	0.486	0.514	-0.028
9	1.076	1.142	1.110	1.161	4.489	0.487	0.513	-0.026
10	1.118	1.192	1.159	1.215	4.684	0.486	0.514	-0.028
					Average	0.486	0.514	-0.027
					High	0.488	0.515	-0.024
					Low	0.485	0.512	-0.030
					Std Dev	0.001	0.001	

Polypropylene High Injection Rate

Normal Runner

	Cavities Weight							
Trial	1A	1B	2A	2B	Total Weight	Flow Group A	Flow Group B	Difference
1	1.222	1.290	1.229	1.302	5.043	0.486	0.514	-0.028
2	1.203	1.269	1.219	1.284	4.975	0.487	0.513	-0.026
3	1.229	1.290	1.218	1.305	5.042	0.485	0.515	-0.029
4	1.196	1.263	1.216	1.282	4.957	0.487	0.513	-0.027
5	1.213	1.283	1.222	1.274	4.992	0.488	0.512	-0.024
6	1.221	1.197	1.254	1.226	4.898	0.505	0.495	0.011
7	1.240	1.229	1.276	1.254	4.999	0.503	0.497	0.007
8	1.219	1.302	1.226	1.301	5.048	0.484	0.516	-0.031
9	1.188	1.254	1.214	1.270	4.926	0.488	0.512	-0.025
10	1.200	1.262	1.213	1.275	4.950	0.487	0.513	-0.025
					Average	0.490	0.510	-0.020
					High	0.505	0.516	0.011
					Low	0.484	0.495	-0.031
					Std Dev	0.008	0.008	

Melt Rotation 0

	Cavities Weight							
Trial	1A	1B	2A	2B	Total Weight	Flow Group A	Flow Group B	Difference
1	1.184	1.260	1.221	1.282	4.947	0.486	0.514	-0.028
2	1.181	1.248	1.213	1.266	4.908	0.488	0.512	-0.024
3	1.184	1.259	1.213	1.278	4.934	0.486	0.514	-0.028
4	1.180	1.259	1.217	1.282	4.938	0.485	0.515	-0.029
5	1.169	1.248	1.209	1.271	4.897	0.486	0.514	-0.029
6	1.184	1.262	1.221	1.281	4.948	0.486	0.514	-0.028
7	1.176	1.249	1.209	1.267	4.901	0.487	0.513	-0.027
8	1.145	1.194	1.172	1.215	4.726	0.490	0.510	-0.019
9	1.177	1.266	1.218	1.292	4.953	0.484	0.516	-0.033
10	1.175	1.253	1.212	1.274	4.914	0.486	0.514	-0.028
					Average	0.486	0.514	-0.027
					High	0.490	0.516	-0.019
					Low	0.484	0.510	-0.033
					Std Dev	0.002	0.002	

Melt Rotation 1

	Cavities Weight							
Trial	1A	1B	2A	2B	Total Weight	Flow Group A	Flow Group B	Difference
1	1.183	1.255	1.216	1.278	4.932	0.486	0.514	-0.027
2	1.095	1.228	1.184	1.234	4.741	0.481	0.519	-0.039
3	1.195	1.275	1.219	1.294	4.983	0.484	0.516	-0.031
4	1.178	1.259	1.217	1.286	4.940	0.485	0.515	-0.030
5	1.199	1.275	1.231	1.295	5.000	0.486	0.514	-0.028
6	1.181	1.262	1.218	1.285	4.946	0.485	0.515	-0.030
7	1.188	1.267	1.222	1.288	4.965	0.485	0.515	-0.029
8	1.188	1.249	1.235	1.273	4.945	0.490	0.510	-0.020
9	1.195	1.274	1.234	1.297	5.000	0.486	0.514	-0.028
10	1.198	1.272	1.231	1.292	4.993	0.486	0.514	-0.027
					Average	0.486	0.514	-0.029
					High	0.490	0.519	-0.020
					Low	0.481	0.510	-0.039
					Std Dev	0.002	0.002	

Melt Rotation 2

	Cavities Weight							
Trial	1A	1B	2A	2B	Total Weight	Flow Group A	Flow Group B	Difference
1	1.186	1.263	1.221	1.286	4.956	0.486	0.514	-0.029
2	1.185	1.264	1.222	1.288	4.959	0.485	0.515	-0.029
3	1.185	1.267	1.223	1.287	4.962	0.485	0.515	-0.029
4	1.149	1.201	1.181	1.229	4.760	0.489	0.511	-0.021
5	1.178	1.256	1.215	1.279	4.928	0.486	0.514	-0.029
6	1.192	1.275	1.226	1.297	4.990	0.485	0.515	-0.031
7	1.177	1.261	1.212	1.282	4.932	0.484	0.516	-0.031
8	1.181	1.262	1.216	1.286	4.945	0.485	0.515	-0.031
9	1.176	1.255	1.212	1.278	4.921	0.485	0.515	-0.029
10	1.205	1.277	1.242	1.303	5.027	0.487	0.513	-0.026
					Average	0.486	0.514	-0.029
					High	0.489	0.516	-0.021
					Low	0.484	0.511	-0.031
					Std Dev	0.001	0.001	

Melt Rotation 3

	Cavities Weight							
Trial	1A	1B	2A	2B	Total Weight	Flow Group A	Flow Group B	Difference
1	1.139	1.191	1.165	1.214	4.709	0.489	0.511	-0.021
2	1.180	1.258	1.216	1.289	4.943	0.485	0.515	-0.031
3	1.174	1.251	1.206	1.276	4.907	0.485	0.515	-0.030
4	1.168	1.249	1.210	1.277	4.904	0.485	0.515	-0.030
5	1.177	1.260	1.228	1.280	4.945	0.486	0.514	-0.027
6	1.153	1.232	1.202	1.263	4.850	0.486	0.514	-0.029
7	1.174	1.253	1.209	1.279	4.915	0.485	0.515	-0.030
8	1.134	1.189	1.165	1.218	4.706	0.489	0.511	-0.023
9	1.185	1.268	1.225	1.294	4.972	0.485	0.515	-0.031
10	1.173	1.256	1.205	1.279	4.913	0.484	0.516	-0.032
					Average	0.486	0.514	-0.028
					High	0.489	0.516	-0.021
					Low	0.484	0.511	-0.032
					Std Dev	0.002	0.002	

Melt Rotation 4

	Cavities Weight							
Trial	1A	1B	2A	2B	Total Weight	Flow Group A	Flow Group B	Difference
1	1.219	1.306	1.258	1.331	5.114	0.484	0.516	-0.031
2	1.201	1.280	1.241	1.313	5.035	0.485	0.515	-0.030
3	1.206	1.290	1.245	1.314	5.055	0.485	0.515	-0.030
4	1.222	1.307	1.263	1.335	5.127	0.485	0.515	-0.031
5	1.234	1.317	1.270	1.343	5.164	0.485	0.515	-0.030
6	1.210	1.292	1.256	1.326	5.084	0.485	0.515	-0.030
7	1.203	1.289	1.247	1.320	5.059	0.484	0.516	-0.031
8	1.223	1.317	1.271	1.340	5.151	0.484	0.516	-0.032
9	1.194	1.271	1.232	1.297	4.994	0.486	0.514	-0.028
10	1.203	1.281	1.238	1.309	5.031	0.485	0.515	-0.030
					Average	0.485	0.515	-0.030
					High	0.486	0.516	-0.028
					Low	0.484	0.514	-0.032
					Std Dev	0.000	0.000	

Melt Rotation 5

	Cavities Weight							
Trial	1A	1B	2A	2B	Total Weight	Flow Group A	Flow Group B	Difference
1	1.198	1.268	1.238	1.299	5.003	0.487	0.513	-0.026
2	1.213	1.277	1.258	1.312	5.060	0.488	0.512	-0.023
3	1.203	1.275	1.252	1.313	5.043	0.487	0.513	-0.026
4	1.173	1.245	1.215	1.273	4.906	0.487	0.513	-0.026
5	1.199	1.275	1.240	1.305	5.019	0.486	0.514	-0.028
6	1.193	1.268	1.233	1.298	4.992	0.486	0.514	-0.028
7	1.201	1.275	1.241	1.306	5.023	0.486	0.514	-0.028
8	1.233	1.297	1.193	1.267	4.990	0.486	0.514	-0.028
9	1.212	1.291	1.252	1.320	5.075	0.486	0.514	-0.029
10	1.170	1.222	1.207	1.252	4.851	0.490	0.510	-0.020
					Average	0.487	0.513	-0.026
					High	0.490	0.514	-0.020
					Low	0.486	0.510	-0.029
					Std Dev	0.001	0.001	

Melt Rotation 6

	Cavities Weight							
Trial	1A	1B	2A	2B	Total Weight	Flow Group A	Flow Group B	Difference
1	1.192	1.257	1.230	1.287	4.966	0.488	0.512	-0.025
2	1.200	1.271	1.241	1.299	5.011	0.487	0.513	-0.026
3	1.167	1.220	1.203	1.251	4.841	0.490	0.510	-0.021
4	1.178	1.247	1.224	1.278	4.927	0.488	0.512	-0.025
5	1.196	1.261	1.232	1.289	4.978	0.488	0.512	-0.025
6	1.186	1.255	1.221	1.282	4.944	0.487	0.513	-0.026
7	1.204	1.228	1.245	1.259	4.936	0.496	0.504	-0.008
8	1.201	1.277	1.241	1.302	5.021	0.486	0.514	-0.027
9	1.182	1.252	1.226	1.285	4.945	0.487	0.513	-0.026
10	1.196	1.261	1.241	1.296	4.994	0.488	0.512	-0.024
					Average	0.488	0.512	-0.023
					High	0.496	0.514	-0.008
					Low	0.486	0.504	-0.027
					Std Dev	0.003	0.003	

Appendix D – Test Results for PA 6

Nylon Low Injection Rate

Normal Runner

	Cavities Weight							
Trial	**1A**	**1B**	**2A**	**2B**	**Total Weight**	**Flow Group A**	**Flow Group B**	**Difference**
1	1.329	1.458	1.368	1.478	5.633	0.479	0.521	-0.042
2	1.328	1.465	1.368	1.487	5.648	0.477	0.523	-0.045
3	1.336	1.478	1.380	1.499	5.693	0.477	0.523	-0.046
4	1.324	1.460	1.364	1.486	5.634	0.477	0.523	-0.046
5	1.316	1.456	1.359	1.478	5.609	0.477	0.523	-0.046
6	1.324	1.458	1.369	1.486	5.637	0.478	0.522	-0.045
7	1.326	1.470	1.377	1.499	5.672	0.477	0.523	-0.047
8	1.325	1.479	1.366	1.504	5.674	0.474	0.526	-0.051
9	1.341	1.474	1.384	1.502	5.701	0.478	0.522	-0.044
10	1.337	1.479	1.390	1.506	5.712	0.477	0.523	-0.045
					Average	0.477	0.523	-0.046
					High	0.479	0.526	-0.042
					Low	0.474	0.521	-0.051
					Std Dev	0.001	0.001	

Melt Rotation 0

	Cavities Weight							
Trial	**1A**	**1B**	**2A**	**2B**	**Total Weight**	**Flow Group A**	**Flow Group B**	**Difference**
1	1.366	1.436	1.414	1.468	5.684	0.489	0.511	-0.022
2	1.345	1.435	1.393	1.468	5.641	0.485	0.515	-0.029
3	1.331	1.439	1.388	1.468	5.626	0.483	0.517	-0.033
4	1.330	1.438	1.385	1.467	5.620	0.483	0.517	-0.034
5	1.335	1.444	1.391	1.475	5.645	0.483	0.517	-0.034
6	1.324	1.443	1.381	1.473	5.621	0.481	0.519	-0.038
7	1.314	1.439	1.372	1.473	5.598	0.480	0.520	-0.040
8	1.319	1.432	1.377	1.466	5.594	0.482	0.518	-0.036
9	1.311	1.432	1.381	1.473	5.597	0.481	0.519	-0.038
10	1.321	1.437	1.394	1.472	5.624	0.483	0.517	-0.034
					Average	0.483	0.517	-0.034
					High	0.489	0.520	-0.022
					Low	0.480	0.511	-0.040
					Std Dev	0.003	0.003	

Melt Rotation 1

	Cavities Weight							
Trial	**1A**	**1B**	**2A**	**2B**	**Total Weight**	**Flow Group A**	**Flow Group B**	**Difference**
1	1.375	1.452	1.417	1.482	5.726	0.488	0.512	-0.025
2	1.362	1.438	1.411	1.472	5.683	0.488	0.512	-0.024
3	1.341	1.445	1.396	1.471	5.653	0.484	0.516	-0.032
4	1.332	1.441	1.386	1.470	5.629	0.483	0.517	-0.034
5	1.322	1.434	1.377	1.467	5.600	0.482	0.518	-0.036
6	1.319	1.442	1.376	1.469	5.606	0.481	0.519	-0.039
7	1.281	1.449	1.395	1.484	5.609	0.477	0.523	-0.046
8	1.341	1.452	1.393	1.486	5.672	0.482	0.518	-0.036
9	1.320	1.444	1.373	1.467	5.604	0.481	0.519	-0.039
10	1.320	1.437	1.382	1.473	5.612	0.481	0.519	-0.037
					Average	0.483	0.517	-0.035
					High	0.488	0.523	-0.024
					Low	0.477	0.512	-0.046
					Std Dev	0.003	0.003	

Melt Rotation 2

Cavities Weight

Trial	1A	1B	2A	2B	Total Weight	Flow Group A	Flow Group B	Difference
1	1.324	1.445	1.385	1.474	5.628	0.481	0.519	-0.037
2	1.331	1.446	1.385	1.477	5.639	0.482	0.518	-0.037
3	1.330	1.436	1.383	1.470	5.619	0.483	0.517	-0.034
4	1.325	1.442	1.380	1.468	5.615	0.482	0.518	-0.037
5	1.324	1.440	1.374	1.470	5.608	0.481	0.519	-0.038
6	1.324	1.441	1.370	1.468	5.603	0.481	0.519	-0.038
7	1.322	1.438	1.374	1.468	5.602	0.481	0.519	-0.037
8	1.322	1.425	1.394	1.484	5.625	0.483	0.517	-0.034
9	1.314	1.439	1.373	1.473	5.599	0.480	0.520	-0.040
10	1.307	1.438	1.368	1.467	5.580	0.479	0.521	-0.041
					Average	0.481	0.519	-0.037
					High	0.483	0.521	-0.034
					Low	0.479	0.517	-0.041
					Std Dev	0.001	0.001	

Melt Rotation 3

Cavities Weight

Trial	1A	1B	2A	2B	Total Weight	Flow Group A	Flow Group B	Difference
1	1.350	1.456	1.399	1.489	5.694	0.483	0.517	-0.034
2	1.327	1.450	1.382	1.480	5.639	0.480	0.520	-0.039
3	1.333	1.446	1.384	1.473	5.636	0.482	0.518	-0.036
4	1.326	1.438	1.380	1.469	5.613	0.482	0.518	-0.036
5	1.323	1.435	1.379	1.465	5.602	0.482	0.518	-0.035
6	1.323	1.434	1.375	1.469	5.601	0.482	0.518	-0.037
7	1.316	1.428	1.369	1.456	5.569	0.482	0.518	-0.036
8	1.326	1.433	1.376	1.463	5.598	0.483	0.517	-0.035
9	1.317	1.441	1.374	1.471	5.603	0.480	0.520	-0.039
10	1.319	1.439	1.370	1.469	5.597	0.480	0.520	-0.039
					Average	0.482	0.518	-0.037
					High	0.483	0.520	-0.034
					Low	0.480	0.517	-0.039
					Std Dev	0.001	0.001	

Melt Rotation 4

Cavities Weight

Trial	1A	1B	2A	2B	Total Weight	Flow Group A	Flow Group B	Difference
1	1.350	1.434	1.399	1.478	5.661	0.486	0.514	-0.029
2	1.321	1.443	1.381	1.477	5.622	0.481	0.519	-0.039
3	1.328	1.435	1.382	1.466	5.611	0.483	0.517	-0.034
4	1.328	1.432	1.383	1.461	5.604	0.484	0.516	-0.032
5	1.327	1.425	1.378	1.455	5.585	0.484	0.516	-0.031
6	1.326	1.429	1.376	1.458	5.589	0.483	0.517	-0.033
7	1.322	1.423	1.380	1.454	5.579	0.484	0.516	-0.031
8	1.323	1.419	1.371	1.456	5.569	0.484	0.516	-0.033
9	1.317	1.430	1.377	1.466	5.590	0.482	0.518	-0.036
10	1.329	1.431	1.382	1.458	5.600	0.484	0.516	-0.032
					Average	0.483	0.517	-0.033
					High	0.486	0.519	-0.029
					Low	0.481	0.514	-0.039
					Std Dev	0.001	0.001	

Melt Rotation 5

Cavities Weight

Trial	1A	1B	2A	2B	Total Weight	Flow Group A	Flow Group B	Difference
1	1.351	1.425	1.395	1.463	5.634	0.487	0.513	-0.025
2	1.325	1.423	1.368	1.449	5.565	0.484	0.516	-0.032
3	1.333	1.432	1.377	1.452	5.594	0.484	0.516	-0.031
4	1.321	1.415	1.375	1.452	5.563	0.485	0.515	-0.031
5	1.323	1.419	1.383	1.458	5.583	0.485	0.515	-0.031
6	1.326	1.426	1.384	1.454	5.590	0.485	0.515	-0.030
7	1.320	1.417	1.379	1.451	5.567	0.485	0.515	-0.030
8	1.334	1.432	1.394	1.458	5.618	0.486	0.514	-0.029
9	1.338	1.427	1.397	1.469	5.631	0.486	0.514	-0.029
10	1.332	1.421	1.379	1.451	5.583	0.486	0.514	-0.029
					Average	0.485	0.515	-0.030
					High	0.487	0.516	-0.025
					Low	0.484	0.513	-0.032
					Std Dev	0.001	0.001	

Melt Rotation 6

Cavities Weight

Trial	1A	1B	2A	2B	Total Weight	Flow Group A	Flow Group B	Difference
1	1.343	1.419	1.387	1.447	5.596	0.488	0.512	-0.024
2	1.325	1.424	1.365	1.467	5.581	0.482	0.518	-0.036
3	1.328	1.426	1.368	1.449	5.571	0.484	0.516	-0.032
4	1.320	1.444	1.376	1.473	5.613	0.480	0.520	-0.039
5	1.291	1.429	1.389	1.472	5.581	0.480	0.520	-0.040
6	1.318	1.427	1.377	1.464	5.586	0.482	0.518	-0.035
7	1.313	1.422	1.372	1.452	5.559	0.483	0.517	-0.034
8	1.319	1.424	1.355	1.449	5.547	0.482	0.518	-0.036
9	1.308	1.420	1.373	1.454	5.555	0.483	0.517	-0.035
10	1.310	1.412	1.357	1.440	5.519	0.483	0.517	-0.034
					Average	0.483	0.517	-0.034
					High	0.488	0.520	-0.024
					Low	0.480	0.512	-0.040
					Std Dev	0.002	0.002	

Nylon Medium Injection Rate

Normal Runner

Cavities Weight

Trial	1A	1B	2A	2B	Total Weight	Flow Group A	Flow Group B	Difference
1	1.512	1.485	1.548	1.518	6.063	0.505	0.495	0.009
2	1.503	1.477	1.538	1.512	6.030	0.504	0.496	0.009
3	1.510	1.481	1.544	1.512	6.047	0.505	0.495	0.010
4	1.514	1.489	1.554	1.525	6.082	0.504	0.496	0.009
5	1.514	1.491	1.551	1.524	6.080	0.504	0.496	0.008
6	1.483	1.479	1.550	1.522	6.034	0.503	0.497	0.005
7	1.516	1.485	1.549	1.518	6.068	0.505	0.495	0.010
8	1.535	1.507	1.551	1.524	6.117	0.504	0.496	0.009
9	1.508	1.487	1.546	1.512	6.053	0.505	0.495	0.009
10	1.501	1.484	1.582	1.520	6.087	0.506	0.494	0.013
					Average	0.505	0.495	0.009
					High	0.506	0.497	0.013
					Low	0.503	0.494	0.005
					Std Dev	0.001	0.001	

Melt Rotation 0

Cavities Weight

Trial	1A	1B	2A	2B	Total Weight	Flow Group A	Flow Group B	Difference
1	1.460	1.501	1.518	1.534	6.013	0.495	0.505	-0.009
2	1.449	1.493	1.503	1.527	5.972	0.494	0.506	-0.011
3	1.450	1.496	1.503	1.526	5.975	0.494	0.506	-0.012
4	1.446	1.490	1.499	1.526	5.961	0.494	0.506	-0.012
5	1.445	1.487	1.489	1.512	5.933	0.495	0.505	-0.011
6	1.441	1.492	1.497	1.522	5.952	0.494	0.506	-0.013
7	1.455	1.498	1.505	1.531	5.989	0.494	0.506	-0.012
8	1.445	1.495	1.496	1.526	5.962	0.493	0.507	-0.013
9	1.439	1.482	1.491	1.520	5.932	0.494	0.506	-0.012
10	1.447	1.487	1.496	1.517	5.947	0.495	0.505	-0.010
					Average	0.494	0.506	-0.012
					High	0.495	0.507	-0.009
					Low	0.493	0.505	-0.013
					Std Dev	0.001	0.001	

Melt Rotation 1

Cavities Weight

Trial	1A	1B	2A	2B	Total Weight	Flow Group A	Flow Group B	Difference
1	1.465	1.493	1.514	1.527	5.999	0.497	0.503	-0.007
2	1.439	1.491	1.489	1.534	5.953	0.492	0.508	-0.016
3	1.455	1.487	1.503	1.520	5.965	0.496	0.504	-0.008
4	1.443	1.478	1.497	1.514	5.932	0.496	0.504	-0.009
5	1.446	1.480	1.498	1.516	5.940	0.496	0.504	-0.009
6	1.445	1.481	1.496	1.512	5.934	0.496	0.504	-0.009
7	1.448	1.483	1.500	1.518	5.949	0.496	0.504	-0.009
8	1.441	1.486	1.495	1.515	5.937	0.495	0.505	-0.011
9	1.444	1.485	1.496	1.514	5.939	0.495	0.505	-0.010
10	1.441	1.478	1.494	1.520	5.933	0.495	0.505	-0.011
					Average	0.495	0.505	-0.010
					High	0.497	0.508	-0.007
					Low	0.492	0.503	-0.016
					Std Dev	0.001	0.001	

Melt Rotation 2

	Cavities Weight							
Trial	1A	1B	2A	2B	Total Weight	Flow Group A	Flow Group B	Difference
1	1.455	1.469	1.512	1.506	5.942	0.499	0.501	-0.001
2	1.468	1.489	1.519	1.527	6.003	0.498	0.502	-0.005
3	1.449	1.485	1.509	1.525	5.968	0.496	0.504	-0.009
4	1.450	1.483	1.497	1.514	5.944	0.496	0.504	-0.008
5	1.439	1.479	1.493	1.511	5.922	0.495	0.505	-0.010
6	1.428	1.470	1.484	1.502	5.884	0.495	0.505	-0.010
7	1.449	1.479	1.485	1.539	5.952	0.493	0.507	-0.014
8	1.445	1.481	1.494	1.511	5.931	0.496	0.504	-0.009
9	1.431	1.471	1.486	1.507	5.895	0.495	0.505	-0.010
10	1.445	1.481	1.498	1.517	5.941	0.495	0.505	-0.009
					Average	0.496	0.504	-0.009
					High	0.499	0.507	-0.001
					Low	0.493	0.501	-0.014
					Std Dev	0.002	0.002	

Melt Rotation 3

	Cavities Weight							
Trial	1A	1B	2A	2B	Total Weight	Flow Group A	Flow Group B	Difference
1	1.446	1.494	1.502	1.535	5.977	0.493	0.507	-0.014
2	1.447	1.499	1.501	1.539	5.986	0.492	0.508	-0.015
3	1.444	1.497	1.484	1.519	5.944	0.493	0.507	-0.015
4	1.439	1.493	1.494	1.527	5.953	0.493	0.507	-0.015
5	1.443	1.488	1.496	1.525	5.952	0.494	0.506	-0.012
6	1.440	1.488	1.494	1.524	5.946	0.493	0.507	-0.013
7	1.428	1.464	1.463	1.528	5.883	0.491	0.509	-0.017
8	1.432	1.468	1.472	1.556	5.928	0.490	0.510	-0.020
9	1.436	1.484	1.486	1.516	5.922	0.493	0.507	-0.013
10	1.436	1.476	1.467	1.497	5.876	0.494	0.506	-0.012
					Average	0.493	0.507	-0.015
					High	0.494	0.510	-0.012
					Low	0.490	0.506	-0.020
					Std Dev	0.001	0.001	

Melt Rotation 4

	Cavities Weight							
Trial	1A	1B	2A	2B	Total Weight	Flow Group A	Flow Group B	Difference
1	1.431	1.490	1.478	1.522	5.921	0.491	0.509	-0.017
2	1.429	1.496	1.485	1.524	5.934	0.491	0.509	-0.018
3	1.438	1.484	1.485	1.521	5.928	0.493	0.507	-0.014
4	1.438	1.489	1.491	1.525	5.943	0.493	0.507	-0.014
5	1.433	1.485	1.478	1.519	5.915	0.492	0.508	-0.016
6	1.423	1.458	1.473	1.529	5.883	0.492	0.508	-0.015
7	1.426	1.476	1.479	1.511	5.892	0.493	0.507	-0.014
8	1.431	1.486	1.480	1.522	5.919	0.492	0.508	-0.016
9	1.429	1.485	1.479	1.513	5.906	0.492	0.508	-0.015
10	1.438	1.484	1.485	1.517	5.924	0.493	0.507	-0.013
					Average	0.492	0.508	-0.015
					High	0.493	0.509	-0.013
					Low	0.491	0.507	-0.018
					Std Dev	0.001	0.001	

Melt Rotation 5

	Cavities Weight							
Trial	1A	1B	2A	2B	Total Weight	Flow Group A	Flow Group B	Difference
1	1.447	1.500	1.496	1.533	5.976	0.492	0.508	-0.015
2	1.438	1.502	1.490	1.531	5.961	0.491	0.509	-0.018
3	1.431	1.490	1.471	1.505	5.897	0.492	0.508	-0.016
4	1.430	1.482	1.480	1.516	5.908	0.493	0.507	-0.015
5	1.434	1.486	1.483	1.519	5.922	0.493	0.507	-0.015
6	1.425	1.477	1.471	1.506	5.879	0.493	0.507	-0.015
7	1.422	1.464	1.470	1.501	5.857	0.494	0.506	-0.012
8	1.413	1.472	1.495	1.524	5.904	0.493	0.507	-0.015
9	1.429	1.485	1.484	1.517	5.915	0.492	0.508	-0.015
10	1.416	1.465	1.468	1.501	5.850	0.493	0.507	-0.014
					Average	0.493	0.507	-0.015
					High	0.494	0.509	-0.012
					Low	0.491	0.506	-0.018
					Std Dev	0.001	0.001	

Melt Rotation 6

	Cavities Weight							
Trial	1A	1B	2A	2B	Total Weight	Flow Group A	Flow Group B	Difference
1	1.451	1.497	1.503	1.545	5.996	0.493	0.507	-0.015
2	1.433	1.499	1.481	1.537	5.950	0.490	0.510	-0.021
3	1.434	1.500	1.484	1.537	5.955	0.490	0.510	-0.020
4	1.435	1.486	1.482	1.519	5.922	0.493	0.507	-0.015
5	1.430	1.488	1.484	1.527	5.929	0.491	0.509	-0.017
6	1.414	1.475	1.470	1.506	5.865	0.492	0.508	-0.017
7	1.420	1.472	1.471	1.512	5.875	0.492	0.508	-0.016
8	1.430	1.476	1.478	1.519	5.903	0.493	0.507	-0.015
9	1.427	1.481	1.476	1.519	5.903	0.492	0.508	-0.016
10	1.419	1.469	1.467	1.508	5.863	0.492	0.508	-0.016
					Average	0.492	0.508	-0.017
					High	0.493	0.510	-0.015
					Low	0.490	0.507	-0.021
					Std Dev	0.001	0.001	

Nylon High Injection Rate

Normal Runner

Cavities Weight

Trial	1A	1B	2A	2B	Total Weight	Flow Group A	Flow Group B	Difference
1	1.499	1.428	1.538	1.469	5.934	0.512	0.488	0.024
2	1.505	1.426	1.531	1.455	5.917	0.513	0.487	0.026
3	1.492	1.417	1.513	1.443	5.865	0.512	0.488	0.025
4	1.486	1.421	1.525	1.450	5.882	0.512	0.488	0.024
5	1.486	1.416	1.519	1.443	5.864	0.512	0.488	0.025
6	1.482	1.417	1.516	1.453	5.868	0.511	0.489	0.022
7	1.481	1.409	1.507	1.439	5.836	0.512	0.488	0.024
8	1.480	1.410	1.512	1.446	5.848	0.512	0.488	0.023
9	1.488	1.417	1.531	1.448	5.884	0.513	0.487	0.026
10	1.494	1.422	1.528	1.454	5.898	0.512	0.488	0.025
					Average	0.512	0.488	0.024
					High	0.513	0.489	0.026
					Low	0.511	0.487	0.022
					Std Dev	0.001	0.001	

Melt Rotation 0

Cavities Weight

Trial	1A	1B	2A	2B	Total Weight	Flow Group A	Flow Group B	Difference
1	1.455	1.449	1.506	1.493	5.903	0.502	0.498	0.003
2	1.438	1.434	1.496	1.467	5.835	0.503	0.497	0.006
3	1.449	1.447	1.501	1.479	5.876	0.502	0.498	0.004
4	1.449	1.441	1.487	1.468	5.845	0.502	0.498	0.005
5	1.411	1.416	1.461	1.437	5.725	0.502	0.498	0.003
6	1.425	1.426	1.463	1.448	5.762	0.501	0.499	0.002
7	1.411	1.413	1.463	1.446	5.733	0.501	0.499	0.003
8	1.419	1.419	1.470	1.451	5.759	0.502	0.498	0.003
9	1.425	1.425	1.475	1.454	5.779	0.502	0.498	0.004
10	1.419	1.418	1.466	1.450	5.753	0.501	0.499	0.003
					Average	0.502	0.498	0.004
					High	0.503	0.499	0.006
					Low	0.501	0.497	0.002
					Std Dev	0.000	0.000	

Melt Rotation 1

Cavities Weight

Trial	1A	1B	2A	2B	Total Weight	Flow Group A	Flow Group B	Difference
1	1.455	1.428	1.493	1.461	5.837	0.505	0.495	0.010
2	1.441	1.425	1.493	1.456	5.815	0.505	0.495	0.009
3	1.427	1.411	1.476	1.444	5.758	0.504	0.496	0.008
4	1.430	1.412	1.477	1.438	5.757	0.505	0.495	0.010
5	1.421	1.410	1.476	1.442	5.749	0.504	0.496	0.008
6	1.410	1.407	1.463	1.433	5.713	0.503	0.497	0.006
7	1.424	1.413	1.474	1.460	5.771	0.502	0.498	0.004
8	1.427	1.418	1.476	1.454	5.775	0.503	0.497	0.005
9	1.420	1.409	1.474	1.446	5.749	0.503	0.497	0.007
10	1.424	1.413	1.480	1.446	5.763	0.504	0.496	0.008
					Average	0.504	0.496	0.008
					High	0.505	0.498	0.010
					Low	0.502	0.495	0.004
					Std Dev	0.001	0.001	

Melt Rotation 2

	Cavities Weight							
Trial	1A	1B	2A	2B	Total Weight	Flow Group A	Flow Group B	Difference
1	1.441	1.420	1.486	1.448	5.795	0.505	0.495	0.010
2	1.440	1.417	1.496	1.460	5.813	0.505	0.495	0.010
3	1.442	1.418	1.492	1.455	5.807	0.505	0.495	0.011
4	1.436	1.417	1.482	1.445	5.780	0.505	0.495	0.010
5	1.425	1.411	1.480	1.445	5.761	0.504	0.496	0.009
6	1.418	1.404	1.468	1.436	5.726	0.504	0.496	0.008
7	1.415	1.407	1.469	1.436	5.727	0.504	0.496	0.007
8	1.419	1.407	1.467	1.440	5.733	0.503	0.497	0.007
9	1.410	1.389	1.449	1.475	5.723	0.500	0.500	-0.001
10	1.398	1.386	1.450	1.416	5.650	0.504	0.496	0.008
					Average	0.504	0.496	0.008
					High	0.505	0.500	0.011
					Low	0.500	0.495	-0.001
					Std Dev	0.002	0.002	

Melt Rotation 3

	Cavities Weight							
Trial	1A	1B	2A	2B	Total Weight	Flow Group A	Flow Group B	Difference
1	1.433	1.424	1.478	1.461	5.796	0.502	0.498	0.004
2	1.418	1.431	1.472	1.459	5.780	0.500	0.500	0.000
3	1.405	1.413	1.459	1.447	5.724	0.500	0.500	0.001
4	1.399	1.407	1.451	1.438	5.695	0.500	0.500	0.001
5	1.399	1.405	1.451	1.440	5.695	0.500	0.500	0.001
6	1.403	1.411	1.459	1.448	5.721	0.500	0.500	0.001
7	1.388	1.394	1.436	1.482	5.700	0.495	0.505	-0.009
8	1.396	1.393	1.436	1.470	5.695	0.497	0.503	-0.005
9	1.409	1.415	1.460	1.454	5.738	0.500	0.500	0.000
10	1.400	1.410	1.467	1.451	5.728	0.501	0.499	0.001
					Average	0.500	0.500	-0.001
					High	0.502	0.505	0.004
					Low	0.495	0.498	-0.009
					Std Dev	0.002	0.002	

Melt Rotation 4

	Cavities Weight							
Trial	1A	1B	2A	2B	Total Weight	Flow Group A	Flow Group B	Difference
1	1.412	1.429	1.462	1.465	5.768	0.498	0.502	-0.003
2	1.401	1.422	1.454	1.459	5.736	0.498	0.502	-0.005
3	1.395	1.419	1.447	1.456	5.717	0.497	0.503	-0.006
4	1.396	1.423	1.446	1.463	5.728	0.496	0.504	-0.008
5	1.399	1.420	1.448	1.460	5.727	0.497	0.503	-0.006
6	1.394	1.412	1.440	1.447	5.693	0.498	0.502	-0.004
7	1.395	1.410	1.458	1.449	5.712	0.499	0.501	-0.001
8	1.393	1.418	1.453	1.454	5.718	0.498	0.502	-0.005
9	1.393	1.414	1.444	1.448	5.699	0.498	0.502	-0.004
10	1.391	1.417	1.437	1.447	5.692	0.497	0.503	-0.006
					Average	0.498	0.502	-0.005
					High	0.499	0.504	-0.001
					Low	0.496	0.501	-0.008
					Std Dev	0.001	0.001	

Melt Rotation 5

	Cavities Weight							
Trial	1A	1B	2A	2B	Total Weight	Flow Group A	Flow Group B	Difference
1	1.411	1.429	1.461	1.469	5.770	0.498	0.502	-0.005
2	1.406	1.429	1.455	1.475	5.765	0.496	0.504	-0.007
3	1.403	1.434	1.458	1.468	5.763	0.496	0.504	-0.007
4	1.396	1.431	1.450	1.464	5.741	0.496	0.504	-0.009
5	1.398	1.419	1.450	1.454	5.721	0.498	0.502	-0.004
6	1.394	1.418	1.440	1.452	5.704	0.497	0.503	-0.006
7	1.390	1.413	1.448	1.448	5.699	0.498	0.502	-0.004
8	1.387	1.409	1.439	1.449	5.684	0.497	0.503	-0.006
9	1.390	1.410	1.446	1.454	5.700	0.498	0.502	-0.005
10	1.396	1.419	1.451	1.460	5.726	0.497	0.503	-0.006
					Average	0.497	0.503	-0.006
					High	0.498	0.504	-0.004
					Low	0.496	0.502	-0.009
					Std Dev	0.001	0.001	

Melt Rotation 6

	Cavities Weight							
Trial	1A	1B	2A	2B	Total Weight	Flow Group A	Flow Group B	Difference
1	1.408	1.430	1.455	1.473	5.766	0.497	0.503	-0.007
2	1.400	1.436	1.445	1.467	5.748	0.495	0.505	-0.010
3	1.400	1.431	1.440	1.465	5.736	0.495	0.505	-0.010
4	1.382	1.417	1.428	1.449	5.676	0.495	0.505	-0.010
5	1.384	1.428	1.447	1.469	5.728	0.494	0.506	-0.012
6	1.377	1.417	1.427	1.451	5.672	0.494	0.506	-0.011
7	1.379	1.414	1.436	1.454	5.683	0.495	0.505	-0.009
8	1.390	1.428	1.438	1.468	5.724	0.494	0.506	-0.012
9	1.387	1.424	1.440	1.467	5.718	0.494	0.506	-0.011
10	1.384	1.419	1.434	1.455	5.692	0.495	0.505	-0.010
					Average	0.495	0.505	-0.010
					High	0.497	0.506	-0.007
					Low	0.494	0.503	-0.012
					Std Dev	0.001	0.001	

Appendix E – Test Results for PBT

PBT Low Injection Rate

Normal Runner

	Cavities Weight							
Trial	**1A**	**1B**	**2A**	**2B**	**Total Weight**	**Flow Group A**	**Flow Group B**	**Difference**
1	2.001	2.063	2.110	2.107	8.281	0.496	0.504	-0.007
2	2.056	1.962	2.154	1.998	8.170	0.515	0.485	0.031
3	2.001	1.974	2.153	2.015	8.143	0.510	0.490	0.020
4	2.003	1.980	2.151	2.004	8.138	0.510	0.490	0.021
5	1.969	2.005	2.132	2.066	8.172	0.502	0.498	0.004
6	2.045	1.987	2.131	2.043	8.206	0.509	0.491	0.018
7	2.001	1.989	2.104	2.039	8.133	0.505	0.495	0.009
8	1.984	1.980	2.112	2.033	8.109	0.505	0.495	0.010
9	1.977	1.988	2.108	2.040	8.113	0.504	0.496	0.007
10	1.989	1.971	2.102	2.016	8.078	0.506	0.494	0.013
					Average	0.506	0.494	0.013
					High	0.515	0.504	0.031
					Low	0.496	0.485	-0.007
					Std Dev	0.005	0.005	

Melt Rotation 0

	Cavities Weight							
Trial	**1A**	**1B**	**2A**	**2B**	**Total Weight**	**Flow Group A**	**Flow Group B**	**Difference**
1	1.933	2.016	2.003	2.048	8.000	0.492	0.508	-0.016
2	1.904	2.017	2.027	2.056	8.004	0.491	0.509	-0.018
3	1.894	1.983	2.001	2.033	7.911	0.492	0.508	-0.015
4	1.859	1.977	1.977	2.024	7.837	0.489	0.511	-0.021
5	1.885	2.009	2.017	2.048	7.959	0.490	0.510	-0.019
6	1.891	1.996	2.012	2.052	7.951	0.491	0.509	-0.018
7	1.868	1.993	1.981	2.032	7.874	0.489	0.511	-0.022
8	1.855	1.988	2.007	2.048	7.898	0.489	0.511	-0.022
9	1.872	1.992	1.994	2.018	7.876	0.491	0.509	-0.018
10	1.812	1.998	1.961	2.048	7.819	0.483	0.517	-0.035
					Average	0.490	0.510	-0.021
					High	0.492	0.517	-0.015
					Low	0.483	0.508	-0.035
					Std Dev	0.003	0.003	

Melt Rotation 1

	Cavities Weight							
Trial	**1A**	**1B**	**2A**	**2B**	**Total Weight**	**Flow Group A**	**Flow Group B**	**Difference**
1	1.943	2.012	2.058	2.059	8.072	0.496	0.504	-0.009
2	1.886	2.001	1.986	2.032	7.905	0.490	0.510	-0.020
3	1.860	1.967	1.988	2.005	7.820	0.492	0.508	-0.016
4	1.892	2.025	1.977	2.058	7.952	0.487	0.513	-0.027
5	1.844	1.979	1.988	2.037	7.848	0.488	0.512	-0.023
6	1.865	1.974	1.981	2.029	7.849	0.490	0.510	-0.020
7	1.852	1.993	1.981	2.033	7.859	0.488	0.512	-0.025
8	1.862	1.995	1.987	2.041	7.885	0.488	0.512	-0.024
9	1.867	2.001	1.997	2.005	7.870	0.491	0.509	-0.018
10	1.903	2.005	2.021	2.072	8.001	0.490	0.510	-0.019
					Average	0.490	0.510	-0.020
					High	0.496	0.513	-0.009
					Low	0.487	0.504	-0.027
					Std Dev	0.003	0.003	

Melt Rotation 2

Trial	Cavities Weight 1A	1B	2A	2B	Total Weight	Flow Group A	Flow Group B	Difference
1	1.918	2.059	2.074	2.005	8.056	0.496	0.504	-0.009
2	1.881	2.021	1.982	2.031	7.915	0.488	0.512	-0.024
3	1.901	1.986	2.024	2.033	7.944	0.494	0.506	-0.012
4	1.896	2.005	2.033	2.050	7.984	0.492	0.508	-0.016
5	1.898	2.013	2.003	2.026	7.940	0.491	0.509	-0.017
6	1.881	2.000	1.969	2.028	7.878	0.489	0.511	-0.023
7	1.831	1.999	1.975	2.029	7.834	0.486	0.514	-0.028
8	1.852	1.958	1.953	2.079	7.842	0.485	0.515	-0.030
9	1.870	2.021	1.963	2.063	7.917	0.484	0.516	-0.032
10	1.856	2.002	1.960	2.033	7.851	0.486	0.514	-0.028
					Average	0.489	0.511	-0.022
					High	0.496	0.516	-0.009
					Low	0.484	0.504	-0.032
					Std Dev	0.004	0.004	

Melt Rotation 3

Trial	Cavities Weight 1A	1B	2A	2B	Total Weight	Flow Group A	Flow Group B	Difference
1	1.892	2.003	2.025	2.045	7.965	0.492	0.508	-0.016
2	1.808	1.971	1.907	1.988	7.674	0.484	0.516	-0.032
3	1.966	2.148	1.924	1.883	7.921	0.491	0.509	-0.018
4	1.814	2.021	1.979	2.081	7.895	0.480	0.520	-0.039
5	1.884	1.999	1.928	2.009	7.820	0.487	0.513	-0.025
6	1.813	1.951	1.937	1.991	7.692	0.488	0.512	-0.025
7	1.879	2.009	1.979	2.028	7.895	0.489	0.511	-0.023
8	1.858	2.005	1.966	2.050	7.879	0.485	0.515	-0.029
9	1.855	1.973	1.964	2.060	7.852	0.486	0.514	-0.027
10	1.841	1.994	1.978	2.045	7.858	0.486	0.514	-0.028
					Average	0.487	0.513	-0.026
					High	0.492	0.520	-0.016
					Low	0.480	0.508	-0.039
					Std Dev	0.003	0.003	

Melt Rotation 4

Trial	Cavities Weight 1A	1B	2A	2B	Total Weight	Flow Group A	Flow Group B	Difference
1	1.894	1.993	2.020	2.040	7.947	0.493	0.507	-0.015
2	1.805	1.935	1.941	1.978	7.659	0.489	0.511	-0.022
3	1.857	2.017	1.979	2.009	7.862	0.488	0.512	-0.024
4	1.861	2.021	1.994	2.047	7.923	0.487	0.513	-0.027
5	1.861	1.984	1.973	2.013	7.831	0.490	0.510	-0.021
6	1.870	2.021	1.995	2.041	7.927	0.488	0.512	-0.025
7	1.842	1.958	1.923	2.077	7.800	0.483	0.517	-0.035
8	1.850	1.993	1.967	2.029	7.839	0.487	0.513	-0.026
9	1.730	1.994	1.965	2.041	7.730	0.478	0.522	-0.044
10	1.860	2.005	1.957	2.029	7.851	0.486	0.514	-0.028
					Average	0.487	0.513	-0.027
					High	0.493	0.522	-0.015
					Low	0.478	0.507	-0.044
					Std Dev	0.004	0.004	

Melt Rotation 5

	Cavities Weight							
Trial	1A	1B	2A	2B	Total Weight	Flow Group A	Flow Group B	Difference
1	1.830	1.968	1.922	2.004	7.724	0.486	0.514	-0.028
2	1.892	2.015	2.008	2.056	7.971	0.489	0.511	-0.021
3	1.826	2.001	1.942	2.047	7.816	0.482	0.518	-0.036
4	1.845	2.005	1.983	2.056	7.889	0.485	0.515	-0.030
5	1.822	2.003	1.876	2.037	7.738	0.478	0.522	-0.044
6	1.826	1.973	1.956	2.011	7.766	0.487	0.513	-0.026
7	1.824	1.973	1.947	2.025	7.769	0.485	0.515	-0.029
8	1.831	1.964	1.973	2.005	7.773	0.489	0.511	-0.021
9	1.760	1.944	1.915	1.982	7.601	0.483	0.517	-0.033
10	1.841	2.013	1.966	2.041	7.861	0.484	0.516	-0.031
					Average	0.485	0.515	-0.030
					High	0.489	0.522	-0.021
					Low	0.478	0.511	-0.044
					Std Dev	0.003	0.003	

Melt Rotation 6

	Cavities Weight							
Trial	1A	1B	2A	2B	Total Weight	Flow Group A	Flow Group B	Difference
1	1.833	1.997	1.966	2.023	7.819	0.486	0.514	-0.028
2	1.847	1.995	1.933	2.029	7.804	0.484	0.516	-0.031
3	1.733	1.940	1.911	1.993	7.577	0.481	0.519	-0.038
4	1.812	1.984	1.953	2.033	7.782	0.484	0.516	-0.032
5	1.825	2.001	1.972	2.032	7.830	0.485	0.515	-0.030
6	1.826	2.008	1.936	2.036	7.806	0.482	0.518	-0.036
7	1.836	2.008	1.930	2.028	7.802	0.483	0.517	-0.035
8	1.809	1.973	1.944	2.037	7.763	0.483	0.517	-0.033
9	1.840	1.974	1.961	2.025	7.800	0.487	0.513	-0.025
10	1.798	1.986	1.975	2.025	7.784	0.485	0.515	-0.031
					Average	0.484	0.516	-0.032
					High	0.487	0.519	-0.025
					Low	0.481	0.513	-0.038
					Std Dev	0.002	0.002	

PBT Medium Injection Rate

Normal Runner

Cavities Weight

Trial	1A	1B	2A	2B	Total Weight	Flow Group A	Flow Group B	Difference
1	2.162	2.013	2.187	2.043	8.405	0.517	0.483	0.035
2	2.144	2.007	2.200	2.069	8.420	0.516	0.484	0.032
3	2.145	2.028	2.168	2.056	8.397	0.514	0.486	0.027
4	2.099	2.005	2.158	2.033	8.295	0.513	0.487	0.026
5	2.164	1.955	2.176	1.973	8.268	0.525	0.475	0.050
6	2.111	2.021	2.184	2.059	8.375	0.513	0.487	0.026
7	2.085	1.998	2.161	2.037	8.281	0.513	0.487	0.025
8	2.110	1.960	2.204	2.005	8.279	0.521	0.479	0.042
9	2.109	2.015	2.175	2.049	8.348	0.513	0.487	0.026
10	2.094	2.017	2.188	2.053	8.352	0.513	0.487	0.025
					Average	0.516	0.484	0.032
					High	0.525	0.487	0.050
					Low	0.513	0.475	0.025
					Std Dev	0.004	0.004	

Melt Rotation 0

Cavities Weight

Trial	1A	1B	2A	2B	Total Weight	Flow Group A	Flow Group B	Difference
1	1.960	2.056	2.041	2.111	8.168	0.490	0.510	-0.020
2	1.971	2.041	2.059	2.123	8.194	0.492	0.508	-0.016
3	1.949	2.044	2.036	2.103	8.132	0.490	0.510	-0.020
4	1.950	2.038	2.020	2.105	8.113	0.489	0.511	-0.021
5	1.972	2.044	2.054	2.117	8.187	0.492	0.508	-0.016
6	1.981	2.056	2.047	2.119	8.203	0.491	0.509	-0.018
7	1.935	2.016	2.045	2.092	8.088	0.492	0.508	-0.016
8	1.947	2.041	2.033	2.120	8.141	0.489	0.511	-0.022
9	1.974	2.059	2.062	2.121	8.216	0.491	0.509	-0.018
10	1.961	2.050	2.042	2.101	8.154	0.491	0.509	-0.018
					Average	0.491	0.509	-0.019
					High	0.492	0.511	-0.016
					Low	0.489	0.508	-0.022
					Std Dev	0.001	0.001	

Melt Rotation 1

Cavities Weight

Trial	1A	1B	2A	2B	Total Weight	Flow Group A	Flow Group B	Difference
1	2.008	2.049	2.098	2.131	8.286	0.496	0.504	-0.009
2	1.978	2.049	2.061	2.126	8.214	0.492	0.508	-0.017
3	1.972	2.044	2.056	2.118	8.190	0.492	0.508	-0.016
4	1.987	2.041	2.063	2.117	8.208	0.493	0.507	-0.013
5	1.970	2.043	2.068	2.110	8.191	0.493	0.507	-0.014
6	1.973	2.037	2.053	2.106	8.169	0.493	0.507	-0.014
7	1.976	2.048	2.054	2.106	8.184	0.492	0.508	-0.015
8	1.986	2.037	2.056	2.112	8.191	0.493	0.507	-0.013
9	1.988	2.062	2.091	2.113	8.254	0.494	0.506	-0.012
10	1.980	2.048	2.067	2.120	8.215	0.493	0.507	-0.015
					Average	0.493	0.507	-0.014
					High	0.496	0.508	-0.009
					Low	0.492	0.504	-0.017
					Std Dev	0.001	0.001	

Melt Rotation 2

	Cavities Weight							
Trial	1A	1B	2A	2B	Total Weight	Flow Group A	Flow Group B	Difference
1	2.016	2.066	2.094	2.129	8.305	0.495	0.505	-0.010
2	2.034	2.070	2.084	2.115	8.303	0.496	0.504	-0.008
3	1.986	2.052	2.086	2.126	8.250	0.494	0.506	-0.013
4	1.974	2.041	2.045	2.123	8.183	0.491	0.509	-0.018
5	1.956	2.025	2.083	2.084	8.148	0.496	0.504	-0.009
6	1.984	2.045	2.088	2.108	8.225	0.495	0.505	-0.010
7	1.977	2.043	2.071	2.114	8.205	0.493	0.507	-0.013
8	1.950	1.992	2.053	2.069	8.064	0.496	0.504	-0.007
9	1.963	2.052	2.090	2.117	8.222	0.493	0.507	-0.014
10	1.988	2.044	2.087	2.112	8.231	0.495	0.505	-0.010
					Average	0.494	0.506	-0.011
					High	0.496	0.509	-0.007
					Low	0.491	0.504	-0.018
					Std Dev	0.002	0.002	

Melt Rotation 3

	Cavities Weight							
Trial	1A	1B	2A	2B	Total Weight	Flow Group A	Flow Group B	Difference
1	2.013	2.057	2.106	2.149	8.325	0.495	0.505	-0.010
2	2.033	2.054	2.112	2.121	8.320	0.498	0.502	-0.004
3	2.006	2.049	2.117	2.111	8.283	0.498	0.502	-0.004
4	2.000	2.021	2.067	2.125	8.213	0.495	0.505	-0.010
5	2.003	2.059	2.075	2.112	8.249	0.494	0.506	-0.011
6	2.009	2.008	2.067	2.133	8.217	0.496	0.504	-0.008
7	1.988	2.041	2.095	2.102	8.226	0.496	0.504	-0.007
8	1.958	2.073	2.072	2.035	8.138	0.495	0.505	-0.010
9	1.974	2.037	2.061	2.109	8.181	0.493	0.507	-0.014
10	1.963	1.990	2.068	2.058	8.079	0.499	0.501	-0.002
					Average	0.496	0.504	-0.008
					High	0.499	0.507	-0.002
					Low	0.493	0.501	-0.014
					Std Dev	0.002	0.002	

Melt Rotation 4

	Cavities Weight							
Trial	1A	1B	2A	2B	Total Weight	Flow Group A	Flow Group B	Difference
1	2.033	2.048	2.128	2.131	8.340	0.499	0.501	-0.002
2	1.995	2.005	2.110	2.082	8.192	0.501	0.499	0.002
3	1.997	2.039	2.106	2.108	8.250	0.497	0.503	-0.005
4	2.001	2.057	2.114	2.093	8.265	0.498	0.502	-0.004
5	1.969	1.979	2.051	2.143	8.142	0.494	0.506	-0.013
6	1.992	2.027	2.069	2.113	8.201	0.495	0.505	-0.010
7	2.004	2.037	2.098	2.114	8.253	0.497	0.503	-0.006
8	1.981	2.004	2.077	2.074	8.136	0.499	0.501	-0.002
9	1.955	2.028	2.088	2.087	8.158	0.496	0.504	-0.009
10	1.976	2.021	2.048	2.099	8.144	0.494	0.506	-0.012
					Average	0.497	0.503	-0.006
					High	0.501	0.506	0.002
					Low	0.494	0.499	-0.013
					Std Dev	0.002	0.002	

Melt Rotation 5

	Cavities Weight							
Trial	1A	1B	2A	2B	Total Weight	Flow Group A	Flow Group B	Difference
1	2.024	2.045	2.088	2.144	8.301	0.495	0.505	-0.009
2	2.009	2.040	2.052	2.067	8.168	0.497	0.503	-0.006
3	1.983	2.032	2.104	2.106	8.225	0.497	0.503	-0.006
4	1.976	1.977	2.041	2.152	8.146	0.493	0.507	-0.014
5	1.993	2.015	2.067	2.089	8.164	0.497	0.503	-0.005
6	1.973	2.037	2.092	2.112	8.214	0.495	0.505	-0.010
7	1.981	2.008	2.087	2.094	8.170	0.498	0.502	-0.004
8	1.940	2.032	2.095	2.072	8.139	0.496	0.504	-0.008
9	1.973	2.001	2.065	2.054	8.093	0.499	0.501	-0.002
10	1.992	2.025	2.102	2.089	8.208	0.499	0.501	-0.002
					Average	0.497	0.503	-0.007
					High	0.499	0.507	-0.002
					Low	0.493	0.501	-0.014
					Std Dev	0.002	0.002	

Melt Rotation 6

	Cavities Weight							
Trial	1A	1B	2A	2B	Total Weight	Flow Group A	Flow Group B	Difference
1	1.988	2.060	2.090	2.130	8.268	0.493	0.507	-0.014
2	1.995	2.051	2.074	2.128	8.248	0.493	0.507	-0.013
3	1.972	2.037	2.056	2.095	8.160	0.494	0.506	-0.013
4	1.967	2.033	2.064	2.095	8.159	0.494	0.506	-0.012
5	1.950	2.029	2.066	2.101	8.146	0.493	0.507	-0.014
6	1.933	1.993	2.066	2.061	8.053	0.497	0.503	-0.007
7	1.920	2.005	2.066	2.067	8.058	0.495	0.505	-0.011
8	1.940	2.049	2.028	2.089	8.106	0.490	0.510	-0.021
9	1.955	1.987	2.009	2.059	8.010	0.495	0.505	-0.010
10	1.887	1.998	2.028	2.099	8.012	0.489	0.511	-0.023
					Average	0.493	0.507	-0.014
					High	0.497	0.511	-0.007
					Low	0.489	0.503	-0.023
					Std Dev	0.002	0.002	

PBT High Injection Rate

Normal Runner

Cavities Weight

Trial	1A	1B	2A	2B	Total Weight	Flow Group A	Flow Group B	Difference
1	2.199	1.966	2.196	2.007	8.368	0.525	0.475	0.050
2	2.169	1.977	2.172	2.025	8.343	0.520	0.480	0.041
3	2.135	1.903	2.227	1.952	8.217	0.531	0.469	0.062
4	2.122	1.982	2.167	2.011	8.282	0.518	0.482	0.036
5	2.140	1.950	2.240	2.002	8.332	0.526	0.474	0.051
6	2.127	1.904	2.184	1.941	8.156	0.529	0.471	0.057
7	2.105	1.988	2.150	2.016	8.259	0.515	0.485	0.030
8	2.177	1.975	2.149	1.974	8.275	0.523	0.477	0.046
9	2.116	1.988	2.155	2.025	8.284	0.516	0.484	0.031
10	2.135	1.990	2.172	2.018	8.315	0.518	0.482	0.036
					Average	0.522	0.478	0.044
					High	0.531	0.485	0.062
					Low	0.515	0.469	0.030
					Std Dev	0.005	0.005	

Melt Rotation 0

Cavities Weight

Trial	1A	1B	2A	2B	Total Weight	Flow Group A	Flow Group B	Difference
1	1.954	2.004	2.098	2.086	8.142	0.498	0.502	-0.005
2	1.978	1.976	2.070	2.080	8.104	0.500	0.500	-0.001
3	2.036	1.992	1.990	2.049	8.067	0.499	0.501	-0.002
4	1.943	1.948	2.059	2.082	8.032	0.498	0.502	-0.003
5	2.001	1.975	2.001	2.032	8.009	0.500	0.500	-0.001
6	1.948	1.961	1.988	2.082	7.979	0.493	0.507	-0.013
7	1.993	1.964	2.024	2.060	8.041	0.500	0.500	-0.001
8	1.968	2.002	1.990	2.045	8.005	0.494	0.506	-0.011
9	1.914	1.912	2.066	2.037	7.929	0.502	0.498	0.004
10	1.918	1.961	2.074	2.054	8.007	0.499	0.501	-0.003
					Average	0.498	0.502	-0.004
					High	0.502	0.507	0.004
					Low	0.493	0.498	-0.013
					Std Dev	0.003	0.003	

Melt Rotation 1

Cavities Weight

Trial	1A	1B	2A	2B	Total Weight	Flow Group A	Flow Group B	Difference
1	2.008	2.016	2.069	2.089	8.182	0.498	0.502	-0.003
2	2.054	2.040	2.071	2.093	8.258	0.500	0.500	-0.001
3	2.001	2.013	2.012	2.082	8.108	0.495	0.505	-0.010
4	1.992	2.004	1.991	2.045	8.032	0.496	0.504	-0.008
5	1.904	1.898	2.070	2.006	7.878	0.504	0.496	0.009
6	1.963	1.996	2.016	2.074	8.049	0.494	0.506	-0.011
7	1.939	1.962	2.005	2.039	7.945	0.496	0.504	-0.007
8	1.996	2.029	2.009	2.063	8.097	0.495	0.505	-0.011
9	2.035	1.923	1.979	1.976	7.913	0.507	0.493	0.015
10	1.968	1.969	1.997	2.049	7.983	0.497	0.503	-0.007
					Average	0.498	0.502	-0.004
					High	0.507	0.506	0.015
					Low	0.494	0.493	-0.011
					Std Dev	0.004	0.004	

Melt Rotation 2

	Cavities Weight							
Trial	1A	1B	2A	2B	Total Weight	Flow Group A	Flow Group B	Difference
1	1.975	2.003	2.050	2.075	8.103	0.497	0.503	-0.007
2	2.035	2.012	2.088	2.106	8.241	0.500	0.500	0.001
3	1.953	1.914	2.060	2.059	7.986	0.503	0.497	0.005
4	2.029	2.033	2.009	2.047	8.118	0.497	0.503	-0.005
5	1.936	1.952	2.057	2.017	7.962	0.502	0.498	0.003
6	1.899	1.950	2.001	2.028	7.878	0.495	0.505	-0.010
7	1.897	1.956	1.970	2.011	7.834	0.494	0.506	-0.013
8	1.918	1.962	2.025	2.045	7.950	0.496	0.504	-0.008
9	1.970	2.001	2.023	2.074	8.068	0.495	0.505	-0.010
10	1.976	1.965	1.999	2.043	7.983	0.498	0.502	-0.004
					Average	0.498	0.502	-0.005
					High	0.503	0.506	0.005
					Low	0.494	0.497	-0.013
					Std Dev	0.003	0.003	

Melt Rotation 3

	Cavities Weight							
Trial	1A	1B	2A	2B	Total Weight	Flow Group A	Flow Group B	Difference
1	1.990	2.013	2.059	2.073	8.135	0.498	0.502	-0.005
2	1.995	2.014	2.074	2.090	8.173	0.498	0.502	-0.004
3	1.970	1.942	2.038	2.033	7.983	0.502	0.498	0.004
4	1.990	1.981	2.055	2.056	8.082	0.500	0.500	0.001
5	2.004	1.968	2.025	2.055	8.052	0.500	0.500	0.001
6	1.971	1.941	2.020	2.025	7.957	0.502	0.498	0.003
7	1.958	1.944	2.029	1.978	7.909	0.504	0.496	0.008
8	1.944	1.967	2.021	2.001	7.933	0.500	0.500	0.000
9	1.949	1.941	1.989	2.009	7.888	0.499	0.501	-0.002
10	1.958	1.957	1.959	2.013	7.887	0.497	0.503	-0.007
					Average	0.500	0.500	0.000
					High	0.504	0.503	0.008
					Low	0.497	0.496	-0.007
					Std Dev	0.002	0.002	

Melt Rotation 4

	Cavities Weight							
Trial	1A	1B	2A	2B	Total Weight	Flow Group A	Flow Group B	Difference
1	1.956	1.963	2.049	2.045	8.013	0.500	0.500	0.000
2	1.998	1.972	2.059	2.071	8.100	0.501	0.499	0.002
3	1.965	1.965	2.035	2.033	7.998	0.500	0.500	0.000
4	1.985	1.882	2.028	2.015	7.910	0.507	0.493	0.015
5	1.918	1.943	2.021	2.029	7.911	0.498	0.502	-0.004
6	1.931	1.925	2.021	2.029	7.906	0.500	0.500	0.000
7	1.979	1.953	1.998	1.991	7.921	0.502	0.498	0.004
8	1.955	1.939	2.039	2.016	7.949	0.502	0.498	0.005
9	1.989	1.971	1.997	2.027	7.984	0.499	0.501	-0.002
10	1.950	1.938	2.021	2.022	7.931	0.501	0.499	0.001
					Average	0.501	0.499	0.002
					High	0.507	0.502	0.015
					Low	0.498	0.493	-0.004
					Std Dev	0.003	0.003	

Melt Rotation 5

	Cavities Weight							
Trial	1A	1B	2A	2B	Total Weight	Flow Group A	Flow Group B	Difference
1	1.969	1.973	2.062	2.052	8.056	0.500	0.500	0.001
2	1.966	1.983	2.037	2.059	8.045	0.498	0.502	-0.005
3	2.011	1.934	2.014	2.032	7.991	0.504	0.496	0.007
4	1.958	1.970	1.977	2.009	7.914	0.497	0.503	-0.006
5	1.969	1.938	1.997	2.043	7.947	0.499	0.501	-0.002
6	1.954	1.943	2.020	2.033	7.950	0.500	0.500	0.000
7	1.937	1.913	2.078	1.940	7.868	0.510	0.490	0.021
8	1.933	1.940	2.004	2.014	7.891	0.499	0.501	-0.002
9	1.882	1.893	2.023	1.973	7.771	0.503	0.497	0.005
10	1.937	1.976	1.992	2.033	7.938	0.495	0.505	-0.010
					Average	0.500	0.500	0.001
					High	0.510	0.505	0.021
					Low	0.495	0.490	-0.010
					Std Dev	0.004	0.004	

Melt Rotation 6

	Cavities Weight							
Trial	1A	1B	2A	2B	Total Weight	Flow Group A	Flow Group B	Difference
1	1.927	1.978	2.025	2.056	7.986	0.495	0.505	-0.010
2	2.001	1.948	2.007	2.011	7.967	0.503	0.497	0.006
3	1.988	1.990	1.999	2.029	8.006	0.498	0.502	-0.004
4	1.926	1.997	2.021	2.041	7.985	0.494	0.506	-0.011
5	1.981	1.961	1.996	2.051	7.989	0.498	0.502	-0.004
6	2.003	1.933	1.988	2.035	7.959	0.501	0.499	0.003
7	1.884	1.919	1.973	2.029	7.805	0.494	0.506	-0.012
8	1.900	1.938	1.980	2.011	7.829	0.496	0.504	-0.009
9	1.974	1.973	1.950	1.986	7.883	0.498	0.502	-0.004
10	1.924	1.943	1.985	2.064	7.916	0.494	0.506	-0.012
					Average	0.497	0.503	-0.006
					High	0.503	0.506	0.006
					Low	0.494	0.497	-0.012
					Std Dev	0.003	0.003	

Vita

Michael John Wolbert Jr., born October 7, 1982, is the son of Michael and Jana Wolbert. He was born in Clarion, Pennsylvania, and grew up in the small town of Crown, Pennsylvania. Grades K-6th he attended North Clarion Elementary. Then 7th-12th grade he attended North Clarion Jr./Sr. High School where he finished in the top 5% of his class.

After graduating from North Clarion Jr./Sr. High school in 2001, Michael attended the Pennsylvania State University at the Behrend Campus in Erie, PA. He received a Bachelor of Science in Plastics Engineering Technology from Penn State in the spring of 2005. While doing his undergraduate work at Penn State Michael participated in the 2003 REU program in the College of Polymers and High Performance Materials at the University of Southern Mississippi. There he performed research on the use of polymers as artificial muscles that respond to electrical stimulation. In the summer of 2004 Michael had an internship with Zurn at their Commerce, Texas plant. He performed multiple tasks from working on the extrusion lines, to mold maintenance, to design, to process optimization. During his senior year at Penn State, Michael worked with Professor Beaumont in the study of shear imbalances and melt rotation as part of his senior project. His work "Shear Imbalance Effects on Gas Distribution in Gas-Assist Injection Molding" was published and presented at ANTEC 2005.

Mid-Summer 2005 Michael started his pursuit of a Masters of Science degree in Mechanical Engineering at Lehigh University. Michael worked under Dr. John Coulter, for it was Dr. Coulter that had convinced Michael to attend Lehigh. Michael spent the next two years working on his Masters of Science Degree; working closely with Dr. Coulter, Kevin Boell of the Plastics CAE Center, and Professor Beaumont of Penn State Behrend.

END OF TITLE